

UNIVERSITY OF NOVA GORICA
GRADUATE SCHOOL

**DEVELOPMENT OF METHODOLOGY FOR THE
EVALUATION OF ANTIMICROBIAL ACTIVITY OF
PREPARED TiO₂ PHOTOCATALYTIC FILMS**

DISSERTATION

Urška Žvab

Mentors:

prof. dr. Urška Lavrenčič Štangar
asst. prof. Martina Bergant Marušič

Nova Gorica, 2014

Zahvala

Zahvaljujem se mentorici Urški Lavrenčič Štangar, da mi je omogočila pridobitev različnih delovnih izkušenj, podporo, mirnost in povezovalnost. Hvala mentorici Martini Bergant Marušič za nasvete v laboratoriju, pri analizi rezultatov in prijaznost. Veliki hvala Mateju za pomoč pri reševanju različnih zapletov. Hvala Markotu Keteju za tehnično pomoč in za rezultate testov s tereftalno kislino. Zahvaljujem se Nataši Novak Tušar, Darji Maučec, Romani Cerc Korošec in Silviji Gross za pomoč pri karakterizaciji materialov in Elsi Fabbretti za fotografijo bakterij pod fluorescentnim mikroskopom. Zahvaljujem se tudi mnogim drugim sodelavcem, za podporo, pomoč, nasvete in družbo. Predvsem Vesni, Andražu, Jani in Fernandu. In še mnogim drugim, ki ste tudi naredili laboratorijski svet lep; med njimi ste bili najpomembnejši Giulia, Vinay in Nina. Seveda hvala tudi Javni agenciji za raziskovalno dejavnost Republike Slovenije, ki je raziskovalno delo in študij finančno omogočila.

Povzetek

Fotokataliza že več desetletij velja za obetaven napredni oksidacijski postopek (angl. advanced oxidation process - AOP) za odstranjevanje organskih in anorganskih onesnaževal iz vode, zraka in s površin. Nanokristalinični anataz titanovega dioksida (TiO_2) je najpogosteje uporabljeni fotokatalitski material. Fotokatalitske prevleke veljajo tudi za trajnostni material, saj potrebujejo le svetlobo, vodo (donor elektronov) in kisik (akceptor elektronov) za svoje delovanje in regeneracijo. Leta 1985 je japonska raziskovalna skupina pod vodstvom prof. Matsunage prva pokazala antimikrobno moč fotokatalize. Sledile so mnoge študije po vsem svetu namenjene razumevanju mehanizmov, udeleženih v fotokatalitsko dezinfekcijo, in preučevanja pogojev, ki določajo dezinfekcijski učinek. Nedavno se je povečalo zanimanje tudi za (eko)toksikološke vplive teh fotoaktivnih nanomaterialov in za oblikovanje standardnih metodologij, namenjenih ovrednotenju njihove aktivnosti, z željo, da bi bili ti dani na trg kot človeku in okolju prijazni materiali in naprave. Mnogi produkti in fotokatalitski materiali so že v prodaji, veliko več pa jih še razvijajo.

Za potrebe standardizacije smo poskusili združiti najprimernejše postopke v metodologije, ki bi omogočile učinkovito ovrednotenje antibakterijske aktivnosti samočistilnih/samodezinfekcijskih površin in tudi prevlek, ki so bile razvite za čiščenje/dezinfekcijo vode. Uporabljene TiO_2 - SiO_2 prevleke smo pripravili s sol-gel postopkom. Sol smo na substrat (keramično ploščico, steklo ali aluminij) nanegli s potapljanjem (angl. dip-coating) ali z razprševanjem. Pripravljene fotokatalizatorje smo karakterizirali z vrstičnim elektronskim mikroskopom (SEM), meritvijo BET (Brunauer, Emmet and Teller) površine, difuzijskih refleksijskih spektrov (DRS), rentgenske praškovne difrakcije (XRD), infrardečo spektroskopijo (FT-IR) in rentgensko fotoelektronsko spektroskopijo (XPS). Pilkington Glass Activ™ smo uporabili kot standardni samodezinfekcijski material. Za dva vzorca smo s termogravimetrično analizo (TG) in diferenčno dinamično kalorimetrijo (DSC) določili tudi termična profila. Preko celotne študije smo kot modelni organizem uporabljali gram-negativno bakterijo *Escherichia coli* (*E. coli*). Samodezinfekcijske prevleke so bile tretirane v dveh osvetljevalnikih, bolj aktivne fotokatalitske prevleke pa v dveh krožnih fotoreaktorjih z različnima zgradbama, v pretočnem in šaržnem reaktorju vrste Carberry (CTP), z različnima zgradbama.

Z namenom poiskati zanesljive, občutljive, ponovljive in hitre metode za zaznavo antibakterijskih učinkov fotokatalitskih prevlek smo poleg standardnega testa štetja kolonij na hranilnih ploščah preizkusili tri različne teste, zasnovane za čitalec mikrotiterskih ploščic. Le preprost test rasti in metabolni test z indikatorjem 2,3-Bis(2-methoxy-4-nitro-5-sulfophenyl)-2H-tetrazolium-5-carboxanilide (XTT) sta bila dovolj občutljiva za ovrednotenje in razlikovanje manj ostrih fotokatalitskih pogojev, značilnih za analize tankih samočistilnih prevlek. Ker dajeta zelo podobne rezultate, bi se sicer lahko uporabljala tudi posamezno. Priljubljeni test LIVE/DEAD[®] *BacLight*[™] (*BacLight*) za prikaz bakterijske viabilnosti z merjenjem integritete celičnih membran ni bil dovolj občutljiv za ovrednotenje samodezinfekcijskih fotokatalitskih površin, vzbujanih z ultravijolično A (UVA) svetlobo. Kljub temu je *BacLight* lahko razlikoval med različnimi fotokatalitskimi pogoji ob osvetljevanju samočistilnih prevlek z dnevno (vidno) svetlobo. Le s testom štetja kolonij, tudi ni bilo možno razlikovati med različnimi samodezinfekcijskimi prevlekami in fotolizo. Pojavnost majhnih različic kolonij (SCV) na trdih gojiščih je kljub vsemu pokazala zamike v rasti kot posledico poškodb tretiranih bakterij.

Tudi v študiji dezinfekcije vode so se na trdih gojiščih razvile SCV. Vendar so bile bakterije v ostrejših pogojih fotokatalitske dezinfekcije vode poškodovane tudi do te mere, da nismo več zaznala rasti na trdih gojiščih. Test *BacLight* v izvedbi z mikroploščico se je pokazal kot najprimernejši za to vrsto fotokatalitskih študij, saj je omogočil sledenje fotokatalitskemu eksperimentu v realnem času in je hkrati predvidel izid testa štetja kolonij, ki je bil dobljen retrospektivno. Ujemanje rezultatov testov *BacLight* in štetja kolonij je tudi pokazal na odsotnost viabilnih bakterij, ki ne rastejo v hranilnih gojiščih (VBNC), v vzorcih po končani fotokatalitski dezinfekciji. Rezultati rastnega in XTT testov v izvedbi z mikroploščico so se ujemali, prav tako so bili v tem primeru primerljivi z rezultati testov štetja kolonij in *BacLight*.

Mešanica AEROXIDE[®] P 25 (P25) in PC500 (ramerje mas 1:1) je bila najboljša med komercialnimi prahovi, ki smo jih dodali TiO₂-SiO₂ nanokristaliničnemu solu, da bi povečali koncentracije fotokatalitsko aktivnih TiO₂ delcev v prevlekah in posledično njihove fotokatalitske aktivnosti ob UVA vzbujanju. Pri uporabi dnevnih luči (pretežno vidna svetloba) so se sicer vsi materiali obnašali podobno, kar pomeni da je bilo dopiranje z dušikom z namenom povečanja aktivnosti materiala pod vidno svetlobo neuspešno. Neaktivni

material, ki je bil dopiran z ogljikom, je bil izločen iz študije že v preliminarnih testih v pretočnem reaktorju.

V zaključku laboratorijskega dela raziskovalnega projekta smo s pomočjo pretočne citometrije preizkusili zmožnost več indikatorjev viabilnosti za ovrednotenje antibakterijskega delovanja fotokatalitskih prevlek. Dvojni barvanji tiazol oranžno (TO)-propidijev jodid (PI) in SYTO 9-PI (*BacLight*) ter enojno barvanje SYTO 9 so se pokazali za najbolj občutljive teste merjenja integritete membran tretiranih *E. coli*. Kot slabše se je izkazalo dvojno barvanje, SYBR[®] Safe DNA Gel Stain (SYBR Safe)-PI. S preostalimi enojnimi barvanji s PI, TO, and SYBR Safe ni bilo mogoče razločiti med različnimi fotokatalitskimi samočistilnimi površinami ter fotolizo. Primeren za ovrednotenje antibakterijskega učinka samočistilnih prevlek se je pokazal tudi indikator Bis-(1,3-dibutilbarbiturinska kislina)trimetin oksonol (DiBAC4(3)), ki meri za viabilnost celice pomembno velikost membranskega potenciala. Test sledenja cepitvi karboksifluorescein diacetata (CFDA) z esterazami, ki nakazuje celično metabolno aktivnost, v naših eksperimentalnih pogojih ni deloval. Iz rezultatov, dobljenih s pretočno citometrijo, lahko zaključimo, da se zdijo TO-PI, SYTO 9-PI ali SYTO 9 merjenja integritete bakterijskih membrane v kombinaciji z DiBAC4(3) meritvami membranskega potenciala najobetavnejša kombinacija za takojšnje, hitro in občutljivo ovrednotenje viabilnosti *E. coli* po izpostavitvi UVA vzbujenim fotokatalitskim samočistilnim plastem.

Testi v mikroploščici in s pretočno citometrijo so se pri ovrednotenje dezinfekcijskih zmožnosti različnih antibakterijskih fotokatalitskih plasti/pogojev pokazali kot dobra alternativa konvencionalnemu testu s štetjem kolonij. Za optimalno izrabo njihovih prednosti morajo biti le-ti pazljivo izbrani in ovrednoteni, pri čemer moramo upoštevati nabor antibakterijskih učinkov, ki jih želimo spremljati, izbrane testne mikroorganizme in fotokatalitsko moč eksperimentalnih pogojev. Testni protokoli morajo biti tudi optimizirani za vsakega izmed izbranih eksperimentalnih pogojev. Dodala bi tudi, da ovrednotenje antibakterijske aktivnosti fotokatalitskih materialov zahteva interdisciplinarni pristop; v enaki meri poznavanje materialov in živih organizmov.

Ključne besede: fotokatalitske prevleke, antimikrobna aktivnost, testni parametri, testi v mikroploščici, testi s pretočno citometrijo

Summary

For many decades now photocatalysis is considered as a promising advanced oxidation process (AOP) for the removal of organic and inorganic pollutants from water, air and surfaces. The nanosized anatase crystalline form of titanium dioxide (TiO₂) is most frequently used as a photocatalyst. Photocatalytic coatings are also seen as sustainable materials, because they only need sunlight, water (electron donor) and oxygen (electron acceptor) for their activation and regeneration. In 1985 Japanese scientific group coordinated by prof. Matsunaga for the first time demonstrated the ability of photocatalysis for the destruction of microorganisms. After that many studies world-wide have been devoted to understanding mechanisms of disinfection and of conditions that influence disinfection outcome. Recently, interest has increased also in (eco)toxicological studies of these photoactive nanomaterials and in the standardisation of evaluation methodologies, including antimicrobial methods, in order to commercialize photocatalytic materials and devices as human- and environment-friendly photocatalytic products. Many applications and materials are already present in the market, but many more are still in the developmental stage.

In accordance to the current standardization demands we strived to unite the most appropriate protocols into methodologies that will enable effective evaluation of antibacterial activity of self-cleaning/disinfecting surfaces and coatings developed for water cleaning/disinfection. TiO₂-SiO₂ coatings employed were prepared by sol-gel process. Sol was deposited on substrate (ceramic tile, glass or aluminum) by dip-coating or spraying. Prepared photocatalysts were characterized by scanning electron microscopy (SEM), by measuring BET (Brunauer, Emmet and Teller) surface area, diffuse reflectance spectra (DRS), X-ray powder diffraction (XRD), Fourier transform infrared spectroscopy (FT-IR) and X-ray photoelectron spectroscopy (XPS). Pilkington Glass Activ™ was used as a standard self-disinfecting film. For some samples also thermogravimetric (TG) and differential scanning calorimetric (DSC) temperature profile was recorded. Model microorganism throughout the whole study was gram-negative bacterium *Escherichia coli* (*E. coli*). Self-disinfecting films were tested in the irradiation chamber, while more active water disinfecting coatings were exposed in two annular reactors, non-continuous and continuous Carrbery type photoreactors (CTP) of different designs.

In order to find reliable, sensitive, reproducible, and fast methods for the detection of antibacterial effects of photocatalytic coatings, three different microplate-based assays were performed in addition to standard colony count. For evaluation of milder photocatalytic conditions that occur in the analysis of thin self-disinfecting coatings under lower light intensities, only basic growth assay and metabolic activity assay with indicator 2,3-Bis(2-methoxy-4-nitro-5-sulfophenyl)-2H-tetrazolium-5-carboxanilide (XTT) were sensitive enough to distinguish between different photocatalytic conditions. Growth and XTT assays may be used also individually as results obtained by these two methods are well in accordance. In a microplate format, commonly used LIVE/DEAD[®] *BacLight*[™] (*BacLight*) assay that measures bacterial viability through membrane integrity was not sensitive enough for the assessment of self-cleaning surfaces following ultraviolet A (UVA)-induced photocatalytic exposure. In contrast, microplate-based *BacLight* assay was capable of discriminating among different experimental conditions after exposure to the daylight. Colony count assay was also insufficient to distinguish between different self-disinfecting films and photolysis. However, appearance of small colony variants (SCV) on nutrient plates indicated growth delay as a consequence of the treatment-related cell injuries.

Small colony variants (SCV) recovered also in the water disinfection study. However, harsher photocatalytic pressure in the water disinfection tests resulted in stronger antibacterial effect, with bacteria being injured also up to unculturable states. Microplate-based *BacLight* assay was found to be the most useful detection assay for this type of studies as it enables following the photocatalytic experiment progression in real time. *BacLight* assay was also in accordance with the standard colony count assay, where the results are obtained in retrospect. This also suggests that the photocatalytic treatment did not trigger viable but nonculturable (VBNC) state of the bacteria tested. Like in the evaluation of self-disinfecting coatings, microplate growth and XTT assays showed similar results, in this case the results were also in accordance to colony count and *BacLight* assays.

The mixture of AEROXIDE[®] P 25 (P25) and PC500 (1:1 mass ratio) was confirmed to be the best among commercial powders that were added to the TiO₂-SiO₂ nanocrystalline sol aiming to increase concentration of photocatalytically active TiO₂ particles in the coatings and, consequently, their photocatalytic activity under UVA. When irradiated by daylight lamps, different materials tested performed very similar. Incorporation of nitrogen-doped titania for improved activity of coating under visible light was unsuccessful. For this reason, non-active

carbon-doped material was eliminated from the study already in preliminary phase performed in a non-continuous CTP. Exploiting advantages of flow cytometry, the capability of different viability indicators to show antibacterial effects of self-disinfecting coatings was evaluated in the last part of the study. Thiazole orange (TO)-propidium iodide (PI) is suggested to be the most sensitive assay to measure membrane integrity of treated *E. coli* followed by SYTO 9-PI (*BacLight*) and SYBR[®] Safe DNA Gel Stain (SYBR Safe)-PI double and SYTO 9 single staining. PI, TO and SYBR Safe single stainings were insufficient to discriminate among different photocatalytic self-disinfecting coatings and photolysis. Bis-(1,3-dibutylbarbituric acid)trimethine oxonol (DiBAC4(3)) measuring membrane potential, another important parameter of live cell, indicated changes in photocatalytically treated *E. coli* and was identified as an appropriate assay for the evaluation of antibacterial effects of photocatalysis. Detecting carboxyfluorescein diacetate (CFDA) cleavage by esterases, which indicates the level of bacterial metabolic activity, was not successful in our experimental settings. To conclude results obtained by flow cytometry: TO-PI, SYTO 9-PI or SYTO 9 membrane integrity assay supported by DiBAC4(3) membrane potential measurements, was observed to be a promising combination for immediate, rapid and sensitive evaluation of *E. coli* viability after exposure to UVA-activated self-disinfecting films.

Microplate-based and flow cytometry assays proved to be very good alternatives to the conventional colony count method in testing different disinfection potential of the antibacterial photocatalytic coatings/conditions. However, for good exploitation of their advantages, they need to be selected and evaluated carefully, taking into account set of antibacterial effects, which are desired to be tested, selected testing microorganisms and photocatalytic strength of the experimental conditions. Testing protocols must be optimized for any of the selected conditions used. In addition, antimicrobial evaluation of photocatalytic materials requires an interdisciplinary approach, bringing together material and life sciences with equal importance.

Keywords: photocatalytic coatings, antimicrobial activity, testing parameters, microplate-based assays, flow cytometry assays

List of Contents

1	Introduction.....	1
2	Photocatalysis and TiO ₂ photocatalyst	4
2.1	General aspects about semiconductor photocatalysis	4
2.2	Immobilized TiO ₂	4
2.3	Mechanisms of the photocatalytic process.....	5
2.4	Enhanced photocatalytic activity	6
2.5	Photocatalytic disinfection	8
2.5.1	Antimicrobial effect of photocatalytic films	8
2.5.2	Mechanism of photocatalytic disinfection	8
2.6	Methodologies for evaluation of antimicrobial efficiency of immobilized photocatalysts.....	10
2.6.1	Testing procedures	12
2.6.1.1	Photocatalytic chambers and reactors for water disinfection.....	12
2.6.1.2	Cleaning and sterilization of photocatalytic coatings	13
2.6.1.3	Preventing leaking of microbiological sample from self-disinfecting surfaces.....	14
2.6.1.4	Removing microorganisms from materials and their storage between sampling and analysis.....	14
2.6.2	Physicochemical parameters affecting antimicrobial efficiency of immobilized photocatalysts.....	15
2.6.2.1	Irradiation	15
2.6.2.2	Temperature.....	17
2.6.2.3	pH.....	18
2.6.2.4	Oxygen presence.....	18
2.6.2.5	Humidity.....	19
2.6.2.6	Composition of testing media.....	19
2.6.3	Microorganisms and culture conditions	21
2.6.3.1	The target microorganisms.....	22
2.6.3.2	Microorganism form	24

2.6.3.3	Microorganism density	25
2.6.4	Detection of antimicrobial effects of photocatalysis	26
2.6.4.1	Culture methods.....	26
2.6.4.2	Fluorescence, luminescence and colorimetric methods.....	28
2.6.4.3	Detection of microbial degradation and specific components of microbial cells.....	30
2.6.5	Presenting antimicrobial effect.....	31
3	Research goals.....	32
4	Materials and methods.....	33
4.1	Materials.....	33
4.1.1	Chemicals and materials for photocatalyst preparation and characterization	33
4.1.2	Chemicals, materials and instruments for antibacterial tests	33
4.2	Preparation of TiO ₂ -SiO ₂ films.....	36
4.2.1	Transparent TiO ₂ -SiO ₂ films with lower activity	36
4.2.2	Opaque TiO ₂ -SiO ₂ films with higher activity	36
4.3	Characterization of TiO ₂ -SiO ₂ films.....	37
4.4	Bacteria and culture conditions	38
4.5	Inactivation of bacteria with photocatalysis.....	38
4.5.1	Inactivation of bacteria on self-disinfecting coatings	39
4.5.1.1	Photocatalytic disinfection procedure in the method development.....	39
4.5.1.2	Photocatalytic disinfection procedure for flow cytometry testings	40
4.5.2	Inactivation of <i>E. coli</i> in simplified water disinfection process	41
4.5.2.1	Non-continuous Carrbery type photoreactor (ncCTP).....	41
4.5.2.2	Carrbery type photoreactor (CTP).....	42
4.6	Detection of antibacterial activity of the films	42
4.6.1	Antibacterial activity evaluation using colony count method.....	42
4.6.2	Antibacterial evaluation using microplate-based <i>BacLight</i> assay	43
4.6.3	Antibacterial evaluation using microplate-based growth and XTT assay	44
4.6.4	Antibacterial activity evaluation by fluorescence microscopy.....	47
4.6.5	Antibacterial activity evaluation by flow cytometry	47
5	Results and discussion.....	51
5.1	Photocatalysts	51

5.1.1	Self-disinfecting coatings used in the development of methodology	51
5.1.2	Coatings for water disinfection.....	57
5.2	Assesment of antibacterial activity of photocatalytic materials	63
5.2.1	Preliminary evaluation of self-disinfecting coatings by fluorescence microscopy.....	63
5.2.2	Antibacterial evaluation of self-disinfecting coatings by microplate-based spectrofluorimetric assays	64
5.2.3	Comparison of microplate-based spectrometric growth and XTT assays and colony count.....	68
5.2.4	Validation of UVA-tested microplate-based assays by visible light-induced photocatalytic coatings	72
5.2.5	<i>E. coli</i> inactivation in simplified water disinfection process	73
5.2.5.1	Disinfection by a prototype ncCTP	73
5.2.5.2	Improved disinfection in CTP reactor.....	78
5.2.6	Flow cytometry assays for the evaluation of antibacterial activity of photocatalytic coatings	86
6	Conclusions.....	95
7	References.....	99

List of Figures

<i>Figure 1: Example of a simple illumination chamber</i>	12
<i>Figure 2: Influence of NaCl concentration on photocatalytic disinfection</i>	21
<i>Figure 3: Scheme of Carberry type photoreactor (CTP) photocatalytic reactor parts</i>	34
<i>Figure 4: UVA (a) and Vis (b) lamps spectra</i>	34
<i>Figure 5: Analysis of relative viability of standard E. coli suspensions by BacLight assay</i> ...	43
<i>Figure 6: Growth (a) and metabolic activity (b) profiles of the unexposed standard E. coli of different densities</i>	44
<i>Figure 7: External calibration curves for quantification of E. coli growth (■) and metabolic activity (□) in microtiter-plate reader</i>	45
<i>Figure 8: BacLight assay (a) and XTT/growth assays (b) programs used in microtiter plate reader</i>	47
<i>Figure 9: Evaluation of PI, TO, SYTO 9, SYBR Safe, DiBAC4(3) and CFDA dyes for flow cytometry analysis</i>	50
<i>Figure 10: SEM corresponding to photocatalytic coatings 19T deposited on ceramic substrate</i>	52
<i>Figure 11: SEM corresponding to photocatalytic coatings P25-PC500 AL deposited on ceramic substrate</i>	53
<i>Figure 12: SEM corresponding to photocatalytic coatings VPC10 (N-doped AL) deposited on aluminum</i>	55
<i>Figure 13: High transparency of 19T films and opaque appearance of P25-PC500 AL films</i>	55
<i>Figure 14: XRD patterns of TiO₂ materials P25-PC500 AL and 19T</i>	56
<i>Figure 15: FT-IR spectra of 19T and P25-PC500 AL</i>	56
<i>Figure 16: TG (a) and DSC curves (b) for 19T and P25-PC500 AL samples</i>	56
<i>Figure 17: SEM corresponding to the photocatalytic coating P25-PC500 deposited on soda-lime glass</i>	58
<i>Figure 18: SEM corresponding to the nitrogen-doped photocatalytic coating VPC10 deposited on a soda-lime glass</i>	58
<i>Figure 19: SEM corresponding to the undoped PC10 analogue of nitrogen-doped VPC10, photocatalytic coating deposited on a soda-lime glass</i>	59

Figure 20: SEM corresponding to photocatalytic coating PC500 deposited on a soda-lime glass.....	60
Figure 21: XRD patterns of TiO ₂ materials P25-PC500 AL and 19T.....	61
Figure 22: FT-IR spectra of P25-PC500, VPC10, PC10 and PC500.....	61
Figure 23: Fluorescence image of stained <i>E. coli</i> after photocatalysis.....	63
Figure 24: Growth and metabolic activity of <i>E. coli</i> exposed to UVA-activated photocatalytic coatings.....	66
Figure 25: Effect of UVA-activated photocatalytic coatings on <i>E. coli</i> membrane integrity.....	67
Figure 26: Effect of photocatalysis and photolysis on <i>E. coli</i> colony size.....	71
Figure 27: Validation of microplate-based assays in the antibacterial evaluation of Vis-activated photocatalytic coatings.....	73
Figure 28: Growth and metabolic activity of <i>E. coli</i> exposed to UVA- and Vis-activated photocatalysts in prototype ncCTP reactor.....	75
Figure 29: Effect of photocatalysis and photolysis on <i>E. coli</i> colony size.....	76
Figure 30: Growth and metabolic activity of <i>E. coli</i> exposed to Vis and Vis-activated photocatalysts in CTP reactor.....	81
Figure 31: Growth and metabolic activity of <i>E. coli</i> exposed to UVA and UVA-activated photocatalysts in CTP reactor.....	82
Figure 32: Growth and metabolic activity of <i>E. coli</i> exposed in dark to photocatalytic plates P25-PC500 in CTP reactor.....	82
Figure 33: Effect of photocatalysis, Vis and UVA light photolysis on <i>E. coli</i> colony size.....	86
Figure 34: Membrane integrity of <i>E. coli</i> exposed to photocatalysis, as indicated by double TO-PI staining.....	87
Figure 35: Membrane integrity of <i>E. coli</i> exposed to photocatalysis, as indicated by double SYTO 9-PI staining.....	88
Figure 36: Membrane integrity of <i>E. coli</i> exposed to photocatalysis, as indicated by double SYBR Safe-PI staining.....	89
Figure 37: Membrane integrity of <i>E. coli</i> exposed to photocatalysis, as indicated by single TO (a) and SYBR Safe (b) staining.....	90
Figure 38: Membrane integrity of <i>E. coli</i> exposed to photocatalysis, as indicated by single stain SYTO 9 and PI staining.....	91
Figure 39: Depolarization of <i>E. coli</i> membranes as indicated by DiBAC4(3) staining.....	92
Figure 40: Metabolic activity of <i>E. coli</i> exposed to photocatalysis, as indicated by esterase substrate CFDA.....	93

List of Tables

<i>Table 1: List of existing and forthcoming ISO and JIS tests for the assessment of antimicrobial activity of photocatalytic coatings.</i>	11
<i>Table 2: List of existing and forthcoming CEN, ISO and JIS standards about irradiation....</i>	16
<i>Table 3: Light power densities for different reactors</i>	35
<i>Table 4: Overview of flow cytometry probes informations, including incubation conditions</i>	48
<i>Table 5: Reaction rates for TPA oxidation obtained for different titania films</i>	51
<i>Table 6: Overview of the main properties of TiO₂-SiO₂ materials tested as self-disinfecting films</i>	57
<i>Table 7: Elemental composition of photocatalysts used in water disinfection tests in CTP...</i>	62
<i>Table 8: Overview of the main properties of TiO₂-SiO₂ coatings tested as materials for water disinfection</i>	62
<i>Table 9: Comparison of two microplate-based assays and the colony count method for the antibacterial evaluation of photocatalytic coatings</i>	69
<i>Table 10: Quantitative outcome of photocatalytic tests performed in ncCTP reactor.....</i>	77
<i>Table 11: Quantitative evaluation of photocatalytic tests performed in CTP reactor</i>	83

Abbreviations

AFM = atomic force microscopy

Activ™ = Pilkington Activ™ Self-Cleaning glass

AOP = advanced oxidation process

ATP = adenosine triphosphate

BacLight = LIVE/DEAD® BacLight™ assay

BET surface = Brunauer, Emmet and Teller surface

CEN = European Committee for Standardization

CF = carboxyfluorescein

CFDA = carboxyfluorescein diacetate

CFU = colony forming unit

CTP = Carberry type photoreactor

DiBAC4(3) = Bis-(1,3-dibutylbarbituric acid)trimethine oxonol

DRS = diffuse reflectance spectra

DSC = differential scanning calorimetry

DSMZ = German Collection of Microorganisms and Cell Cultures

E. coli = *Escherichia coli*

EDTA = ethylenediaminetetraacetic acid

EtOH = ethanol

EU = European Union

FRET = fluorescence resonance energy transfer

FT-IR = Fourier transform infrared spectroscopy

IARC = International Agency for Research on Cancer

iPrOH = isopropanol

ISO = International Organization for Standardization

JIS = Japanese Industrial Standards

LB = Luria-Bertani

Menadione = 2-methylnaphthalene-1,4-dione

n = number of measurements

ncCTP = non-continuous CTP

OD = optical density

P25 = AEROXIDE® P 25

PBS = phosphate buffered saline

PI = propidium iodide
PYE = peptone-yeast extract
ROS = reactive oxygen species
Saline = physiological saline solution, i.e., 0.9% NaCl
SCV = small colony variants
SD = standard deviation
SEM = scanning electron micrographs
SYBR Safe = SYBR[®] Safe DNA Gel Stain
TEOS = tetraethoxysilane
TG = thermogravimetric
TO = thiazole orange
TOC = total organic carbon
TPA = terephthalic acid
UV = ultraviolet light
UVA or UVC = ultraviolet A or C light
VBNC = viable but nonculturable
Vis = visible light
XPS = X-ray photoelectron spectroscopy
XTT = 2,3-Bis(2-methoxy-4-nitro-5-sulfophenyl)-2H-tetrazolium-5-carboxanilide
WHO = World Health Organization

1 Introduction

Advanced oxidations processes (AOP), by exploiting high reactivity of hydroxyl radical (OH•), are effective in destruction of persistent chemicals that are difficult to remove by other methods, such as ozonation alone (Andreozzi et al. 1999; World Health Organization (WHO) 2011). AOP include photolysis (ultraviolet (UV) or vacuum-UV), hydrogen peroxide (H₂O₂)-based techniques, ozone (O₃)-based techniques and heterogeneous photocatalysis (Andreozzi et al. 1999; Pera-Titus et al. 2004; Melemi et al. 2009). Paleologou et al. (2007) compared different AOP with other techniques for water disinfection and the following efficiency order was proposed: UVA/TiO₂/H₂O₂ > UVA/TiO₂ > UVA/H₂O₂ > UVA. TiO₂ photocatalysis has been investigated very intensively during the last few decades due to its ability to effectively degrade biotic and abiotic contaminants of water, air and surfaces, being cheap and easy to use (Mills and Lee 2002; Carp et al. 2004; Fujishima et al. 2008). Many studies were performed with TiO₂ suspensions, as photocatalytic reaction occurs at the liquid-solid interface. Therefore, the overall rate is expected to be lower for corresponding immobilized photocatalysts as only a part of the photocatalyst is in contact with the reactant (Cernigoj et al. 2006), e.g., microorganism. However, methods with the immobilized photocatalyst are more convenient and environmentally friendly mostly because they do not require any post-treatment for the removal of the suspended material, and because the leakage of photoactive material in nanoparticle size to the environment is reduced. Use of a support also helps to prevent coagulation of TiO₂ powder as a consequence of interaction between TiO₂ nanoparticles, pollutants and their intermediates, which could lead to reduced TiO₂ surface area and activity (Li Puma et al. 2008).

Simple and very common route for preparing photocatalytic films is using traditional sol-gel method with photocatalyst material being well dispersed in the appropriate solvent, followed by the deposition (e.g., dip-coating or spin-coating) of stable colloidal solution onto an inert substrate, evaporation of a solvent and thermal annealing process (Mills et al. 2003a; Grinis et al. 2008). The prepared sol-gel samples have high photocatalytic activity, which could be manipulated by thickness of the coating, surface area (porous and rough materials), doping and crystallinity (Carp et al. 2004; Fujishima et al. 2008; Fresno et al. 2014). However, the sol-gel films, especially the multilayer films, generally tend to crack, are fragile and optically opaque, on the other hand industrial Chemical Vapor Deposition (CVD) produced films

(including glass products Pilkington Activ™ Self-Cleaning glass) are mechanically more robust and optically clear, but have 4-8 fold lower quantum yield than sol-gel films (Mills et al. 2003a).

Nowadays the spread of infectious diseases is greatly facilitated due to the increased mobility of people and products, rise of population and megacities with severe health care deficiencies, environmental degradation, increase of drug-resistant microbes and slow development of new antibiotics (Gannon 2000; Shlaes et al. 2013). An association was also found between health problems and indoor bioaerosols (Pal et al. 2008; Chen et al. 2010). Additionally, in certain places, like medical facilities or pharmaceutical industry, regular and effective disinfection is even more required. Conventional method of manual surface disinfection with wiping is not long-term effective, cannot be standardized, is time- and staff-intensive and may have non-target residual activity. Aggressive antimicrobial chemicals are also rather unfriendly to humans and the environment (in Kuhn et al. 2003a; Cushnie et al. 2010). Removal of potentially harmful microorganisms is required also in the preparation of drinking water (McCullagh et al. 2007; WHO 2011) and in food industry: in growing vegetables (Muszkat et al. 2005), breeding animals and in the storage (Chawengkijwanich and Hayata 2008) and processing (Cushnie et al. 2010) of food. Disinfection with the UVC light is usually not satisfactory, as the depth of penetration is not adequate - any shadow decreases the microorganisms' inactivation, microorganisms could reactivate, and it presents potential occupational risks (Kuhn et al. 2003a). Chlorination and ozonation are problematic due to the formation of disinfection by-products and were observed not to be always effective in removal of pathogens (WHO 2011). Additionally, the widespread use of UVC light or chemical treatments can result in the bacterial resistance (Chollet et al. 2009). Waterborne infectious diseases, transmission of infections by air or by contact and infections of medical devices could be reduced also by antimicrobial coatings (Tiller 2008; Cushnie et al. 2009). Thus, antimicrobial photocatalytic materials represent one of the attractive options required today to cope with these issues.

Antimicrobial activity of the photocatalysts is most frequently evaluated through the determination of the colony forming units (CFU). This method is, however, very time-demanding, results could be obtained only in retrospects and might not to be sensitive enough to detect activity of the thin photocatalytic films. Limitations arise also with the microbial strains tending to clump or having a slow growth such as mycobacteria (Elguezabal et al.

2011). Besides that, microorganisms could be in different physiological states with different antimicrobial susceptibility and pathogenicity, which is not always evident from the number of colonies growing on nutrient plates (Oliver 2005; Proctor et al. 2006). Colony count is therefore not very useful to distinguish small differences among samples, which are essential in the functional characterization of the thin photocatalytic films with moderate activity. Therefore a need for the introduction of more effective methods for the evaluation of the antimicrobial activity of immobilized photocatalysts was indicated and eventually satisfied in this study.

2 Photocatalysis and TiO₂ photocatalyst

2.1 General aspects about semiconductor photocatalysis

Photocatalysis is generally thought as the catalysis of the photochemical reaction at a solid surface, usually a semiconductor with TiO₂ is the most widely used photocatalyst due to its superior characteristics as being chemically and biologically inert, very photoactive in its nanostructured, mainly anatase form, abundant in nature, cheap and easy to manipulate (Mills and Lee 2002; Carp et al. 2004). TiO₂ is also commercially available at various crystalline forms and particle sizes. Photocatalytic activity of TiO₂ is the result of an interplay between a number of parameters, e.g., phase composition, electronic structure, particle size, exposed surface area, surface hydroxyl group density, surface acidity, number and nature of trap sites (both in the lattice and at surface), adsorption/desorption characteristics, degree of aggregation, mobility of charge carriers, presence of impurities, amount and kind of defects, adsorption of molecules from gas or aqueous phase, lateral interactions between adsorbed species, nature of solvent, etc. (Carp et al. 2004; Bahnemann et al. 2010). The plurality of variables driving the nature of the photocatalytic activity presents a challenge when trying to understand the kinetics and mechanisms underlying photocatalytic process (Bahnemann et al. 2010), although photocatalytic processes have become an extremely well researched field in the past 20 years due to the practical interest in the air and water remediation (loaded with low concentration of toxic organic pollutants) (Li Puma et al. 2008 and reference therein), and self-cleaning/sterilizing surfaces. Partial or complete oxidation of many toxic organic molecules, including pesticides, pharmaceuticals, surfactants and dyes, and also reduction of some toxic inorganic ions can be achieved with photocatalysis (Mills et al. 2003a; Carp et al. 2004). There is also an effort to use photocatalysis for light-assisted production of hydrogen (Fujishima et al. 2008). The fundamental aspects of photocatalysis are still actively researched and have recently become quite well understood. The mechanisms by which many types of organic compounds are completely decomposed to carbon dioxide and water, for example, have been delineated (Fujishima et al. 2008).

2.2 Immobilized TiO₂

TiO₂ was (and is often still) considered as non-harmful for humans and environment (Carp et al. 2004; Malato et al. 2009; Nakata and Fujishima 2012). On the other hand, there are evidences today that TiO₂ nanoparticles could be toxic and phototoxic for aquatic organisms

(Federici et al. 2007; Battin et al. 2009; Xiong et al. 2011; Miller et al. 2012), terrestrial invertebrates (Valant et al. 2012; Wu et al. 2012), plants (Ghosh et al. 2010) and human cells (Vamanu et al. 2008; Li et al. 2008; Ghosh et al. 2010; Petkovic et al. 2011). International Agency for Research on Cancer (IARC) also classified TiO₂ as possibly carcinogenic to humans and carcinogenic for experimental animals (Group 2B) (IARC 2010). However, unintended environmental impacts could be prevented with immobilization and appropriate production and disposal of TiO₂ nanoparticles. For water treatment applications it is also simpler if photocatalytic material is immobilized (Blake 2001; Grieken et al. 2010), and most of the work on air treatment has been performed with immobilized photocatalysts (Blake 2001). Plenty of literature is focused on the development of different antimicrobial photocatalytic coatings. However, requirements for a good photocatalytic disinfection coating are similar for various applications. Desired photocatalytic coatings have to be (i) photocatalytically active, with long term activity (ii), well adhered, (iii) mechanically stable, and (iv) have to inactivate microorganisms under sunlight or indoor light (Mills et al. 2003a; Mills et al. 2003b; Paz 2010). Self-cleaning films should additionally be transparent to retain substrate appearance, but it is acceptable that they are less active, which is usually the case of such thin films. To use efficiently near-UV (320-380 nm), coming from sunlight or UVA lamps they must be relatively thick, i.e., typically >1 μm (Mills et al. 2003b; Taranto et al. 2009). Coatings for water and air disinfection could be opaque, allowing them to be thicker than self-cleaning films and consequently more active.

2.3 Mechanisms of the photocatalytic process

The photocatalytic reaction mechanisms are initiated by the absorption of the light with energy equal or greater than material band gap, which elevates the electron from valence band to the conduction band. Therefore electron/hole pairs are formed within the semiconductor material. In most cases charge carriers recombine, by radiative and thermal processes, either directly or indirectly through structural defects in the bulk or at the surface of the semiconductor and no chemical change occurs. However, if the charges are localized by trapping at the surface states their mean lifetime can be long enough to allow their transfer to adsorbed or surface chemical entities behaving as e⁻ donors or acceptors. In case the resulting radicals or radical-ions react or are transformed before back e⁻ transfer with semiconductor occurs, a photocatalytic redox reaction is initiated. Generation, trapping and recombination of conduction band electrons and valence band holes occur on the femto, pico

and nano time scales and interfacial surface reactions on the millisecond and second scales (reviewed in Bahnemann et al. 2010). The ratio of the chemical changes to the unproductive charge recombination determines the overall quantum yield (Pichat et al. 2000). A fact that was early recognized about photocatalytic reactions was that the quantum yields are low (Bahnemann et al. 2010). During the photocatalytic processes there are at least two reactions occurring simultaneously, the first involving oxidation, from photogenerated holes, and the second involving reduction, from photogenerated electrons. However, there are plenty of possible photochemical, chemical and electrochemical reactions that can occur on the photocatalyst surface. Some changes involving the surface and bulk structure and even decomposition of the photocatalyst, could lead to the inactivation of the photocatalyst (Fujishima et al. 2008). For TiO₂, in the case of humid and aerated environment, oxygen (O₂) is considered to be the e⁻ acceptor and is transformed into superoxide ion (O₂^{•-}). This reaction prevents e⁻/h⁺ recombination, in the absence of other e⁻ acceptors. The e⁻ donors are (in the absence of other compounds) surface adsorbed water (H₂O) and hydroxyl ions (OH⁻), which are transformed to hydroxyl radicals (OH[•]). Following transformations other reactive oxygen species (ROS) can be produced, including hydrogen peroxide (H₂O₂) (Benabbou et al. 2007). Although, for example, H₂O₂ acts also on a long distance, it is assumed that degradation reactions take place mainly at the interface between the titania particles and the fluid phase, i.e., on the surface of the NPs, where adsorption plays a critical role (Bahnemann et al. 2010). This may be connected in a large extent to the very reactive OH[•], which are produced at the source of the photocatalyst action, presumably in high amounts. On the other hand, some authors argue that photocatalytic reactions can also occur at distances remote (tens of micrometers) from the illuminated surface (in Fujishima et al. 2008).

2.4 Enhanced photocatalytic activity

Different modifications in terms of structure, crystallinity and morphology have been introduced to improve TiO₂ performance (Carp et al. 2004; Fujishima et al. 2008; Fresno et al. 2014). Rutile-anatase mixed-phases show very good photocatalytic activity, in TiO₂ AEROXIDE[®] TiO₂ P 25 (P25) for example, where also higher wavelengths are actinic for the rutile phase (Hurum et al. 2003; Carp et al. 2004). According to Bickley et al. (1991) increased photocatalytic activity of this form of TiO₂ results from the enhancement in the magnitude of the space-charge potential, which is created by the contact between different phases and by the presence of localized electronic states from the amorphous phase. Both of

them slow down electron-hole recombination, which is the main route by which the absorbed photonic energy is dissipated. Hurum et al. (2003) proposed rutile-anatase nanoclusters in P25, with transition points allowing rapid electron transfer from rutile to anatase. According to Hurum et al. (2003), rutile absorbs visible light photons that are further stabilized in lower energy anatase lattice trapping sites. Diffuse reflectance spectrum of P25 has also been observed to be closer to pure rutile than to the 80/20 anatase/rutile mixture of P25 (Bickley et al. 1991). On the other hand, Datye et al. (1995) and Ohtani et al. (2010) studies of P25 suggested independent behavior of anatase, rutile and amorphous particles of P25, with no interactions between different phases. Addition of pure anatase, with a large (specific) surface area, e.g. PC500, to rutile/anatase mixture of crystallites P25 with medium surface area was also suggested to be beneficial for some applications (Arslan et al. 2000; Pizzaro et al. 2005; Bui et al. 2008). Photocatalysis can also be enhanced by the preparation of TiO₂ composites with substances that have narrower band gap, e.g. by dye sensitization, or by non-metal doping (e.g. N, C, S) that improves response to visible light (Vis). Substitutional doping of N (for O) in the anatase TiO₂ crystals, followed by the band gap narrowing was proposed by Asahi et al. (2001) as the most effective among C, N, F, P, or S replacements. Differently, Di Valentin et al. (2005) suggested formation of localized states in the band gap of TiO₂ by N atoms; with substitutional nitrogen states just above the valence band and interstitial nitrogen states higher in the gap. Excitations from these isolated states to the conduction band may account for the absorption edge shift toward lower energies (visible region). They also proposed easier formation of oxygen vacancies in N-doped TiO₂ (Di Valentin et al. 2005). Lee et al. (2009) suggested better efficiency of photocatalysis through interstitial N (NO_x)-doping states rather than substitutional N-doping states, probably due to the variation in the number and location of the impurity levels (active recombination sites) in the energy band gap. According to Wu et al. (2013), band gap narrowing is limited to heavy (≥ 8.3 at.%) nitrogen doping, while for light nitrogen doping formation of N-isolated states is expected, substitutional rather than interstitial. Furthermore, photocatalytic activity can be increased by deposition of transition metals on the titanium dioxide surface, such as silver or copper that provides additional antimicrobial effect and serves as electron scavengers to reduce recombination, and by applying electrical potential or additional oxidants (Blake 2001; He et al. 2005; Zaleska 2008). Other semiconductors tested for photocatalytic activity have been in general found less active than titanium dioxide, and anatase is the most active among the three common crystalline forms of titania (anatase, brookite and rutile) (Blake 2001; Hermann 2005; Blanco-Galvez et al. 2007). Photocatalytic rate of disinfection is affected also

by the amount of catalyst loaded on the substrate (Lee et al. 2004; Alrousan et al. 2009). SiO₂ presence was also shown to influence photocatalytic performance of TiO₂ coatings (Cheng et al. 1995; Guan 2005; Hu et al. 2012). And worth to mention, in contrary to small organic pollutants, meso or micro porous photocatalytic films are not advantageous for microorganism inactivation due to the size exclusion (Dunlop et al. 2008; Alrousan et al. 2009).

2.5 Photocatalytic disinfection

2.5.1 Antimicrobial effect of photocatalytic films

Photo-oxidative processes that produce ROS can damage any cell macromolecule (Boelsterli 2007). Therefore, photocatalytic coatings are expected to have also antimicrobial effects, as was shown for the first time by Matsunaga et al. in 1985. Bactericidal effect of natural sunlight was already described more than a century ago (Downes and Blunt 1877). However, total disinfection by solar, UVA or even UVC illumination is not always possible and the microorganisms can recover, if inactivation is not complete (Goswami et al. 1997; Lee et al. 2004; Sichel et al. 2007; Gomes et al. 2009; Rincon and Pulgarin 2004a; Quek and Ho 2008). The addition of nanostructured (photoactive) TiO₂ enhances efficiency of solar, UVA and UVC light and prevents recontamination (Goswami et al. 1997; Rincon and Pulgarin 2004a; Lee et al. 2004; Shang et al. 2009). In addition to loss of viability, UVA-illuminated TiO₂ films are also capable of microbial detoxification and cell degradation (Sunada et al. 1998; Jacoby et al. 1998).

2.5.2 Mechanism of photocatalytic disinfection

Microorganisms can be completely photocatalytically degraded (mineralized) to carbon dioxide, water and mineral acids (Dunlop et al. 2008), including microbial toxins (Sunada et al. 1998 and 2003), mostly due to the action of hydroxyl radicals (OH•) (Rincon and Pulgarin 2003; Cho et al. 2004). Extremely reactive hydroxyl radical (OH•) (oxidizing potential = 2.80 V, exceeded only by fluorine) with estimated lifetime of 10⁻⁹ s reacts with any biological molecule of microorganism in its immediate vicinity and there is no known biological scavenger of OH• (Burton and Jauniaux 2011). However, total decomposition of cells usually does not occur (Hara-Kudo et al. 2006; Baram et al. 2011). Deactivation of *Escherichia coli* (*E. coli*) as a function of light intensity has a similar kinetic shape as the degradation of

organic compounds, probably because some photochemical mechanisms are common for both processes (Rincon and Pulgarin 2003). However, when comparing photocatalyst activity toward simple molecules versus organisms, some differences can be expected (Benabbou et al. 2007). On photocatalytic self-disinfecting surfaces, most organisms will be in contact with the photocatalyst, especially at low cell densities, and therefore in contact with $\text{OH}\cdot$ (Ditta et al. 2008). Due to its indiscriminative activity it is not very likely that microbes will develop resistance toward TiO_2 disinfection (Chollet et al. 2009). Reduction of dissolved oxygen generates additional reactive oxygen species including superoxide radical anion ($\text{O}_2^{\cdot-}$), hydroperoxyl radical ($\text{HO}_2\cdot$) and hydrogen peroxide (H_2O_2). Formed by $1e^-$ -transfer to O_2 , charged $\text{O}_2^{\cdot-}$ is membrane impermeable (Burton and Jauniaux 2011), at least in the initial phase of a photocatalytic reaction. Adsorbed oxygen gets reduced also by $2e^-$ -transfer to H_2O_2 , which is also formed by disproportionation reaction of $\text{O}_2^{\cdot-}$. $\text{O}_2^{\cdot-}$ reduction to H_2O_2 could also be performed by microbial intracellular or extracellular superoxide dismutase (SOD) (Gerlach et al. 1998). H_2O_2 acts in degradation pathway as electron acceptor or could be a direct source of hydroxyl radicals after a homolytical scission or in Fenton reactions performed by microorganisms (Carp et al. 2004; Fujishima et al. 2008; Burton and Jauniaux 2011). H_2O_2 could be detoxified to water by microbial catalase and glutathione peroxidase. $\text{O}_2^{\cdot-}$ could be oxidised to the singlet oxygen ($^1\text{O}_2$), a strong oxidant (Carp et al. 2004; Fujishima et al. 2008; Burton and Jauniaux 2011), which has been suggested to be responsible for photocatalytic disinfection under Vis using N- and S-doped catalyst (Rengifo-Herrera et al. 2009). Neutral species H_2O_2 , $\text{HO}_2\cdot$ and $^1\text{O}_2$ are also able to diffuse and act farther away from the source of their production (Tatsuma et al. 2001; Naito et al. 2006).

Different studies suggested that the cell wall is the primary site of ROS attack, causing changes in the membrane integrity, lipid peroxidation and inhibition of cellular respiration. This is followed by oxidative attack on internal cellular components, which eventually leads to the cell death (Maness et al. 1999; Dunlop et al. 2002; Gogniat et al. 2006). Under less stringent photocatalytic conditions initial lag phase is observed as a result of defense mechanisms that microorganisms activate against ROS. Lag phase progresses to logarithmic phase when ROS production and ROS-mediated damages overcome antioxidative and repair mechanisms of cells (Rengifo-Herrera et al. 2009). Intermittent illumination of a photocatalytic system was also shown to increase the time required for *E. coli* inactivation. Interruption of illumination presumably gives bacteria time to recover and thus improves its viability. However, there are also reports of increasing efficiency of intermittent illumination

over a continuous one. If the exposure is harmful enough for a microbial population, e.g., if it is long enough, its population decrease continues in the period post irradiation. However, in the last phase of photo-treatment, inactivation of microorganisms becomes extremely slow because only a few remaining active organisms in the irradiated solution compete for OH• with both, the inactivated microorganisms and metabolites released during the photo-process (overviewed in Rincon and Pulgarin 2003).

2.6 Methodologies for evaluation of antimicrobial efficiency of immobilized photocatalysts

Procedures for testing antimicrobial effects of photocatalytic coatings are diverse. They are tailored to optimally exploit mechanisms, kinetics and efficiency of different materials in certain environmental conditions, and against the target contaminations (examples in Sunada et al. 1998 and 2003; Dunlop et al. 2010; Cushnie et al. 2010). For practical reasons testing methods also reflect available instrumentation, material (e.g. microorganism species) and laboratory conditions (i.e. biosafety level) of particular research laboratory. Compliance with the standard water testing procedures in the case of photocatalytic coating for water disinfection (example in Grieken et al. 2010) and furthermore reliability, improved sensitivity and speed of testing could also contribute to the decision about the experimental methodology used. When deciding for experimental conditions, it is desired to identify and simulate appropriate parameters (i.e. temperature, exposure time, irradiation, humidity, oxygen pressure, media) that result in elimination of microorganisms from certain coating, or from certain media (water, air) and which represent or could be extrapolated to the real target environment of the final product. Recent implementation of some standard methods (Table 1) to the antimicrobial testing is very encouraging and can provide a good starting point when deciding for an optimal antimicrobial testing. Fast progress in research and development nevertheless requires a constant improvement and harmonisation of testing procedures, including the standard methods (Mills et al. 2012). In the next sections, some of the major testing parameters that can influence performance and outcome of an antimicrobial testing will be presented and discussed.

Table 1: List of existing and forthcoming ISO and JIS tests for the assessment of antimicrobial activity of photocatalytic coatings.

ISO 27447:2009 (Published)	Fine ceramics (advanced ceramics, advanced technical ceramics) -- Test method for antibacterial activity of semiconducting photocatalytic materials
ISO 13125:2013 (Published)	Fine ceramics (advanced ceramics, advanced technical ceramics) -- Test method for antifungal activity of semiconducting photocatalytic materials
ISO/NP 17721 (Under development)	Quantitative determination of antibacterial activity of ceramic surfaces -- Test methods for photocatalytic and non-photocatalytic ceramic tile surface
ISO/CD 18061 (Under development)	Fine ceramics (advanced ceramics, advanced technical ceramics) -- Determination of antiviral activity of semiconducting photocatalytic materials - - Test method using bacteriophage Q-beta
ISO/DIS 17094 (Under development)	Fine ceramics (advanced ceramics, advanced technical ceramics) -- Test method for antibacterial activity of semiconducting photocatalytic materials under indoor lighting environment
JIS R 1702:2012 (Valid)	Fine ceramics (advanced ceramics, advanced technical ceramics) -- Test method for antibacterial activity of photocatalytic products and efficacy
JIS R 1705:2008 (Valid)	Fine ceramics (advanced ceramics, advanced technical ceramics) -- Test method for antifungal activity of photocatalytic products under photoirradiation
JIS R 1705:2008/Amendment 1:2010 (Valid)	Fine ceramics (advanced ceramics, advanced technical ceramics) -- Test method for antifungal activity of photocatalytic products under photoirradiation (Amendment 1)
JIS R 1706:2013 (Valid)	Fine ceramics (advanced ceramics, advanced technical ceramics) -- Determination of antiviral activity of photocatalytic materials -- Test method using bacteriophage Q-beta
JIS R 1752:2013 (Valid)	Fine ceramics (advanced ceramics, advanced technical ceramics) -- Test method for antibacterial activity of photocatalytic products and efficacy under indoor lighting environment
JIS R 1756:2013 (Valid)	Fine ceramics (advanced ceramics, advanced technical ceramics) -- Determination of antiviral activity of photocatalytic materials under indoor lighting environment -- Test method using bacteriophage Q-beta

2.6.1 Testing procedures

2.6.1.1 Photocatalytic chambers and reactors for water disinfection

A proposed standard reactor system from International Organization for Standardization (ISO) ISO 27447:2009 (Table 1) for antibacterial testing of self-disinfecting films and textile is described in Mills et al. (2012). In the film adhesion method, a sterilized paper is placed at the bottom of the glass Petri dish and moisturized with sterile water. U-shaped glass rod is then placed on the top of moistened filter paper and this serves as a holder for photocatalytic films. In the glass adhesion method, intended for textile testing, photocatalytic film is replaced with a glass plate holding the test sample on top of it. In both cases, Petri dish is covered with a glass cover. UV light source is placed above the photocatalytic cell and light intensity could be modified by altering lamp position or may be attenuated by using a metal sheet perforated with holes (Mills et al. 2012). Similar systems have been used by some other groups (Sunada et al. 2003; Ditta et al. 2008; Kim et al. 2008; Cushnie et al. 2010). Illumination chamber used by Sunada et al. (2003) was air tight to prevent drying, which is unnecessary if the Petri dish is covered. Irradiation chamber must also be closed, to avoid exposure of researchers to the UV light (Figure 1).

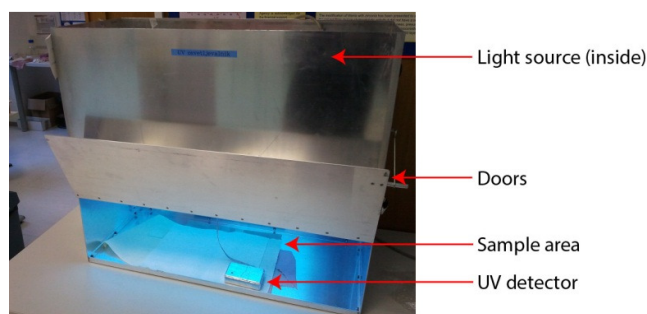


Figure 1: Example of a simple illumination chamber (from aluminium) for the assessment of antimicrobial effect of self-disinfecting coatings (Photo: M. Kete).

No ISO or Japanese Industrial Standards (JIS) standards exist describing reactor settings for the assessment of antimicrobial activity of photocatalytic materials for water (and air) disinfection (Table 1). However, wide variety of reactor designs and configurations have already been tested for water treatment (Bahnemann 2004; Blanco-Galvez et al. 2007;

McCullagh et al. 2011). Among them, by employing immobilized photocatalyst, tubular membrane reactor (Matsunaga et al. 1988), fiberglass mesh in sleeve system (Ireland et al. 1993), compound parabolic, parabolic and V-groove reactors (McLoughlin et al. 2004), stirred tank reactor (Lee et al. 2004; Alrousan et al. 2009), tube reactor with TiO₂ filter (Hara-Kudo et al. 2006), annular wall photoreactor (Grieken et al. 2010; Sordo et al. 2010; Marugan et al. 2010), bottles with photocatalyst inside and lamp above (Lonnen et al. 2005) or irradiated in solar collector (Gelover et al. 2006), glass bottles with TiO₂ film on internal lumen (Fisher et al. 2013), photoelectrocatalytic reactor (Dunlop et al. 2002; Dunlop et al. 2008; Cho et al. 2011), fixed bed reactor (Subrahmanyam et al. 2008; Sordo et al. 2010; Pablos et al. 2011), and thin-film fixed-bed reactor (TFFBR) (Belhacova et al. 1999; Khan et al. 2012). Huge variety of designs makes it difficult to compare all these studies. Existing ISO settings for determination of photocatalytic activity of surfaces in aqueous medium (Mills et al. 2012) or other relevant JIS standards, could possibly be adapted also for disinfection tests. Alternatively, testing of coatings, designed for water disinfection, together with an appropriate reference sample and by using settings for self-disinfecting material, could serve as an orientation for material performance in more complex reactor systems and enable comparison with other materials. This principle has already been partially applied in some water disinfection studies (Baram et al. 2007; Reddy et al. 2007; Xiong and Hu 2013). According to Paz (2009), model development could facilitate comparison between experiments that were carried out in reactors of different configurations.

2.6.1.2 Cleaning and sterilization of photocatalytic coatings

Cleaning and sterilization of photocatalytic coatings could be obtained by ultrasonification in disinfection media (e.g. 70% ethanol (EtOH) or methanol (MeOH)) (Ditta et al. 2008; Cai et al. 2013), by gently shaking in disinfection media (Ditta et al. 2008) or simply by wiping with EtOH soaked cotton (Kim et al. 2008). Ultrasonification produces more damage on photocatalysts than shaking (Ditta et al. 2008). In order to reuse photocatalysts after disinfection testing, Baram et al. (2011) immersed photocatalysts in solution of ethanolamine and DMF 1:1 (v/v) at 70 °C for 10 min, and after that rinsed them with deionized water. Dry sterilization was used by Sunada et al. (1998) – at 180 °C for 2 h and Muranyi et al. (2010), at 180 °C for 10 h. Despite its convenience, dry sterilization can not be used for some substrates, such as paper, textile or plastic, where autoclaving is more suitable. Although it could result in inactivation of photocatalytic films (Ditta et al. 2008), autoclaving was used

by Akhavan (2009) and Caballero et al. (2009) and is also the recommended method in ISO 27447:2009 (Table 1) (Mills et al. 2012). Ireland et al. (1993) disinfected reactor system prior to experiment with concentrated sodium hypochlorite for 24 h and flushed it with 20 reactor volumes of distilled water. A need for regeneration treatment of TiO₂ after several cycles of *E. coli* inactivation was noticed by Baram et al. (2011), although it is not expected to be required for all pollutants (Tasbihi et al. 2007; Baram et al. 2011). In contrary, Belhacova et al. (1999) preserved stability of photocatalytic layer in fixed bed reactor for many months under mild conditions with diluted neutral or acidic aqueous solution applied.

2.6.1.3 Preventing leaking of microbiological sample from self-disinfecting surfaces

According to ISO 27447:2009 (Table 1), an adhesive film or glass with a transparency greater than 85% for UV between 340 and 380 nm may cover the test sample (Mills et al. 2012), presumably to evenly spread bacterial sample throughout photocatalytic film and to prevent sample runoff from the photocatalyst. According to Kim et al. (2008) sample covering also facilitates attachment of microbial cells to the TiO₂ surface. Sample runoff from UV-induced superhydrophilic photocatalytic surface can be prevented also by placing a frame around examined surface (Sunada et al. 1998; Cushnie et al. 2010).

2.6.1.4 Removing microorganisms from materials and their storage between sampling and analysis

It is important to confirm that microorganisms are completely removed from photocatalytic surfaces prior to any further viability assessment in order to avoid overestimation of the photocatalytic effect. Microorganisms could be removed from immobilized photocatalysts by washing them with nutrient broth, e.g. by gently shaking or vortexing (Wong et al. 2006; Cao et al. 2009), or with water (Ditta et al. 2008; Cai et al. 2013). Bacteria in nutrient broth can be also simply aspirated from photocatalytic surface, without further washing (Li et al. 2013). Cushnie et al. (2010) pipetted bacteria exposed in distilled water into a microcentrifuge tube already consisting 1 mL of water. Remaining bacteria were then removed with moistened cotton swab tip, which was then immersed into bacterial suspension; solution was further vortexed (3 x 10 s) and prepared for detection. ISO standard procedure for photocatalyzing films instead requires samples to be placed in a Stomacher bag containing nutrient broth with two surfactants. Photocatalytic surfaces are then rubbed from outside to remove attached

bacteria (Mills et al. 2012). If the analysis is not performed immediately after sampling, e.g. if it is required that samples from different irradiation times are analyzed together, samples should be kept under protective conditions (i.e. media, temperature and oxygen pressure) in order to sustain bacterial viability but to prevent regenerative mechanisms.

2.6.2 Physicochemical parameters affecting antimicrobial efficiency of immobilized photocatalysts

2.6.2.1 Irradiation

Higher light intensity is expected to improve antimicrobial effect of light (Rincon and Pulgarin 2003; Lee et al. 2004; Chen et al. 2009b) and photocatalysis (Chen et al. 2009b; Marugan et al. 2010; Grieken et al. 2010; Khan et al. 2012a; Xiong and Hu 2013). In addition to higher direct photon attack on microorganisms (Xiong and Hu 2013), high light intensity results also in an increased ROS generation on the TiO₂ surface (Chen et al. 2010). In most photocatalytical experiments, optimal light power utilization is achieved only at lower light intensities (Ohko et al. 1997; Belhacova et al. 1999; Herrmann 1999; Chen et al. 2009b; Xiong and Hu 2013). However, in a electrophotocatalytic experiment performed by Dunlop et al. (2008), linear response between rate constant for *Clostridium perfringens* inactivation and high incident light intensity from ca. 70 to 200 W/m² of UVA was observed. Additionally, indoor natural light with low UVA part was not able to induce photoreaction for a fungal inhibition (Chen et al. 2009c). Low transparency, caused by turbidity, color or high pollutant concentration reduces the amount of light reaching TiO₂ surface, which leads to a reduction in inactivation rate and higher intensities of light required for the effective photocatalysis (Rincon and Pulgarin 2003; Hashimoto et al. 2005; Rodriguez et al. 2007). For the same UV dose, faster inactivation was obtained with high light intensities for a short time in comparison to low light intensities for a longer time (Xiong and Hu 2013). Lower incident radiation also results in longer initial delay in the inactivation profile (Marugan et al. 2010). Sterilization surely depends also on the light wavelength, with UVC being the most deleterious (Wegelin et al. 1994; Nhung et al. 2012; Pigeot-Remy et al. 2012). For the bacterial reduction in the air was suggested that UVA-photocatalysis is competitive with UVC photolysis (Sanchez et al. 2012). Intermittent solar light illumination resulted in the prolonged time required for *E. coli* inactivation (Rincon and Pulgarin 2003). Intermittent illumination is expected in part of the real applications, i.e., in the outdoor applications as

sunlight intensity varies with the time and in non-continuous reactor systems. However, controlled intermittent periodic illumination (possible with LEDs) could give higher photonic efficiencies and high energy savings (Chen and Elimelech 2007). Recently, the mostly used fluorescent mercury black light (UVA) and white light (visible) lamps have been replaced with LEDs in some photocatalytic disinfection experiments (Cheng et al. 2011; Nhung et al. 2012; Ye et al. 2012; Xiong and Hu 2013; Cai et al. 2013), LEDs have some advantages over the standard incandescent lamps, but there are also some drawbacks. In addition to freely available ultraviolet emission from the indoor daylights, outdoor sunny areas offer economical and practical opportunity for photocatalytic disinfection. Sunlight alone is able to inactivate microorganisms due to the synergistic effect of UV, Vis and IR part of solar spectrum (Wegelin et al. 1994; Rincon and Pulgarin 2004a). Sunlight could be also simulated by using solar lamps (Rincon and Pulgarin 2003; Gumy et al. 2006). However, it was suggested that UVA part of the solar spectrum is mainly responsible for disinfection, and that global solar energy is not a good parameter for evaluating the process efficiency (Sichel et al. 2007; Baram et al. 2011). Photocatalytically most active and therefore mostly used anatase crystalline phase of TiO₂ has a band gap of 3.2 eV, corresponding to absorption wavelength upper limit of 384 nm. To examine Vis-responding photocatalysts, the UV part has to be blocked, e.g. by UV-blocking window film, eliminating wavelengths below 400 nm (Fisher et al. 2013) or by using optical filter (Akhavan 2009), to eliminate effect of the UV part of the daylight (Figure 4b) or sunlight lamps.

Table 2: List of existing and forthcoming CEN, ISO and JIS standards about irradiation conditions and measurement of these conditions in photocatalytic tests.

FprCEN/TS 16599 (Under approval)	Photocatalysis - Irradiation conditions for testing photocatalytic properties of semiconducting materials and the measurement of these conditions
ISO 10677:2011 (Published)	Fine ceramics (advanced ceramics, advanced technical ceramics) -- Ultraviolet light source for testing semiconducting photocatalytic materials

Table 2 continues to the next page↓

ISO/FDIS 14605 (Under development)	Fine ceramics (advanced ceramics, advanced technical ceramics) -- Light source for testing semiconducting photocatalytic materials used under indoor lighting environment
JIS R 1709:2007 (Valid)	Light source for test of photocatalytic materials used under ultraviolet
JIS R 1750:2012 (Valid)	Fine ceramics -- Light source for testing semiconducting photocatalytic materials used under indoor lighting environment

Pre-irradiation of photocatalytic materials may increase efficiency of disinfection (Liu et al. 2007; Chen et al. 2009c), but not necessarily (Sawada et al. 2005), and there is no pre-irradiation step recommended in the ISO 27447. For photoinduced superhydrophilicity (PSH), which correlates with disinfection activity (Guan 2005; Liu et al. 2007), is known that it takes some time (usually days) in the dark after the irradiation that the surface returns to its original, more hydrophobic inactive form (Mills et al. 2003b) and that heat (e.g., dry sterilization) can improve back-transformation. Considering that photocatalytic systems are developed for different parts of the globe and for different seasons, having different irradiation conditions, it is understandable that irradiation conditions vary significantly among studies, making them difficult to compare (Dunlop et al. 2008). European Committee for Standardization (CEN), ISO and JIS standards dealing with irradiation in photocatalytic tests are listed in Table 2.

2.6.2.2 Temperature

Small temperature fluctuations only have a minor effect on photocatalytic reactions and temperatures in the range of 20-80 °C are optimal for photocatalysis (Fox and Dulay 1993; Hermann 2005), however, temperature is critical for microbial growth and pathogen resistance. Decay is usually faster at higher temperatures and may be further mediated by UV radiation. Photocatalytic studies including water disinfection (Herrera Melian et al. 2000; Dunlop et al. 2002; Lonnen et al. 2005; Marugan et al. 2010) and air purification (Vohra et al. 2006; Josset et al. 2007; Modesto et al. 2013) are mostly performed at ambient temperature. It was shown that microbial inactivation is enhanced at higher temperatures (Lee et al. 2004; Sawada et al. 2005), while lower temperatures reduce the antibacterial activity (Sawada et al. 2005; Foster et al. 2012). However, Cushnie et al. (2010) observed a satisfactory antibacterial

effect of photocatalytic film also at 10 °C, a working temperature for the food and drink industry. Inactivation of *Staphylococcus aureus* was even faster at lower than at ambient temperature (25 °C) and this was attributed to the inhibition of cold shock response by UV. Nevertheless, temperature dependence of microbial elimination is expected to vary among different microbial species and their physiological state, e.g., fungal spores being less sensitive to the temperature increase from 10 °C to 25 °C than vegetative bacterial cells (Sawada et al. 2005). In order to prevent temperature fluctuation during experimentation as a consequence of illumination and stirring, or to obtain lower temperatures in water cleaning systems, heat dissipation using cooling fans (Karunakaran et al. 2011) or circulating cooling water (Dunlop et al. 2002; Lee et al. 2004) can be applied.

2.6.2.3 pH

pH is an influential parameter for organism viability. A neutral pH near 7 is optimal for many biological processes. However, extreme pH environments are occurring in nature. Among microorganisms, cyanobacteria and many bacteria can not grow at low pH. Differently, some algae, fungi and archaea are extreme acidophiles (Rothschild 2002; Ray 2005). Most natural waters have pH between 6.0 and 8.5, although lower and higher values also occur (Chapman and Kimstach 1996). Experiments using different microorganisms showed that pH values in the range of 5-9 generally do not have a major effect on the antimicrobial efficiency of photocatalytic coatings (Alrousan et al. 2009; Baram et al. 2011; Khan et al. 2012). Some however reported enhanced inactivation of bacteria at lower pH, which has been attributed to increased strength of electrostatic forces between bacteria and photocatalyst and increased concentration of H₂O₂ (Baram et al. 2011; Schwegmann et al. 2013), but could also be related to the effect of suboptimal pH itself (Khan et al. 2012).

2.6.2.4 Oxygen presence

Oxygen presence is required for photocatalytic process as it acts as a strong electron acceptor of light-excited electrons, suppresses charge recombination and induces ROS formations, which in excess destroy biological systems, including microorganisms (Carp et al. 2004).

Oxygen alone is known to be at the same time required and beneficial, but also potentially damaging for biological systems (Burton and Jauniaux 2011). Oxygen fuels mitochondrial oxidative phosphorylation for maximal adenosine triphosphate (ATP) production in aerobic cells (Jones and Thompson 2009) and it is converted to different ROS, which could still be

required, but on the other hand could also be toxic for cells (Apel and Hirt 2004). Study of Khaengraeng and Reed (2005) showed greater resistance of aerobically grown facultative anaerobe *E. coli* over their anaerobically grown counterparts to the simulated sunlight and a direct relation between inactivation and oxygen content of the water during the illumination, with hypo-oxygenated treatment being less harmful. They suggested therefore that studies of bacteria exposed to UVA or sunlight must consider effect of oxygen at every stage of the procedure (Cho et al. 2004; Khaengraeng and Reed 2005). In photocatalytic water disinfection studies, air purging is mostly applied to provide oxygen and this has been proven to increase photo-killing (Liu and Yang 2003; Dunlop et al. 2008). Oxygen concentration is generally not measured in photocatalytic disinfection experiments. In addition to oxygen, presence of other electron acceptors, such as hydrogen peroxide, superoxide, singlet oxygen, peroxysulfate and peroxydisulfate, chlorite, chlorate, bromate, periodate, nitrous oxide, ozone or persulfate were observed to enhance photocatalysis (Ireland et al. 1993; Belhacova et al. 1999; Blake 2001; Rincon and Pulgarin 2004b). According to Blanco-Galvez et al. (2007), addition of electron acceptors also gives opportunity to extend the use of heterogenous photocatalysis to complicated waste waters.

2.6.2.5 Humidity

Humidity influences photocatalytic processes and prevention of desiccation is required by ISO 27447:2009 (Mills et al. 2012). A certain degree of humidity is necessary to maintain hydroxylation of photocatalysts and to prevent its blockage by partly oxidized products (Carp et al. 2004). Aerosolized microorganisms in air disinfection photocatalytic applications are much more likely exposed to low humidity levels than microorganisms tested on self-disinfecting coatings, which are usually studied caught in water droplets. In addition, different microorganism dependence on humidity level was observed in a conventional drop test as compared to air disinfection systems (Gotswami et al. 1997; Ko et al. 2000; Muranyi et al. 2010). In the drop test, the desiccation effect can be further reduced by making water base in the testing chamber and by covering the sample with a lid or film (Cushnie et al. 2010; Mills et al. 2012).

2.6.2.6 Composition of testing media

Composition of testing media greatly influences photocatalytic action in real systems and under experimental conditions. Organic and inorganic substances significantly slowed the

photocatalytic killing of *E. coli* performed in nutrient broth with total organic carbon (TOC) 34.2 mg/L (Baram et al. 2011). Photocatalysis is known to be retarded also in presence of small amounts of organic and inorganic molecules, which are present in tap water or added to stabilize proteins (e.g. albumin or mannitol) (Sunada et al. 2003; Rincon and Pulgarin 2004b; Baram et al. 2011). Inhibition is based on competition of organic and inorganic molecules for hydroxyl radicals, radical scavenging, poisoning of the catalyst, and absorption or diffraction of light by broth components (Lee et al. 2004; Rincon and Pulgarin 2004b; Alrousan et al. 2009), and by preventing close contact between test organism and catalyst, which is crucial for an efficient microbial inactivation (Foster et al. 2011). Degradation of organic matter also releases complex elements and compounds, like phosphorus and silica, and form low molecular weight compounds, which enhance microbial survival (Alrousan et al. 2009). Most inorganic compounds and ions present in real water samples and different testing media negatively influence photocatalytic antimicrobial action. It was reported that PO_4^{3-} , HCO_3^- , SO_4^{2-} , NO_3^- , Cl^- , K^+ , and Ca^{2+} decrease photocatalytic elimination of *E. coli* (Rincon and Pulgarin 2004b; Alrousan et al. 2009) as well as phage MS2 (Koizumi and Taya 2002), with almost no effect of Na^+ and Br^- ions. Hyper- or hypo-osmotic conditions of the testing medium represent an osmotic stress, which can enhance oxidative damage caused by photocatalysis (Blake et al. 1999). Based on the differences in the cell wall structure, fungi, algae, and gram-positive bacteria can withstand higher osmotic stress than most of the gram-negative bacteria (Blake et al. 1999; Cushnie et al. 2009; Grieken et al. 2010). However, in the study of Grieken et al. (2010), differences in the sensitivity of two bacterial species to osmotic stress in deionized water did not lead to different sensitivities to photocatalytic treatment. Moreover, there are reports that isotonic 0.15 M NaCl (physiological saline solution (saline)) can enhance photocatalytic disinfection (Ditta et al. 2008; Cushnie et al. 2009).

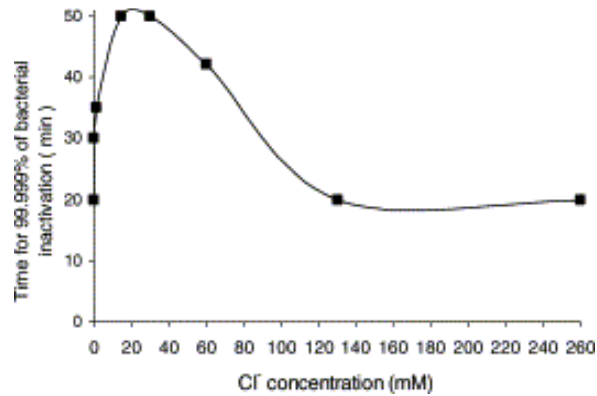


Figure 2: Influence of NaCl concentration on photocatalytic disinfection. Time required to reach 99.999% of *E. coli* inactivation by photocatalysis as a function of NaCl concentration between 0.02 and 260 mM. Initial bacterial density: 10^7 CFU/mL (0.25 g/L of TiO₂) (taken from Rincon and Pulgarin 2004b).

E. coli inactivation versus Cl⁻ conc. (0-260 mM) curve was measured by Rincon and Pulgarin (2004b) (Figure 2). In contrary, phosphate-buffered saline (0.1 M PO₄-P), a widely used biological buffer, strongly adsorbs onto the TiO₂ and decreases disinfection and for this reason it is not recommended as a testing medium (Belhacova et al. 1999; Rincon and Pulgarin 2004b; Gogniat et al. 2006). Although the addition of 0.1% (w/v) peptone or other nitrogenous substances could reduce microbial stress during the experimental procedure (Straka and Stokes 1956), organic compounds severely impede photocatalytic efficiency (Cushnie et al. 2009). Humic acid (major natural organic matter in water supplies) was observed to be the main inhibitor of photocatalytic disinfection in surface water (Alrousan et al. 2009; Marugan et al. 2010; Khan et al. 2012b). General findings about influence of salts and of organic molecules on photocatalysis obtained from studies in liquid media are helpful in designing disinfection studies in gas media. However, compounds causing enhancement or retardation of photocatalytic air disinfection systems are different (Paz 2009; Sanchez et al. 2012), and their involvement in air disinfection has not been yet studied systematically.

2.6.3 Microorganisms and culture conditions

Antimicrobial evaluation cannot be performed for each pathogen since it would be too demanding. The suggested practical approach by WHO (2011) in case of drinking water quality management is to derive targets for reference pathogens representing groups of pathogens (e.g., bacteria, archaea, algae, fungi, protozoa, and viruses (Pelczar 2013)) and this approach could also be applied for antibacterial activity assessment of immobilized

photocatalysts. Within microbial groups, biological differences are smaller. However, high difference in sensitivity to photocatalysis may exist inside the major groups of microorganisms, also among different strains of the same species (Sawada et al. 2005; Sichel et al. 2007; Baram et al. 2011). Using the same standard microorganism by different researchers is the approach that allows direct comparison of their results. However, if materials are developed for certain application, e.g., water disinfection, relevant water pathogens must be tested. Use of standard strains can overestimate potential activity against organisms likely to be encountered in “in use” situations (McCullagh et al. 2007; Dunlop et al. 2010; Foster et al. 2012). In summary, representative model microorganisms have to be decided, whose selection must consider not only (i) (diverse) susceptibility to photocatalytic and other antimicrobial treatments, (ii) incidence (prevalence) and severity of infections for certain application, but also (iii) convenience in handling of the microorganisms, i.e., by deciding for non-pathogenic and conventional strain. Last condition is especially important in the initial evaluations of antimicrobial photocatalysts that are preferably performed at low cost with basic microbiological equipment.

2.6.3.1 *The target microorganisms*

Bacteria are generally the most vulnerable microorganisms for disinfection (Fujioka and Yoneyama 2002; Heaselgrave et al. 2006). The most important water contaminants are: *Vibrio cholerae*, *Campylobacter*, *E. coli* O157, *Shigella* and *Salmonella* (WHO 2011). *E. coli* is a standard laboratory microorganism. The most commonly used non-pathogenic strain K12 is also simple and inexpensive to work with. In addition, *E. coli* is a common inhabitant of human and animal intestine and is therefore a suitable indicator of drinking and bathing water contamination with faecal coliform bacteria (together with streptococci) (Directive 2006/7/EC; Directive 98/83/EC; WHO 2011). Namely, the greatest microbial risks are associated with ingestion of water that is contaminated with faeces from humans or animals (including birds) (WHO 2011). Moreover, *E. coli* serotype O157:H7 is also an emerging cause of foodborne or waterborne diseases (EPA; Gannon 2000), which all together makes *E. coli* a relevant testing microorganisms, especially in water disinfection studies. Consequently, the most studied microorganism in antimicrobial photocatalytic experiments is gram-negative bacteria *Escherichia coli* (reviewed in McCullagh et al. 2007 and Foster et al. 2011). Human pathogen *Staphylococcus aureus* is another frequently used (gram-positive) bacteria (Wong et al. 2006; Cushnie et al. 2009; Cushnie et al. 2010; Dunlop et al. 2010), different

bacteriophages serve as model viral organisms (Belhacova et al. 1999; Koizumi and Taya 2002; Ditta et al. 2008; Zheng et al. 2013), mold fungi *Aspergillus niger* was used for testing self-cleaning and air disinfection materials (Vohra et al. 2006; Chen et al. 2009a), agricultural pathogens are used for testing self-cleaning and water disinfection materials (Sawada et al. 2005; Sichel et al. 2007; Cheng et al. 2011; Khan et al. 2012; Xiong and Hu 2013), while different protozoa or algae species are used for assessment of water treatment photocatalysts (Lee et al. 2004; Ochiai et al. 2010) and self-cleaning surfaces (Graziani et al. 2013). Regarding UVC light susceptibility a wide divergence among different *E. coli* strains was found (Sommer et al. 2000). In addition, environmental microbial strains were observed to be less sensitive to UVA and UVA/TiO₂ compared to lab-strains (Hijnen et al. 2006; Dunlop et al. 2010). To assess the effectiveness of virus removal in water disinfection studies, coliphages, *Bacteroides fragilis* phages and enteric viruses may be used as indicators (Fujioka and Yoneyama 2002; WHO 2011). However, regarding drinking water monitoring, rotaviruses, enteroviruses and noroviruses have been identified as potential reference pathogens. Water contaminated by human waste could contain high amount of all three species. However, only for enteroviruses a routine culture-based analysis for measuring infective particles is available. Since they are smaller than other pathogens, viruses are also more difficult to remove (WHO 2011). Regarding parasites, *Giardia* infections are generally more common than *Cryptosporidium*. However, *Cryptosporidium* is smaller and hence more difficult to remove by physical processes, it is also more resistant to oxidizing disinfectants, and there is also some evidence that it survives longer in aquatic environments (WHO 2011). For drinking water *Clostridium perfringens* (including spores) content is also monitored for water originates from or influenced by surface water, to measure the effectiveness of the protozoa removal (WHO 2011; Directive 98/83/EC). It is used as an indicator of virus and protozoa absence (WHO 2011). For water offered for sale in bottles or containers, also the presence of *Pseudomonas aeruginosa* and enumeration of culturable microorganisms at 22 °C and 37 °C is examined. Additional microorganisms may be monitored, such as bacteriophages or bacterial spores, if potential danger to human health is detected and in verification of water safety plan (WSP), e.g., in evaluation of new water disinfection technology using photocatalysis (Directive 98/83/EC; WHO 2011). Under specific circumstances, *Cryptosporidium*, *Giardia lamblia*, *Legionella*, guinea worm (*Dracunculus medinensis*), toxic cyanobacteria and enteric viruses may be of public health importance (WHO 2011; EPA). For bathing waters, monitoring of cyanobacteria (source of cyanotoxins), macro algae and marine phytoplankton is recommended when water profile indicates that

there is a high potential for their proliferation (Directive 2006/7/EC). In 2000, infectious diseases were a leading cause of death worldwide and the third leading cause of death in the USA (Zhang and Powers 2012). Acute lower respiratory infectious diseases, including pneumonia and influenza, diarrheal diseases and measles, appear to have peaked at high incidence level. More lethal variants of influenza are also posing a threat (Gannon 2000). Multi-drug resistant bacteria infecting the hospitals and being therefore relevant for photocatalytic studies are: *Staphylococcus aureus*, *Enterococcus faecium*, *Klebsiella pneumoniae*, *Acinetobacter baumannii*, *Pseudomonas aeruginosa* and *Enterobacter spp.* Antibiotic-resistant bacteria are increasingly present and have raised concern also in aquatic environments (Xiong and Hu 2013). Overall, microorganisms causing household contaminations, like molds in kitchens and bathrooms, fungi growing on house walls, or biofilms on ship hulls, are also very relevant (Tiller 2008), as well as food-poisoning microorganisms; such are *Staphylococcus aureus*, *Clostridium perfringens*, and *Bacillus cereus* (Madigan et al. 2003). Currently used antibiotics and other chemical disinfectants have adverse effect on the environment. In addition, pathogens developed resistance towards certain antibiotics (Khan et al. 2012a). Antibiotic-resistant microbes have already been tested with photocatalytic disinfection, and it was suggested that antibiotic multi-resistance does not confer increased tolerance to UVA or UVA/TiO₂ exposure (Sousa et al. 2013; Xiong and Hu 2013).

2.6.3.2 Microorganism form

Resistance is usually related also to the cellular or growth characteristics of microbes. It has been shown that the survival rate for spores is significantly higher than for vegetative cells, which is related to structural differences (Sawada et al. 2005; Sichel et al. 2007). Enhanced photocatalytic activity by external electrical bias was observed to significantly increase the rate of photocatalytic disinfection of *Clostridium perfringens* spores (Dunlop et al. 2008). Another important parameter is microbial growth pattern. Planktonic microorganisms are more sensitive to photocatalytic disinfection than microbial communities grown in biofilms (Polo et al. 2011) and bacteria from the exponential growth phase are generally more sensitive than bacteria from the stationary growth phase (Rincon and Pulgarin 2004c; Guillard et al. 2008). Planktonic *E. coli* was mostly tested on photocatalytic coatings. However, 60-80% of human microbial infections are caused by bacteria growing as a biofilm, e.g., highly virulent methicillin-resistant *Staphylococcus aureus* (MRSA) is capable of

biofilm formation with a 10-1000-fold increase in antibiotic resistance. *Staphylococcus aureus* and *Staphylococcus epidermis* infections originate from biofilms on implantable medical devices and are common causes of infective endocarditis. Biofilms have also been identified on various other medical devices (Zhang and Powers 2012). Biofilms may be formed also in water distribution systems, which are colonized with amoebae, heterotrophic bacterial and fungal species, including strains of *Citrobacter*, *Enterobacter* and *Klebsiella*. However, most microorganisms in the drinking water biofilms don't have adverse health effects in the general population, with exceptions of *Legionella*, which could colonize water systems in buildings and severely affect immunocompromised people (WHO 2011). Microorganisms in water bodies (bacteria, viruses, protozoa) are also typically protected by the attachment to particulates; although disinfection is usually performed after the removal of particulate matter (WHO 2011).

2.6.3.3 Microorganism density

According to WHO (2011) there is up to 1×10^7 /mL *E. coli* and *Klebsiella*, 1000/mL *Camylobacter spp.*, 1×10^5 /mL *Vibrio cholerae*, 1/mL Enteroviruses, 5/mL Rotaviruses, 10/mL *Cryptosporidium*, 10/mL *Giardia intestinalis* in untreated wastewaters or raw waters. Conventional wastewater treatment commonly reduces microbial densities by one or two orders of magnitude before the wastewater is discharged into the surface water (WHO 2011). Regarding management of bathing water quality in European Union (EU), inland waters of excellent quality or good quality must contain less than 2 or 4 CFU of intestinal enterococci per mL and less than 5 or 10 CFU of *E. coli* per mL. Coastal waters and transitional waters contain even lesser, 1 or 2 enterococci and 2.5 or 5 CFU per mL, for excellent or good quality bathing waters (Directive 2006/7/EC). Regarding EU directive on the quality of water intended for human consumption, this water must be free of any microorganisms or parasites, following single-hit principle, i.e., that even a single pathogen is enough to cause infection and disease. There must be no *E. coli* and enterococci present. For the bottled water *Pseudomonas aeruginosa* count must be 0 and colony count at 22 °C and 37 °C must not exceed 100 and 20 CFU/mL, respectively (Directive 98/83/EC, WHO 2011). Although it was expected that high initial density of microorganisms could negatively affect photocatalysis, the influence of microorganism loading on disinfection rate still remains ambiguous (Belhacova et al. 1999; Grieken et al. 2010). It has been also shown that even high experimental bacterial density of 10^6 - 10^7 CFU/mL (3.7 mg/L) represent only half of the TOC

found in the surface waters (Alrousan et al. 2009; Baram et al. 2011), suggesting low impact of microorganism density on photocatalytic disinfection rate and on the efficiency of photocatalysis in general. However, inhibition of photocatalysis with high bacterial density (10^6 and 10^7 per object) loaded on self-disinfection coating was observed and explained by the limited light transfer to the photocatalytic surface and the reduced amount of cells having direct contact with the surface (Muranyi et al. 2010).

2.6.4 Detection of antimicrobial effects of photocatalysis

Affordable instrumentations, including maintenance costs, quick and immediate analysis to follow progression of reactions in real time, and, finally, well-developed analytical protocols with high standardization potential are important parameters for an effective detection of antimicrobial effects of photocatalytic coatings. There are some powerful analytical techniques that gave important contribution to the understanding of the antimicrobial process of photocatalysis, but currently they don't fulfill criteria of being fast, reliable and affordable detection techniques for the evaluation of antimicrobial effect of photocatalytic coatings. Advanced microscopy and spectroscopy techniques that fit into this frame are scanning electron microscopy (SEM), transmission electron microscopy (TEM) and attenuated total reflection Fourier transform infrared spectroscopy (ATR-FTIR) together with atomic force microscopy (AFM). SEM was used to indicate visible cell surface damages (Kim et al. 2013), while ATR-FTIR revealed formation of peroxidation products on *E. coli* cell membranes during TiO₂ photocatalysis. Time-dependent ATR-FTIR experiments also provided the evidence that changes in *E. coli* cell wall membranes are precursors leading to cell lysis that was shown by AFM. TEM on the other hand indicated interactions of TiO₂ aggregates with the bacterial surface (Nadtochenko et al. 2005). Other detection methods, which better satisfy criteria of being rapid and effective evaluation techniques, are overviewed in the following subchapters.

2.6.4.1 Culture methods

The classical method for determining the viability in microbial samples is plate count technique assessing bacterial growth on a nutrient agar after a period of incubation (Villarino et al. 2000; Davey 2011). Spread plate or pour plate variants of the methods are also mostly used also for the detection of antimicrobial effect of photocatalysis. The method is based on the numeration of the colonies formed after cultivation of the tested sample or its dilutions,

presented as number of CFU. Results from culture method techniques, such as broth cultures or previously mentioned agar-based bacterial media and cell cultures for viruses and phages, present living and culturable microorganisms, in which reduction is normally expressed in terms of \log_{10} reduction (WHO 2011). It should be noted that plate count detects only a fraction of microorganisms, which are able to grow and form colonies in a given medium and in a selected incubation period. Numerous pathogenic bacteria can enter the viable but nonculturable (VBNC) state that constitutes an important reservoir of pathogens in the environment (Oliver 2010). Different stressors, including oxidative stress, could render microorganisms non-culturable in standard laboratory media for some period, but they are still viable and can recover with time (Nowakowska and Oliver 2013). Also photocatalytically injured microorganisms in VBNC could be missed with culture-based methods, e.g. plate count method, leading to the overestimation of the photocatalytic efficiency (Kaur et al. 2013). H_2O_2 has been indeed recognised as an inducer of the VBNC state (Mizunoe et al. 1999). For improved detection of small colony variants (SCV), Khaengraeng and Reed (2005) and Khan et al. (2012b) used agar medium supplemented with the peroxide scavenger or prereduced medium, while Pal et al. (2008) and Cushnie et al. (2010) followed regrowth by repeating counting of colonies after longer incubation times in addition to usual the 20 or 24 h. On the other hand, sublethal injuries are not considered in enumeration results, what is especially important when evaluating antimicrobial effect of moderately active thin films or photocatalysis in less harmful conditions, such as under low sunlight and high flow rates or for short exposure times, i.e., at conditions, when total disinfection is not achieved (Ede et al. 2012; Khan et al. 2012b). Detecting (and presenting) SCV originating from sublethally injured cells is important not only to better distinguish among different photocatalytic conditions, but also to detect potential growth delay or slower proliferation rate in addition to the complete elimination of microbes. SCV have been associated also with higher infectivity of bacteria (reviewed by Proctor et al. 2006). Relative simplicity allows plate count to be performed in almost every lab equipped with basic microbiological equipment and with minimal training. This is probably one of the main reasons that despite all the limitations of the method, most of the existing standard methods for the antimicrobial evaluation of photocatalytic coatings are based on plate count. However, the plate count method is based upon the premise that a single microorganism can grow and divide to give an entire colony, and this amplification provides also a high level of sensitivity for culturable microorganisms, with the capability to detect viable bacteria at densities of 10 per mL without the need for pre-analysis concentration (Davey 2011).

2.6.4.2 Fluorescence, luminescence and colorimetric methods

Several fluorescent and coloured indicators exist that enable to assess cell viability without culturing cells, either at the single-cell level (epifluorescent microscopy, flow cytometry, solid state cytometry) or in total cell population (spectrophotometry, fluorimetry and luminometry). Indicators display different levels of cellular integrity or functionality (Berney et al. 2007b). Methods are based on the exclusion, uptake or metabolic conversion of coloured, luminescent, fluorescent or fluorogenic stains. Their main advantages are that (i) they are based on a direct observation of cells after antibacterial treatment, (ii) they do not require bacterial growth in adequate growth conditions and can detect also bacteria in VBNC state, and (iii) they allow targeting specific characteristics of the microbial cell (membrane permeability, metabolic activity, energetic status of the cell, DNA/RNA content etc.). However, one needs to be careful when selecting appropriate stain among number of stains available, taking into account predicted effects of a photocatalytic sample on microbial cell and characteristics of the selected microbial model system. Careful consideration should be given also to the preparation of appropriate control samples to optimally match the expected mode of antimicrobial effects in photocatalytically stressed samples in order to avoid false negative or positive results. In the field of photocatalytic coatings, increasing number of studies use double staining method based on microbial membrane integrity, which is the first site of photocatalytic attack. A thorough review of fluorescence based probes for bacterial cytoplasmic membrane research is given in Trevors (2003). The most frequently used method for the bacterial viability testing is commercially available LIVE/DEAD[®] *BacLight*[™] Bacterial Viability kit (*BacLight*) (Life Technologies), which utilises two DNA dyes, SYTO 9 and propidium iodide (PI). SYTO 9 labels all cells while PI binds only to dead cells, which allows a total and a viable count at the same time. The method has been tested in many fields and with different microorganisms (manufacturer's indication). As an inexpensive alternative, PI alone can be used to stain bacterial cells with compromised membranes (Kim et al. 2013). SYTO 9 could be replaced by other total stains, such as SYBR Green (Barbesti et al. 2000) or thiazole orange (TO) (McHugh and Tucker 2007). Bis-(1,3-dibutylbarbituric acid)trimethine oxonol (DiBAC4(3)) could be used in addition for the evaluation of cells membrane potential to obtain more integral information about the cell wall status (Jepras et al. 1995). *BacLight* and similar methods are robust methods for determination of microbial viability also in photocatalytic material evaluation (Josset et al. 2007; Cai et al. 2013). They aim to simplify the performance of microbial viability determination, but often they still need

adaptation for the specific organism of interest and the instruments available. Commonly used metabolic activity indicators tetrazolium salts, such as 3-(4,5-dimethylthiazol-2-yl)-2,5-diphenyltetrazolium bromide (MTT) and 2,3-Bis(2-methoxy-4-nitro-5-sulfophenyl)-2H-tetrazolium-5-carboxanilide (XTT), get reduced by live (eukaryotic and prokaryotic) cells into colored formazane compounds. XTT transformation depends on cellular reductive capacity, including the activity of mitochondrial/electron transport system (ETS) dehydrogenases, cytochrome P450 system, as well as flavoprotein oxidases (Kuhn et al. 2003b). However, this method does not allow immediate and direct observation of injured cells. Two metabolic activity indicators, which can overpass these limitations, are carboxyfluorescein diacetate (CFDA), a cell-permeable substrate for cell esterase (Hoefel et al. 2003; Berney et al. 2008), and ATP measurement (Hong et al. 2005; Berney et al. 2008), which, however, could be interfered by the free ATP, released from cells during photocatalytic disinfection (Hammes et al. 2008).

Microscopy represents basic approach for direct observation of antimicrobial effects on a single cell level. After staining, analysis can be done immediately, either manually or in an automated fashion (image analysis). Image analysis makes the method less fastidious and time-consuming, providing rapid acquisition of data related to statistically significant numbers of cells. Flow cytometry is another method for direct single cell evaluation. The level of automatization, sample handling and rapid analysis of thousands of cells overcome some shortcomings of epifluorescence microscopy. Multiple cell properties can be evaluated at the same time providing more detailed picture about physiological changes and microbiota than can be obtained with single stain or growth on an agar plate. The major drawback of this method is that (apart from the cost of basic equipment and maintenance) a careful evaluation of different stains and staining conditions is needed for every microorganism (or microbial community) used or any antimicrobial method tested (Fallani et al. 2010; Strauber and Muller 2010; Davey 2011). Although a very potent method, the complexity of protocol optimization and data analysis makes this method less suitable for the basic antimicrobial evaluation of photocatalytic coatings. Still, flow cytometry stays a valuable tool in studies elucidating mechanisms of photocatalytic action on the microbial cell (Gogniat et al. 2006) as well as in basic microbial viability assessment after photocatalytic exposure (Kumar et al. 2011; Kaur et al. 2013).

Almost any stain (e.g. DNA stains PI and SYTO 9, CFDA, DiBAC4(3), quantum dot streptavidin conjugates, Fluo-4) can be adapted for the use in high-throughput format of microplate readers, where multiple samples can be evaluated in an automated fashion (Fuller et al. 2000; Alakomi et al. 2005; Beckman et al. 2008; Clementi et al. 2012). Although the basic method does not allow direct single-cell evaluation, it can provide information about the status of the whole tested microbial population in a quantitative manner. At variance with the colony count, this method is able to detect various levels of cell injuries, caused by a photocatalytic treatment, of a whole microbial population but not at the single-cell level like flow cytometry or microscopy.

2.6.4.3 Detection of microbial degradation and specific components of microbial cells

Evaluating the presence and condition of selected components of the microbial cell does not give direct information about microbial elimination and has a limited potential for standardised antimicrobial testing as compared to more conventional antimicrobial methods. Usually it is a method of choice when degradation of particular microbial component is important, e.g., endotoxins (Sunada et al. 1998; Smit et al. 2005), cyanobacteria and algae compounds in water treatment processes (Hargesheimer and Watson 1996; Madigan et al. 2003) or dust mite antigens in air cleaning systems (Vohra et al. 2006). More robust approach is evaluation of the photocatalytic damage at the whole cell, DNA or protein level. In contrast to photocatalytic degradation of organic compounds, concentration of TOC is not a good measure of photocatalytic efficiency, because microorganisms often do not degrade completely (Dunlop et al. 2008; Baram et al. 2011). Measuring degradation products such as malondialdehyde (MDA) and ion release could still give some information about the photocatalysis-induced cell damage (Wu et al. 2011). Non-selectivity of the photocatalytic attack was traced also by using agarose and sodium dodecyl sulfate polyacrylamide gel electrophoresis (SDS-PAGE), showing damage in plasmid and genomic DNA of *E. coli* (Kim et al. 2013) as well as fragmentation and degradation of *E. coli* cellular proteins (Chollet et al. 2009). Polymerase chain reaction (PCR) amplification of nucleic acid enables identification and quantification of treated microbiom. It has been used by Sanchez et al. (2012) to follow photocatalytic air disinfection in realistic conditions. However, the method does not detect the physiological state of treated microorganisms and requires trained operators and a well equipped laboratory.

2.6.5 Presenting antimicrobial effect

When presenting microorganism decay by the photocatalytic treatment, percentages must be avoided as they could lead to overestimated impression about photocatalyst activity in this interdisciplinary research field, where 99.9% reduction of initial chemical may be enough, but in case of initial 10^3 CFU/mL, this still represents 1 CFU/mL, which is enough for the infection transmission through water (Directive 98/83/EC). This problem was exposed by McCullagh et al. (2007). Survival rates (percentages) were used by many authors (Liu et al. 2008; Sousa et al. 2013). Sunada et al. (1998) also used percentages to emphasize endotoxin detoxification in their studies, where final concentrations of *E. coli* endotoxin were 8.4×10^5 and 5.2×10^5 endotoxin units (EU)/m³, which is still very high, as indicated by Smit et al. (2005). On the other hand, survival rates could also be presented in a way that all remaining microorganisms are emphasized (Baram et al. 2007; Muranyi et al. 2010). According to the example from drinking water management, theoretical considerations show that risks are directly proportional to the arithmetic mean of the ingested dose. Therefore, use of arithmetic mean of variables, such as density of microorganisms in raw water and its removal by treatment (e.g., by photocatalysis) is recommended (WHO 2011). However, usual practice, including photocatalytic treatment, is to convert densities and treatment effects to log values and to do further calculations or specifications on the log scale (Ditta et al. 2008; WHO 2011). Such calculations results in the estimates of geometric mean rather than arithmetic mean, and these may significantly underestimate the risk (WHO 2011). However, effect of photocatalytic disinfection could be simply represented as raw values, e.g., by numbers of colonies (Guillard et al. 2008).

3 Research goals

My first aim is to prepare well adhered and mechanically stable photocatalytic coatings, with prolonged activity towards individual organic molecules and microorganisms. Different TiO₂-SiO₂ photocatalytic coatings will be prepared by sol-gel method, dip-coating deposition or spraying of colloidal solution on substrates followed by thermal annealing process.

The second goal is to develop sensitive, reproducible and fast methodology for the evaluation of antimicrobial activity of different self-disinfecting coatings with the moderate activity. Development of high-throughput microplate-based spectrophotometric and spectrofluorimetric detection methods is crucial in this part of the study. Methodology developed in the first part will be used also for other applications; e.g. the evaluation of water disinfection systems with higher photocatalytic pressure.

In the last part of research additional viability indicators will be tested at the single-cell level by flow cytometry. This will serve to understand better previous results obtained in the microplate format and to find potential direct indicators of bacterial viability after photocatalysis.

4 Materials and methods

4.1 Materials

4.1.1 Chemicals and materials for photocatalyst preparation and characterization

Titanium dioxide AEROXIDE[®] TiO₂ P 25 (P25) was from Evonik Industries, Germany. PC500 titania powder was purchased from Cristal Global, France. Titanium isopropoxide and 1-propanol (≥99%) were bought from Fluka, Switzerland. Nitrogen-doped TiO₂ powder VPC10 and its undoped analogue PC10 were donated by TitanPE Technology, China. Carbon-doped titania KRONOcLen 7000 was ordered from Kronos[®]. TiO₂ aqueous suspensions denoted UNG2 (150 g/L TiO₂) and UNG9 (270 g/L TiO₂) were products of Cinkarna Celje, Slovenia. Tetraethoxysilane (TEOS) (95%) was purchased from Acros Organics, Belgium and colloidal silica dispersion Levasil 200/30% from AkzoNobel, Sweden. EtOH (96%) and hydrochloric acid (HCl) (32%) were from Itrij, Slovenia. Absolute EtOH was from AppliChem, Germany. Pilkington Activ[™] Self-Cleaning glass (Activ[™]) was donated by Pilkington, UK.

4.1.2 Chemicals, materials and instruments for antibacterial tests

Peptone from soybean, yeast extract, sodium chloride, agar (bacteriology grade) and XTT were purchased from AppliChem, Germany or Biolife, Italy. Menadione – 2-methylnaphthalene-1,4-dione was obtained from Sigma-Aldrich, Germany. Luria-Bertani (LB) media was prepared from yeast extract powder (Himedia, India), and tryptone (Merck, India). For solid LB media also bacto agar (BD, France) was added. To prepare staining buffer for flow cytometry we used sodium chloride (extrapure AR, Sisco Research Laboratories, India), potassium chloride (A.R., Himedia, India), sodium phosphate dibasic dihydrate (Sigma-Aldrich, Germany), potassium dihydrogen phosphate GR (Merck, India), Pluronic F-68 (Himedia Laboratories, India), sodium azide (SDFCL, India) and EDTA (disodium salt dehydrate) (Fluka, Germany). Menadione was obtained from Sigma-Aldrich, Germany. LIVE/DEAD[®] BacLight[™] Bacterial Viability Kit L7012, (5(6)-CFDA) - mixed isomers, DiBAC4(3) and SYBR[®] Safe DNA Gel Stain (SYBR Safe) were from Life

Technologies, USA. Agar nutrient media were prepared in 92 mm Petri dishes without ventilation cams, Sarstedt, Germany.

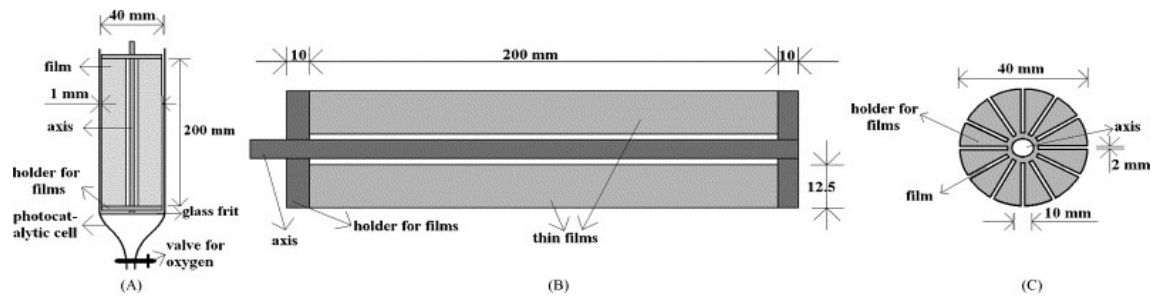


Figure 3: Scheme of Carberry type photoreactor (CTP) photocatalytic reactor parts: (A) photocatalytic cell with sample holder, (B) longitudinal section of the holder, (C) cross-section of the holder with 12 gouges for photocatalytic films deposited on glass slides (taken from Cernigoj et al. 2006).

For the XTT and the growth assay, 96-well polystyrene, transparent and crystal-clear plates with the flat bottoms were used, while for SYTO 9 and PI fluorescence we used 96-well polystyrene black FLUOTRAC 200 – medium binding plates. Lids allowed optimum oxygen supply for the cultivated cells and were used also for *BacLight* assay, to improve safety of method based on toxic DNA-intercalating dyes.

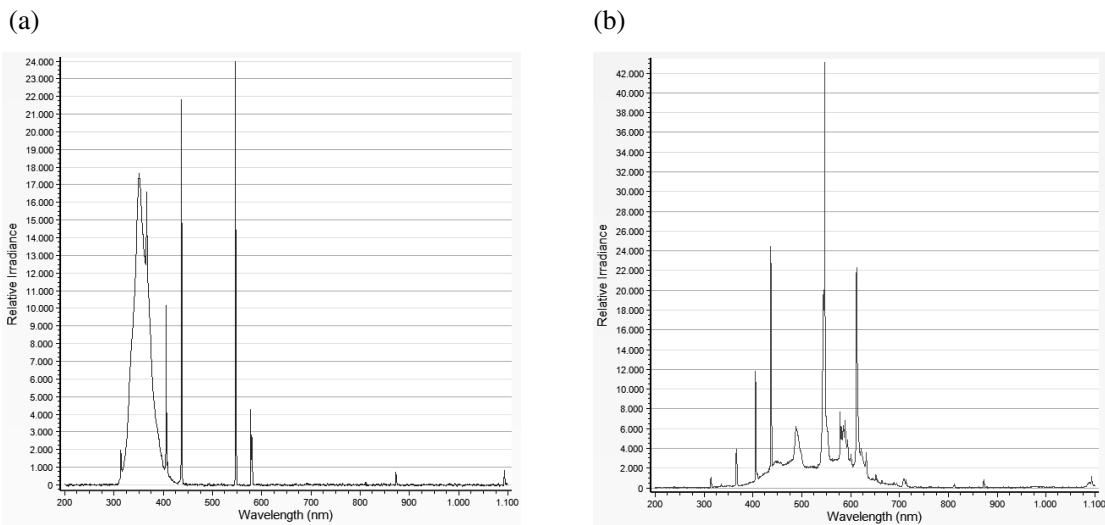


Figure 4: UVA (a) and Vis (b) lamps spectra. Relative irradiances are given for photons of different wavelengths.

Lids and plates were purchased from Greiner bio-one, Germany. Plates were analyzed by micro titer plate reader Infinite[®] 200 from Tecan, Switzerland. Flow cytometry analyses were

done on BD FACSCanto II, USA. The irradiations of bacteria on the TiO₂-photocatalytic layers were performed in the UVA transparent DUROPLAN[®] Petri dishes of the DURAN group, Germany, made of borosilicate glass, placed in the illumination chamber (Figure 1).

Table 3: Light power densities for different reactors, measured with sensors for 300-400 nm and 300-800 nm wavelength range.

Reactor	Lamp	300-400 nm Light Intensity (W/m ²)	300-800 nm Light Intensity (W/m ²)
Illumination Chamber	UVA: 40 W L 40/79K, 2x 20W Cleo Compact	23.3	23.3
	Vis: F18W/865 T8, 2x L15W/840 T8	0.2	46
CTP Reactor	UVA: 2x 20W Cleo Compact	65.2	65.2
	Vis: 6x L15W/840 T8	5.5	252
ncCTP Reactor	UVA: 3x 15W Cleo Compact	12.3	12.3
	Vis: 6x L8W/954 T5	Not measured	Not measured

Differently, flow cytometry experiments were performed in another photoreactor set up, described in Priya et al. (2011). Reaction vessel was replaced by borosilicate Petri dish. Water disinfection research was done in a Carberry type photoreactor (CTP) described in Cernigoj et al. (2006) (Figure 3). Some preliminary experiments were performed also in non-continuous CTP (ncCTP) (Kete et al. 2012). In all experiments with CTP, eleven photocatalytic films were fixed on a sample holder. In contrast to the original setting we didn't apply spinning of the holder, as mixing of the bacterial solution was sufficiently achieved by synthetic air purging. Hydrophilic syringe filters CHROMAFIL[®] CA from Macherey-Nagel, Germany with pore sizes of 0.20 µm were used to filter sterilise XTT/menadione solution, saline for *BacLight* assay and phosphate buffered saline (PBS) buffer for flow cytometry. UVA radiation source were mercury fluorescent lamps with broad peak at 355 nm, 40 W L 40/79K Osram (for chamber), 20W Cleo Compact (for chamber and CTP) and 15W Cleo Compact (for ncCTP), Philips, Netherlands. Visible lamps were mercury

fluorescent lamps F18W/154 T8 (now replaced by F18W/865 T8 according to producer) from Sylvania (for chamber), L15W/840 T8 from Osram (for chamber and CTP) and L8W/954 T5 also from Osram (for ncCTP). Lamps spectra (Figure 4) were taken by Tristan USB minispectrometer from mut (Germany). The light power density was measured with Atlas, Germany sensors, i.e. SunCal BB 300-400 for the wavelength range between 300 and 400 nm and SunCal WB 300-800 BST for the wavelength range between 300 and 800 nm. The values are presented in Table 3. As (simulated) filter uncoated quartz was considered, according to transmittances of different reactor glasses given by Malato et al. (2013). The microscope slides and the square cover slips (20 mm) were from Menzel-Glaser, Germany.

4.2 Preparation of TiO_2 - SiO_2 films

4.2.1 Transparent TiO_2 - SiO_2 films with lower activity

H₂O, silica binder solution (made from Levasil colloidal silica and TEOS precursor) and EtOH were added to the aqueous titania suspension UNG9, according to the patented procedure (Cernigoj and Lavrencic Stangar 2009). The final concentration of TiO₂ in the sol was 2.2% and the molar ratio Si/Ti was 1.9. Thin films were deposited onto already calcined ceramic tiles with air spraying nozzle in the amount of 0.078 g/dm². Films on the tiles were heat-treated in the temperature range from 50 °C to 400 °C. The final temperature was achieved in 30 min by gradual heating and then the tiles were left in the oven for additional 30 min to cool down gradually. Coated tiles were cut to 9 cm² squares for antibacterial tests. These samples were named 19T.

4.2.2 Opaque TiO_2 - SiO_2 films with higher activity

P25-PC500 (AL) TiO₂-SiO₂ coating solution was prepared according to the procedure described in Suligoj et al. (2010). P25 and PC500 titania powders were homogeneously dispersed in a binder sol prepared from titanium isopropoxide, Levasil colloidal silica and TEOS precursors. The final concentration of TiO₂ in the sol was 6.8% and the molar ratio Si/Ti was 2. Thin films were deposited on 9 cm² ceramic tiles squares by dip-coating technique (pulling speed 5 cm/min) and heat-treated at 400 °C. Nitrogen-doped AL analogues were prepared in a similar manner but nitrogen-doped titania VPC10 powder replaced P25 and PC500 titania, to improve antibacterial activity under Vis (Wong et al. 2006). Film was deposited on aluminum strip by brush and was subsequently cut to 4.5 cm² pieces. Samples

were heat-treated in the temperature range between 100 and 200 °C for one hour. For water disinfection tests P25-PC500 (AL), nitrogen-doped VPC10 and for ncCTP also carbon-doped KRONOcLean 7000 incorporated sols were three times sequentially, in thin layers, deposited by dip-coating technique on aluminum slides in case of ncCTP and on soda-lime glass support for CTP reactor. Each individual layer was heat-treated at 150 °C for one hour. Differently from patented procedure, glass substrate was used instead of aluminium slides for CTP, because of better adherence of photocatalysts on glass and also protective silica layer between the catalyst and the substrate is not required as in case of aluminum sheets. Sol enrichment with titania is according to the patent (Suligoj et al. 2010) obtained with P25 and PC500 powders added in equal amounts. To improve catalyst activity in visible, enrichment was done additionally with carbon- or nitrogen-doped titania instead, and with undoped analogue powder (from the same producer as the nitrogen-doped one). To achieve better dispersion of TiO₂-particles in binding TiO₂-SiO₂ sol primary 5 min ultrasonification step was prolonged to 10 minutes. For easier preparation of uniform coatings, deposition by brush from original procedure was replaced with manual dip-coating technique. However, in this way a higher quantity of coating solution is needed and quite some solution is wasted at the end of the deposition. Slides (substrates for film deposition) had dimensions 12 mm × 2 mm × 240 mm for CTP and 28 mm × 0.8 mm × 280 mm for ncCTP. One film had approximately 100 cm² of active geometric surface and weighed 80 mg for CTP, while for ncCTP it reached 162 cm² and ca. 220 mg.

4.3 Characterization of TiO₂-SiO₂ films

Surface structure and thickness of films were determined by SEM. The microscope used was Zeiss Supra[®] 3VP, Germany. Energy dispersive X-ray (EDX) system (Oxford Instruments, UK) of the same instrument provided elemental composition information of the photocatalysts. Characterization of elemental composition and chemical states were determined also with X-ray photoelectron spectroscopy (XPS) that was performed on a Perkin-Elmer Φ 5600ci spectrometer, USA. The UV/Vis spectrophotometer Lambda 650 (with 150 mm integrating sphere) from Perkin-Elmer, USA was used to measure diffuse reflectance spectra (DRS) of TiO₂ powders and films, which were converted to Kubelka-Munk function used to obtain band gap from Tauc plot (Morales et al. 2007). Specific surface area was obtained by BET (Brunauer, Emmet and Teller) method, employing a Micromeritics[®] TriStar 3000 instrument, USA. BET measurements were conducted at the

National institute of Chemistry, Ljubljana. X-ray powder diffraction (XRD) patterns were obtained on a PANalytical X'Pert PRO high-resolution diffractometer, Netherlands. SEM and XRD analyses were taken by Darja Maučec at the National Institute of Chemistry (Ljubljana, Slovenia). Photocatalytic activity of various films was proved by a fluorescence test with solid organic contaminant containing terephthalic acid (Cernigoj et al. 2010). To determine weight reduction profile in relation to temperature, thermogravimetry (TG) was performed and to determine heat flow in and out of sample with temperature increase, differential scanning calorimetry (DSC) was carried out, both on TG/SDTA 851^o instrument Mettler Toledo, USA. The Fourier transform infrared spectroscopic (FT-IR) analysis of the P25-PC500 AL, 19T VPC10 (N-doped) and PC10 powders mixed with ca. 99% of dry KBr in pellets, was performed in absorption mode in the frequency range from 4000 to 400 cm⁻¹ with a resolution of 4 cm⁻¹ using a FT-IR Spectrum 100 spectrometer Perkin-Elmer, USA.

4.4 Bacteria and culture conditions

E. coli K12 498 (German Collection of Microorganisms and Cell Cultures (DSMZ)) was sub-cultured from -20 °C bacterial cultures and maintained on nutrient agar for 1 month maximum. Nutrient medium used was peptone-yeast extract (PYE) with the addition of 1.5% (w/v) agar. Bacterial colonies were inoculated in 5 mL (for tests with self-disinfecting surfaces) or 6 mL (for water disinfection tests) of nutrient broth in a 15 mL tube and the culture was incubated at 37 °C in an orbital shaker at 175 rpm in lying position to achieve better aeration. For water disinfection with ncCTP experiment, requiring more bacteria, 100 mL overnight culture was prepared in 250 mL Erlenmeyer flask, with shaking at 75 rpm. For flow cytometry analysis performed at the Indian Institute of Science (Bengalore, India), we used different *E. coli* strain and procedure. *E. coli* K12 MG1655 (ATCC – American Type Culture Collection) was grown in Luria-Bertani (LB) nutrient medium. Colonies were inoculated in 100 mL of nutrient broth in a 250 mL of Erlenmeyer flask and incubated at 37 °C at 200 rpm.

4.5 Inactivation of bacteria with photocatalysis

Experiments evaluating antibacterial activity of photocatalysis were repeated two or more times with similar results. Results are presented either as means±standard deviation (SD) of all experiments performed or one representative experiment of at least two performed is shown. Proper description for each particular experiment is added to the Figure legends. Validation

of UVA-tested microplate-based assays by Vis-induced self-disinfecting coatings and preliminary tests of water disinfection in ncCTP were performed only once (Figure 27 and 28). For blank experiments, where negative effects of exposure on bacteria were not expected, overlapping measurements of samples with control were already considered as confirmation of no difference between sample and control (e.g. Chapter 4.5.1.2).

4.5.1 Inactivation of bacteria on self-disinfecting coatings

4.5.1.1 Photocatalytic disinfection procedure in the method development

After 18-20 h of incubation when cells were in a stationary growth phase, the estimations of cell densities were determined by measuring optical density (OD) at 600 and 670 nm with the UV/Vis double-beam spectrometer Lambda 650 from Perkin-Elmer, USA and by conventional spread-plate technique (Koch 1994). There were approx. 4×10^9 CFU/mL and *E. coli* density was approx. 1×10^{10} bacteria/mL in overnight cultures (OD 670 and OD 600 of 10× diluted overnight cultures was 0.3 and 0.4, respectively). Cells were harvested from 1.2 mL of suspension by centrifugation at $1000 \times g$ for 10 min and washed with saline. For experiments with UVA and self-disinfecting surfaces, 10-times, and for experiment with self-disinfecting surfaces and Vis, 20-times and 2000-times dilutions were prepared in saline. All photocatalyst samples were first lined with silicone to prevent leaching of bacteria culture from surfaces and then sterilized by dry sterilization (2 h, 160 °C). Autoclaving was not suitable, because it resulted in deactivation of photocatalytic materials, which was already observed by Ditta et al. (2008). Based on the smell present during autoclaving, we believe that contaminations from the previous autoclaving cycles or from other materials, e.g., nutrient media in the same autoclaving process, together with physical characteristics of the autoclaving process, may deactivate photocatalytic samples. Bacteria were applied onto the sample materials in a volume of 0.5 mL or 0.25 mL (for twice smaller N-doped VPC10 samples) drops, without spreading. 2 mL of sterile distilled water was added to the dishes bottom to prevent desiccation (Ditta et al. 2008). Experiments were performed in tailor-made chamber photoreactor (illumination chamber) using three UVA or daylight florescent lamps. Each photocatalytic sample was used for one irradiation time point only. One set of the substrate material of the same dimensions as coated ones was used for the photolysis

determination and one set of each, coated and blank samples, were kept in dark under aluminum foil. Bacterial samples were exposed to the photocatalysis according to the indicated times and then subjected to analyses. After collecting the bacteria, sample materials were washed twice with nutrient medium ($2 \times 500 \mu\text{L}$) and pooled together with the collected bacteria in a total volume of 1.5 mL. It is important that microorganisms are completely removed from photocatalytic surfaces prior any further viability assessment in order to avoid overestimation of the photocatalytic effect. Colony count and *BacLight* assay were performed immediately after sample retrieval, while bacterial samples intended for microplate-based XTT and growth assays were hand-mixed and kept on ice ($0 \text{ }^\circ\text{C}$), in protective conditions (Chapter 2.6.1.4), until the analysis of all the collected samples was started, but not more than 6 h.

4.5.1.2 *Photocatalytic disinfection procedure for flow cytometry testings*

After 14-16 h of incubation when cells were in stationary phase of growth, the estimations of cell densities were obtained by measuring optical density (OD) at 600 and 670 nm with the UV/Vis spectrophotometer T60, PG instruments, UK, and by conventional spread-plate technique (Koch 1994). There were approx. 4×10^9 CFU/mL and *E. coli* densities were approx. 1×10^{10} bacteria/mL in overnight cultures (OD 670 and OD 600 of $10\times$ diluted overnight cultures was approx. 0.3). Cells were harvested from 1.2 mL of suspension by centrifugation at 4000 rpm for 10 min and washed with saline, and furthermore 10-times diluted to prepare working bacterial solution. All photocatalyst samples were first lined with silicone to prevent leaching of bacteria culture from surfaces and then sterilized by dry sterilization (2 h, $160 \text{ }^\circ\text{C}$). Materials were used up to three times. Reused photocatalysts were cleaned by 2 h shaking in 70% technical EtOH and UVA irradiation. Bacteria were applied onto the sample materials in the volume of 0.5 mL drops, without spreading. 2 mL of sterile distilled water was added to the dishes bottom to prevent desiccation (Ditta et al. 2008). Experiments were performed in tailor-made chamber photoreactor (illumination chamber) described in Priya et al. (2011) by using a UVA lamp. Each photocatalytic sample was used up to three experiments and for one irradiation time point only. One substrate material of the same dimensions as coated one was used for the photolysis evaluation in every experiment. Uncoated substrate in dark was used as negative control in every experiment. Coated material with the highest photocatalytic activity was also tested in dark. No effect on bacteria was

observed and, therefore, this combination was not used further in the study as a negative control. Bacterial samples were exposed to photocatalysis for 4 h. After collecting the bacteria, sample materials were washed twice with nutrient medium ($2 \times 500 \mu\text{L}$) and pooled together with the collected bacteria in a total volume of 1.5 mL. Bacteria were then washed twice with PBS and diluted to final 1×10^7 bacteria/mL used in flow cytometric assays.

4.5.2 Inactivation of *E. coli* in simplified water disinfection process

4.5.2.1 Non-continuous Carrbery type photoreactor (ncCTP)

Inactivation of bacteria in water disinfection system was performed using ca. 1750 mL volume of bacterial solution circulating through ncCTP. Detailed description of the photosystem is found elsewhere (Kete et al. 2012). In short, photocatalytic cell was filled with 12 aluminum slides with immobilized photocatalyst or was left empty for blank experiment. UVA or daylight lamps were used as a light source (Chapter 2.6.2.1; Figure 4; Table 3). Bacterial solution was purged with synthetic air for mixing and providing oxygen for bacteria and photocatalysis. Flow of the bacterial solution was controlled. In the sampling port was also possible to measure temperature, pH and O_2 pressure. Photocatalytic system was sterilized before and after experiments by soaking overnight in 70% technical ethanol. 50 mL of overnight culture was harvested by centrifugation at $8000 \times g$ for 10 min, at room temperature. Cells were then dissolved in saline and introduced into 1750 mL of saline in reactor, where final bacteria density was $2\text{-}4 \times 10^8$ *E. coli*/mL ($5\text{-}9 \times 10^7$ CFU/mL). In order to obtain homogeneous solution, bacterial solution was purged with synthetic air 30-45 min before starting with the irradiation. For the control of dark adsorption and bacterial density, one bacterial sample was taken just before the irradiation and compared to 10 mL bacterial sample having the same density, which was prepared in 50 mL centrifuge tube on the benchtop from the same stock bacterial solution as bacterial solution in the photocatalytic cell. Additional 1.5 mL samples were taken from the cell at different irradiation times, up to 6 h of exposure and prepared for the analysis by three different microplate-based assays and, in addition, certain exposure times also for the colony count assay. Colony count and *BacLight* assay were performed immediately after sample retrieval, while bacterial samples intended for microplate-based XTT and growth assays were diluted three times with liquid nutrients, hand-mixed and kept on ice (0°C) until the analysis of all samples together for a long-lasting (ca. 16 h) continuous point measurements in microtiter plate reader was started.

4.5.2.2 Carrbery type photoreactor (CTP)

The main water disinfection study was performed by using 250 mL photocatalytic cell in a CTP reactor (Figure 3). Photocatalytic cell was filled with 11 glass slides with immobilized photocatalysts or with uncoted glass substrates in blank experiments. One slide position was left empty, allowing sampling with 2 mL serological pipette. Source of irradiation were 6 daylight or 2 UVA lamps (Table 3; Figure 4). Disinfection ability of 6 UVA lamps was also tested. To evaluate photocatalyst dark activities, all experiments were performed also in the aluminum-wrapped photocatalytic cell. Bacteria solution was purging with synthetic air like in ncCTP. Photocatalytic coatings and photocatalytic cell were disinfecting by soaking in 70% technical EtOH overnight, followed by washing once or twice with sterile ddH₂O the next day. 4 mL of *E. coli* overnight culture was harvested by centrifugation at 8000 × g for 10 min, at room temperature. Cells were afterwards dissolved in saline and introduced into 240 mL of saline in reactor cell, where final bacteria density was 1-2 × 10⁸ *E. coli*/mL (2-6 × 10⁷ CFU/mL). Experiments, sampling and final analysis were made like with ncCTP. The 30-45 min pre-irradiation phase was performed in the photocatalytic cell placed outside of the reactor as lamps in the reactor were switched on during this time in order to obtain stable irradiation from the beginning of experiments.

4.6 Detection of antibacterial activity of the films

4.6.1 Antibacterial activity evaluation using colony count method

Following conventional spread-plate technique (Koch 1994) we evaluated the capability of exposed bacteria to form colonies on solid nutrient medium. Serial dilutions were prepared by adding 100 µL or 50 µL of bacteria culture into 900 µL or 950 µL of sterile saline in order to obtain 10× or 20× dilutions, respectively. 100 µL of the appropriate dilutions were plated onto nutrient agar plates. Lower volumes (20 or 10 µL) have been avoided for the sake of better accuracy. Agar plates were stored in fridge 2 to 7 days after the preparation, and were preheated at 37 °C for 20 minutes just before the use. Inoculated plates were counted after 20-24 h of incubation at 37 °C. Two replicas were prepared for each sample and all experiments were repeated at least two times.

4.6.2 Antibacterial evaluation using microplate-based BacLight assay

LIVE/DEAD[®] BacLight[™] Bacterial Viability Kit L7012 (Life Technologies) was used according to the manufacturer's instructions. Staining mixture contained PI (30 μ M final concentration) and SYTO 9 (5 μ M final concentration) diluted in filter-sterilized deionized water. Instead of PI solution from the kit, 1 mg/mL solution of PI powder in ddH₂O was used in some experiments, and was stored in the refrigerator up to 1 year. Bacteria from all the samples were washed in saline (autoclaved only) prior to analysis. 100 μ l of bacteria (2×10^8 *E. coli*/mL) and 100 μ L of staining solution were mixed in the wells of a microtiter plate. Excitation and emission wavelengths were 485 ± 10 and 535 ± 12.5 nm for SYTO 9 and 485 ± 10 and 625 ± 17.5 nm for PI, respectively. Measurements were performed at $24.5 (\pm 0.5)$ °C. For the assessment of relative bacterial viability a calibration curve was done by mixing viable and isopropanol-killed bacteria in different proportions (Figure 5). Standards were prepared according to the manufacturer's instructions. By measuring fluorescence of the standards every six months approx. gains were optimized. Program of measurements is given in Figure 8, part a.

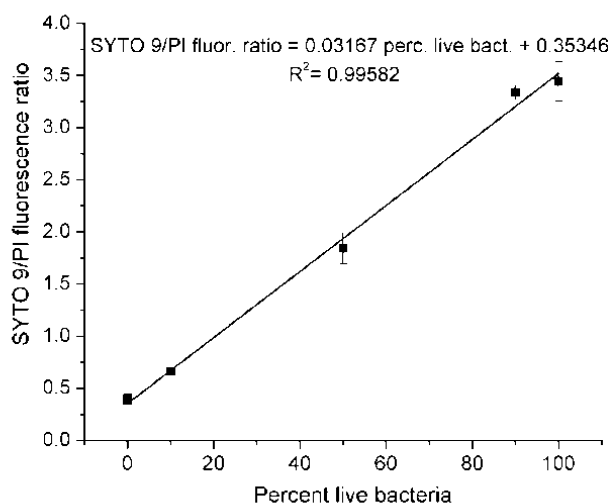


Figure 5: Analysis of relative viability of standard *E. coli* suspensions by BacLight assay (Life Technologies). Samples of *E. coli* were prepared following manufacturer's instructions. Arithmetic means and SD of two repeats ($n=2$) are displayed and used to construct calibration curve.

4.6.3 Antibacterial evaluation using microplate-based growth and XTT assay

XTT assay was performed according to Pettit et al. (2005) with the following modifications. XTT was dissolved in saline. Menadione solution was stored at $-80\text{ }^{\circ}\text{C}$. Reagent was prepared just before use and was filter sterilized. $150\text{ }\mu\text{L}$ of bacterial sample and $50\text{ }\mu\text{L}$ of XTT/menadione reagent were added to each well and bacteria were grown at $37\text{ }^{\circ}\text{C}$ and 87.6 rpm . Formazan accumulation was followed recording the absorbance at $492 \pm 5\text{ nm}$. For the growth assessment, $50\text{ }\mu\text{L}$ of PYE nutrient media was introduced into wells instead of XTT/menadione reagent. Bacterial growth was followed at $595 \pm 5\text{ nm}$. Quantitative analyses of growth- and XTT-generated data were performed by extracting recovery times at which different bacterial samples reached certain absorbance thresholds. To set the absorbance thresholds, we used standard bacterial samples – untreated bacteria of different densities and set the thresholds in the middle of exponential phases of bacterial growth (Lowdin et al. 1993) (Figure 6a) or XTT conversion (Figure 6b).

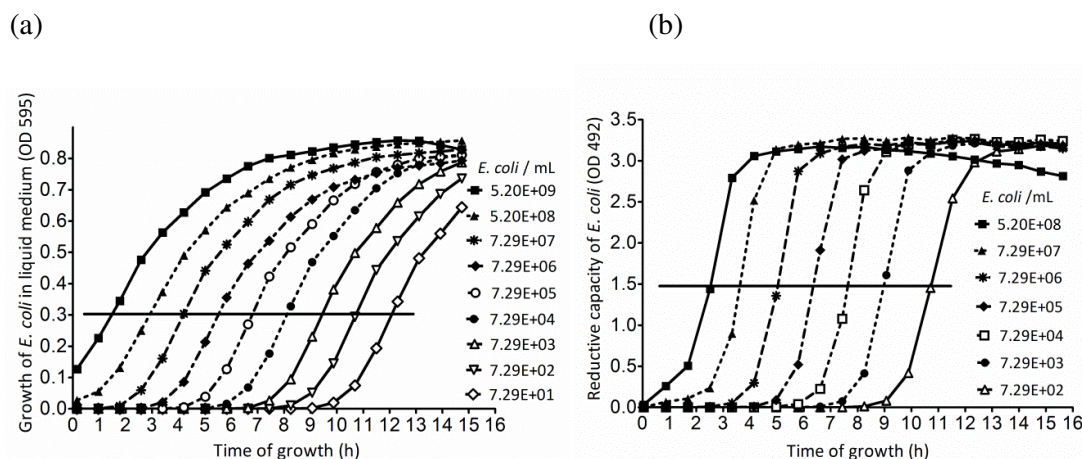


Figure 6: Growth (a) and metabolic activity (b) profiles of the unexposed standard *E. coli* of different densities. Intersection lines are fixed at the threshold values 0.3 on the curves from microplate-based growth assay (a) and at 1.5 on the curves from microplate-based metabolic activity – XTT assay (b). Growth periods, which correspond to marked threshold values (0.3 and 1.5) were subsequently used for the preparation of calibration curves. Results of one experiment out of three performed are presented.

For standard bacteria samples, high linear correlation between bacterial number and extracted threshold times in a broad range of bacterial densities were obtained for both assays: R-

squared values were 0.99 for both, growth and XTT assays, obtained by plotting the threshold times as a function of logarithm of bacteria densities; 1×10^2 to 1×10^9 *E. coli*/mL (Figure 7). In our experimental conditions we set threshold values at OD 595 = 0.3 for growth assay and at OD 492 = 1.5 (coincides with half-saturation point) for XTT assay. Measuring program used in microtiter-plate reader is given in Figure 8, part b.

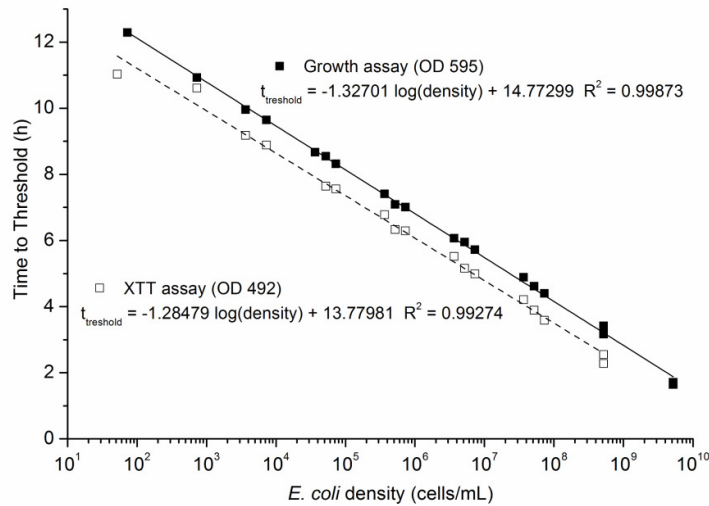


Figure 7: External calibration curves for quantification of *E. coli* growth (■) and metabolic activity (□) in microtiter-plate reader. Time periods in which bacteria reached the threshold value 0.3 (at OD 595) in the growth assay and 1.5 (at OD 492) in the XTT assay versus *E. coli* (unexposed bacteria samples) density were plotted to obtain dependencies, which allow calculations of corresponding densities from treated bacterial samples threshold times (Time to Threshold). Data originated from three independent measurements.

(a)

Plate Description: [GRE96fb_chimney] - Greiner
 96 Flat Black
 Plate with Cover: Yes
 Barcode: No
 Part of Plat
 Range: D2:D11 (range varied)
 Temperature Mode: On
 Temperature: 24,5 °C
 Wait for Temperature

(b)

Plate Description: [GRE96ft] - Greiner 96
 Flat Transparent
 Plate with Cover: Yes
 Barcode: No
 Part of Plate
 Range: A1:H12 (range varied)
 Temperature Mode: On
 Temperature: 37,0 °C
 Wait for Temperature
 Minimum Temperature: 36,5 °C
 Maximum Temperature: 37,5 °C

Figure 8 continues to the next page↓

Minimum Temperature: 24,0 °C
Maximum Temperature: 25,0 °C
Shaking
Duration: 120 sec
Mode: Orbital
Amplitude: 1 mm
Frequency: 87,6 rpm
Wait (Timer)
Wait Time: 00:13:00
Wait for injection: No
Ignore wait for last kinetic cycle: No
Fluorescence Intensity
Excitation Wavelength: 485 nm
Excitation Bandwidth: 20 nm
Emission Wavelength: 625 nm
Emission Bandwidth: 35 nm
ReadingMode: Top
Lag Time: 0 µs
Integration Time: 20 µs
Number of Reads: 25
Settle Time: 0 ms
Gain: Manual
Gain Value: 76
Label: pi
Fluorescence Intensity
Excitation Wavelength: 485 nm
Excitation Bandwidth: 20 nm
Emission Wavelength: 535 nm
Emission Bandwidth: 25 nm
ReadingMode: Top
Lag Time: 0 µs
Integration Time: 20 µs
Number of Reads: 25
Settle Time: 0 ms

Figure 8 continues to the next page↓

Kinetic Cycle
Number of Cycles: 30 (Time of
measurements is modifiable)
Shaking
Duration: 120 sec
Mode: Orbital
Amplitude: 1 mm
Frequency: 87,6 rpm
Wait (Timer)
Wait Time: 00:01:00
Wait for injection: No
Ignore wait for last kinetic cycle: No
Absorbance
Measurement Wavelength: 492 nm
Measurement Bandwidth: 10 nm
Number of Reads: 20
Settle Time: 0 ms
Label: xtt
Multiple reads per well type: FilledCircle
Multiple reads per well size: 5 x 5
Border: 1200 µs
Shaking
Duration: 120 sec
Mode: Orbital
Amplitude: 1 mm
Frequency: 87,6 rpm
Wait (Timer)
Wait Time: 00:01:00
Wait for injection: No
Ignore wait for last kinetic cycle: No
Absorbance
Measurement Wavelength: 595 nm
Measurement Bandwidth: 10 nm
Number of Reads: 20
Settle Time: 0 ms
Label: od595

Gain: Manual	Multiple reads per well type: FilledCircle
Gain Value: 70	Multiple reads per well size: 5 x 5
Label: syto9	Border: 1200 μ s
	Shaking
	Duration: 600 sec
	Mode: Orbital
	Amplitude: 1 mm
	Frequency: 87,6 rpm

Figure 8: *BacLight* assay (a) and XTT/growth assays (b) programs used in microtiter plate reader. Programs were optimized for *E. coli* strain 498 (DSMZ) viability evaluation. Underlined texts indicate commands, which were different for individual experiments.

4.6.4 Antibacterial activity evaluation by fluorescence microscopy

Preliminary, we checked if LIVE/DEAD[®] *BacLight*[™] Bacterial Viability Kit L7012 (Life Technologies) could be used for the evaluation of bacterial samples, stressed by photocatalysis at conditions as described in Chapter 3.5.1.1. Bacterial samples for microscopy were prepared following the producer's instructions. Staining mixture was prepared as in Chapter 4.6.2. 1000 μ L of bacteria (adjusted to 2×10^8 *E. coli*/mL) and 10 μ L of the staining solution were mixed thoroughly and incubated at room temperature in the dark for 15 minutes. 10 μ L of the prepared stained bacterial suspension were in the next step trapped between a microscopic slide and 20 mm square cover slip. Samples were observed with inverted phase and fluorescence microscope Axio Observer Z1 Zeiss, Germany. Filter cubes used were "red": EX BP 587/25, BS FT 605, EM BP 647/70 for PI and "green": EX BP 470/40, BS FT 495, EM BP 525/50 for SYTO 9.

4.6.5 Antibacterial activity evaluation by flow cytometry

PI, total dyes TO, SYTO 9, SYBR Safe, DiBAC4(3) or CFDA or the combinations of PI-TO, PI-SYTO 9, PI-SYBR Safe was added to 200 μ L of bacterial suspension with the density of 10^7 cells/mL. Labeled bacteria were then incubated and finally, 30,000 labeled cells were measured using a flow cytometer. Probes information, including incubation times are given in Table 4. All dyes were evaluated by using mixtures of viable and isopropanol-killed bacteria (*BacLight* protocol) in different proportions (Figure 9). Killing of cells for CFDA assay was tried to be achieved also by heat and EtOH exposure. Final staining protocols were based on protocols of Barbesti et al. (2000), Hoefel et al. (2003), Berney et al. (2008), manufacturer's

instructions and our previous experiences with microplate-based *BacLight* assay. 488-nm blue laser was used as an excitation source in all experiments.

Table 4: Overview of flow cytometry probes informations, including incubation conditions.

Probes, storage	Stock Solution	Volume added to cells	Final Concentration	Incubation
PI, 4°C	1.3 mg/mL (1.9 mM)	10 µL	62 µg/mL (90.5 µM)	15 min, RT, Dark
TO, -20°C	0.081mg/mL (0.170 mM)	5 µL	2 µg/mL (4.14 µM)	15 min, RT, Dark
SYTO 9, -20°C	0.334 mM	2 µL	3.31 µM	15 min, RT, Dark
SYBR Safe, 4°C	1000x conc.	1 µL	1x conc.	15 min, RT, Dark
DiBAC4 (3), -20°C	0.5 µg/mL (1 mM)	2 µL	5 ng/mL (10 µM)	20 min, RT, Dark
CFDA, -20°C	4.6 µg/mL (10 mM)	0.2 µL	4.6 ng/mL (10 µM)	15, 30, 45 min, 35 °C, Dark

For detection of the emitted light, 515-545 nm FITC filter was used for TO, SYTO 9, SYBR Safe, DiBAC4(3) and CFDA. PI emission was collected through 564-606 nm PE filter. Matching of the emission and excitation spectra of DNA-binding dyes with the emission filters and laser were examined with Fluorescence SpectraViewer (Life Technologies). Measured data were analysed with FCS Express software. Position and length of the markers (M1 and M2) for each individual fluorescence dye was set according to the standard samples histogram (Figure 9) and additionally adjusted for the photocatalytic samples considering also spectra of the negative (Dark) and positive (most active photocatalyst P25-PC500) controls.

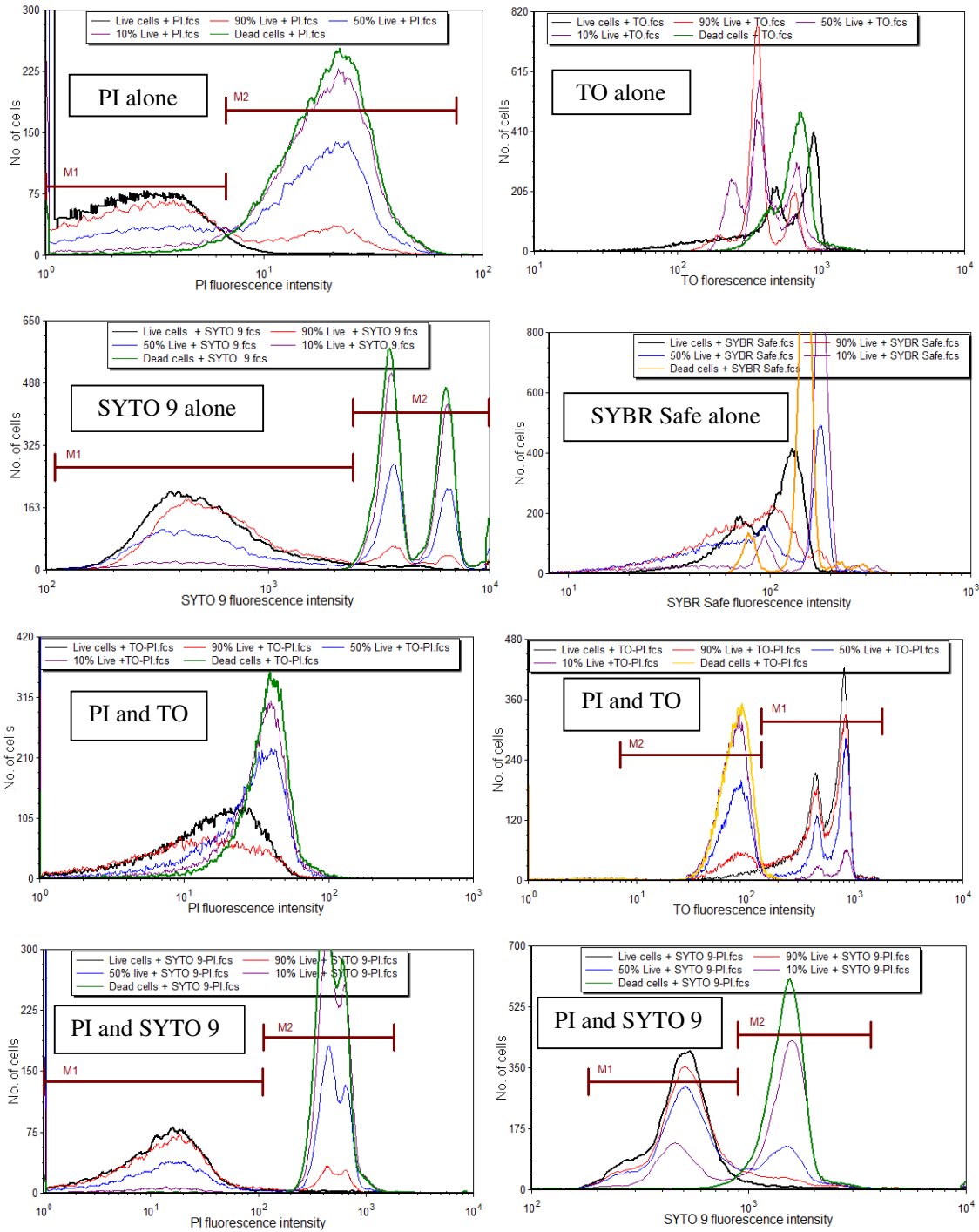


Figure 9 continues to the next page ↓

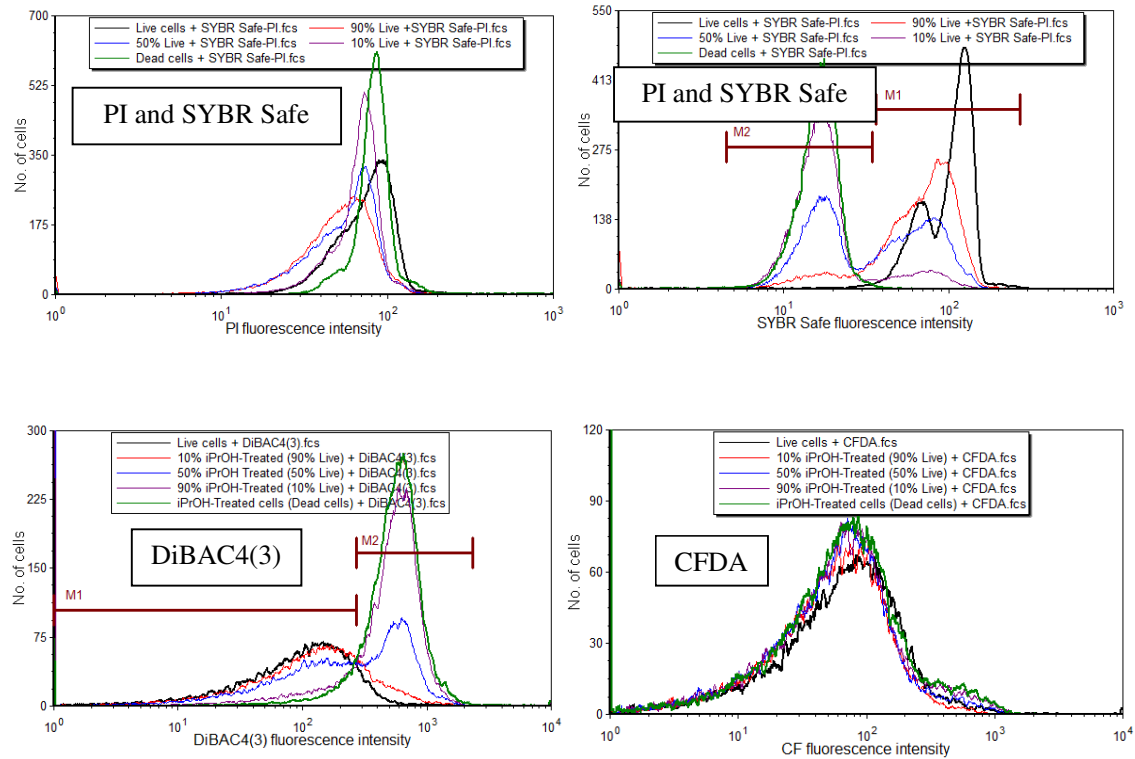


Figure 9: Evaluation of PI, TO, SYTO 9, SYBR Safe, DiBAC4(3) and CFDA dyes for flow cytometry analysis, by using mixtures of viable and isopropanol-killed bacteria (BaLight protocol) in different proportions. Probes for membrane integrity assessments were tested also in pairs and intensity of fluorescence from both dyes was measured. Markers distinguish between untreated/healthy (M1) and treated/impaired (M2) cells. Results of one representative experiment out of two or three performed are presented.

5 Results and discussion

5.1 Photocatalysts

5.1.1 Self-disinfecting coatings used in the development of methodology

Four different titania films with variable capacity of photooxidizing organic matter were used for development of methodology for evaluation of antibacterial effects of photocatalytic coatings (Table 5). Opaque P25-PC500 AL film was used as highly active material. The 19T film was a thin and transparent coating intended for self-cleaning surfaces and was considered as a material with lower activity. In addition, commercial photocatalyst Pilkington Activ™ Self-cleaning Glass (UK) (Mills et al. 2003b) was used as a standard material. Activ™ was suggested to be a suitable reference photocatalytic film for self-cleaning coatings as it is physically well-defined, photocatalytically active, with reproducible activity, mechanically stable, available and cheap, which do not apply for films prepared from P25 that is the usual standard titania photocatalyst (Mills et al. 2003a; Ditta et al. 2008). The fourth coating in this study was the nitrogen-doped titanium dioxide film, expected to have an improved antibacterial activity under the Vis (Rengifo-Herrera et al. 2009).

Table 5: Reaction rates for TPA oxidation obtained for different titania films (measured according to Cernigoj et al. 2010 by M. Kete).

Samples	19T	P25-PC500 (AL)	Activ™	VPC10 (N-doped)
k1 (M/min)	2.46×10^{-7}	2.54×10^{-6}	2.54×10^{-9}	1.41×10^{-6}

By visual eye observation 19T films appeared smooth and transparent. This was also confirmed by UV-Vis spectroscopy (Figure 13). SEM showed some microcracks on the uniform surface of 1 µm thick 19T coatings (Figure 10).

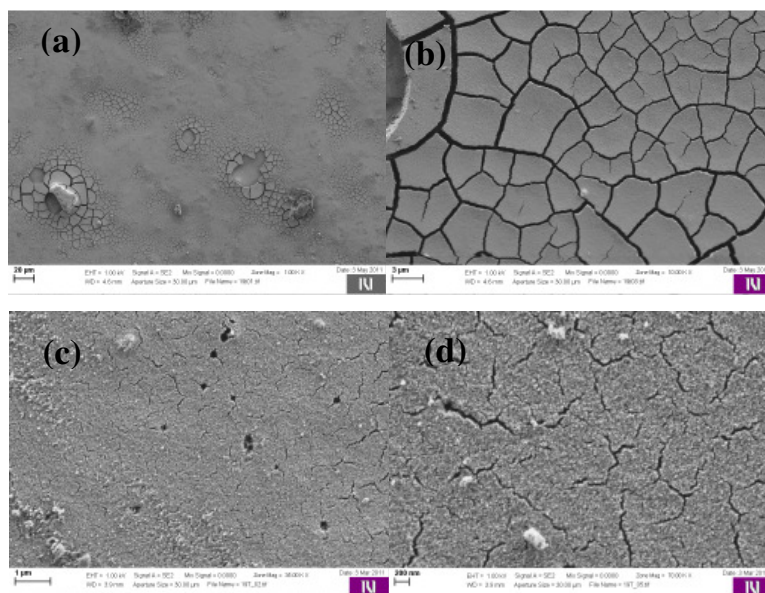


Figure 10: SEM corresponding to photocatalytic coatings 19T deposited on ceramic substrate (Nica4), at different magnifications. Scale at the bottom left of micrographs is: 20 μm (a), 3 μm (b), 1 μm (c), 200 nm (d).

Cracks may influence durability of the material (Ramier et al. 2008), but were not big enough for *E. coli* to be trapped inside. Cracks of the same size were observed also on the other two prepared materials (Figures 11a and 12a). Specific surface area (BET surface) was quite high – 217 m^2/g . For the comparison, SA_{BET} of 30 nm P25 is $50 \pm 15 \text{ m}^2/\text{g}$ and of 5-10 nm crystallites of PC500 $>250 \text{ m}^2/\text{g}$ (Rachel et al. 2002). High specific area allows adsorption of larger amount of substrate (Ohtani et al. 2010) and can therefore improve photocatalytic reaction rate. However, larger crystallites with smaller surface area possess smaller density of crystalline defects (Ohtani et al. 2010), which contributes to charges recombination, therefore to reaction retardation. P25 is an extremely active photocatalytic material, even though its surface area is not high. X-ray analysis employing (101) peak of anatase and the Scherrer's equation indicated that 19T sample contains grains with average size of 14 nm, i.e. the effective size of coherently scattering domains (Klug and Alexander 1973). XRD pattern (Figure 14) confirms presence of pure anatase phase nanoparticles in this sample (Reyes-Coronado et al. 2008). Films P25-PC500 AL are thick and white in color – they are non-transparent, in comparison to the transparent 19T samples (Figure 13). SEM images indicate 20-25 μm thick coatings with textural sponge-like porosity (Figure 11).

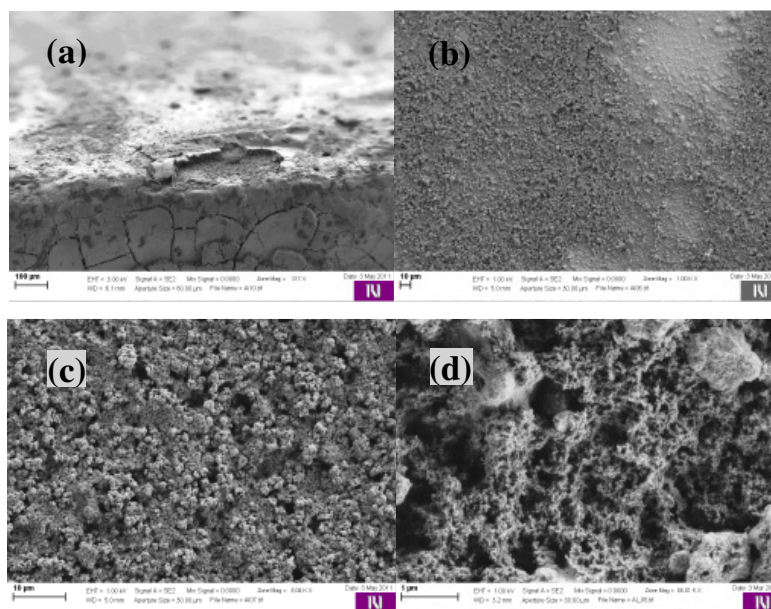


Figure 11: SEM corresponding to photocatalytic coatings P25-PC500 AL deposited on ceramic substrate (Nica4), at different magnifications. Scale at the bottom left of micrographs is: 100 μm (a), 10 μm (b), 10 μm (c), 1 μm (d).

Its BET was 175 m^2/g , and it formed crystalline grains with average size of 41 nm. Even if we increased the temperature as compared to the original procedure, porous surface structure was retained. XRD pattern of P25-PC500 AL (Figure 14) indicates prevailing presence of anatase crystalline form, as expected, but rutile phase is also evident (Reyes-Coronado et al. 2008). FT-IR analysis (Figure 15) evidences presence of the significant amounts of hydroxyl groups (HOH, Ti-OH, Si-OH and H-bonds) in both materials, with characteristic vibration peaks at 3100-3600 and 1620 cm^{-1} (Gao et al. 2004; Yan et al. 2005; Wu 2005). They are traps for photogenerated holes, forming reactive hydroxyl radicals, and therefore prevent recombination of charges, thus enhance photocatalysis. Surface hydroxylation is also important for maintaining hydrophilicity, which additionally contributes to self-cleaning ability of TiO_2 thin films (Guan 2005). From the broad band centered at 400-700 cm^{-1} , Ti-O bonds in the TiO_2 lattice are also evident (Gao et al. 2004; Beranek and Kisch 2008) and in the band occurring at ca. 700-1400 cm^{-1} , Ti-O-Ti, Si-O-Si, Ti-O-Si and Si-OH vibrations are contained (Ingo et al. 2001; Yan et al. 2005; Wu 2005) (Figure 15). TG analysis for 19T and AL films showed expected loss of weight, i.e. 8-10% up to 600 $^\circ\text{C}$ for 19T and up to 400 $^\circ\text{C}$ for AL, which could be correlated with DSC endothermic falls and were explained by the removal of differently bound water from the samples. Exothermal phase transition from anatase to rutile (in Marinescu et al. 2011) at higher temperatures was not observed (Figure

14 and 16); therefore high photocatalytic activity of anatase phase was preserved during calcination of 19T and AL, performed up to ca. 400 °C, which was used to produce a harsh, robust coat of titanium dioxide on the substrate (Mills et al. 2003a). However, we see that hydroxylation, and consequently most probably activity, would be higher if lower curing temperatures, e.g. 150 °C would be used, like it was in the procedure of catalysts preparation for water disinfection study. Weakly adsorbed water and probably most of the remaining solvents are removed already up to 100 °C, and in the range 150-400 °C the mass loss was attributed to decomposition of OH groups and organic components and formation of Ti-O-Ti, Si-O-Si and Ti-O-Si bonds (Ingo et al. 2001; Wu 2005; Nakayama and Hayashi 2008). In the last part of this temperature range, a relatively big and sharp fall of mass for P25-PC500 AL sample was evident, suggesting that AL sample presumably contained OH groups or organic compounds that were stable at lower calcination temperatures. However, all these reactions are exothermic processes (Nakayama and Hayashi 2008), which are not seen from DSC curves. However, the sum of thermal changes is much more endothermic for 19T than for P25-PC500 AL sample; therefore, exothermic processes could be hidden in the DSC plot behind endothermic removal of water molecules and remaining solvents from the photocatalyst (Figure 16). Ti-O stretching vibrations (shoulder broad peak at ca. 600 cm⁻¹) are also stronger for 400 °C AL compared to 19T, which indicates higher amount of TiO₂ in P25-PC500 AL than in 19T (all the others peaks are smaller) (Figure 15). And finally, high activity of P25-PC500 AL could also at least partly be explained by relatively high presence of OH vibrations compared to Ti-O-Ti, Si-O-Si, Ti-O-Si and Si-OH vibrations. However, comparison of the amount of surface hydroxyl groups contained in different photocatalysts as shown by FT-IR method used is difficult, because it is not simple to obtain pressed pellets with the same thickness and density. Band gap of P25-PC500 AL and 19T was calculated to be 3.42 and 3.36 eV, respectively, corresponding to absorption wavelength upper limit of 363 and 370 nm, thus both belong to UVA, and not Vis active photocatalysts. Capability of photocatalysts for hydroxylation of terephthalic acid (TPA) was decreasing in order P25-PC500 AL > 19T > Pilkington Activ™ (Table 5). SEM images of nitrogen-doped catalyst (Figure 12) indicate dynamic microsurface of the coating. Thickness of the film was 5-6 µm. Other characterizations of N-doped VPC10 film were done in the next step, in which material was deposited on glass and tested for photocatalytic water disinfection (Chapter 4.1.2). The main properties of all the photocatalysts employed are listed in Table 6.

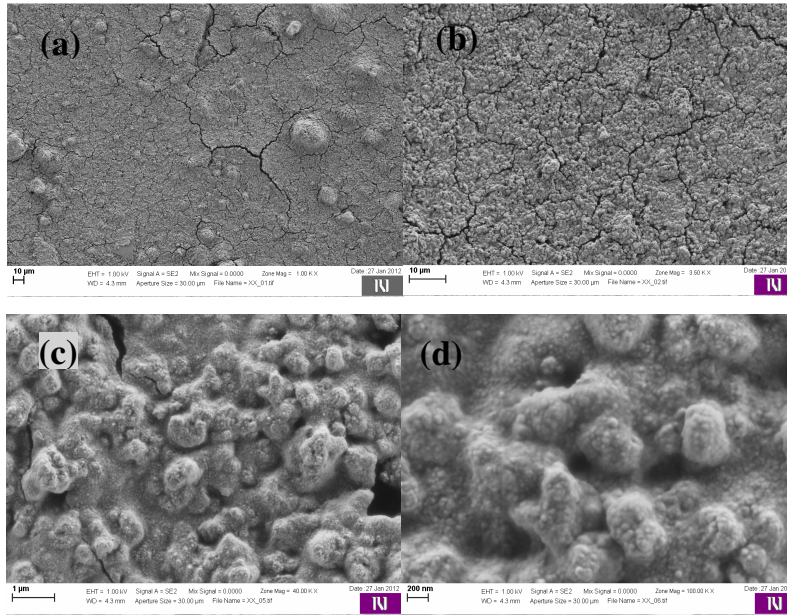


Figure 12: SEM corresponding to photocatalytic coatings VPC10 (N-doped AL) deposited on aluminum, at different magnifications. Scale at the bottom left of micrographs is: 10 μm (a), 10 μm (b), 1 μm (c), 200 nm (d).

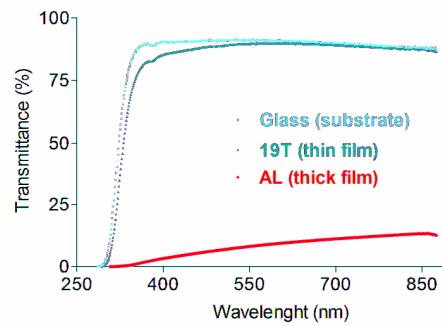


Figure 13: High transparency of 19T films and opaque appearance of P25-PC500 AL films, both deposited on glass, as seen by UV-Vis absorption spectroscopy.

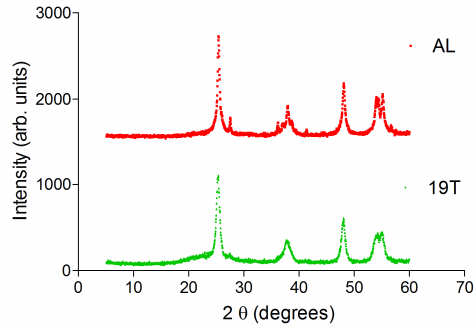


Figure 14: XRD patterns of TiO_2 materials P25-PC500 AL and 19T scratched from ceramic substrate Nica4.

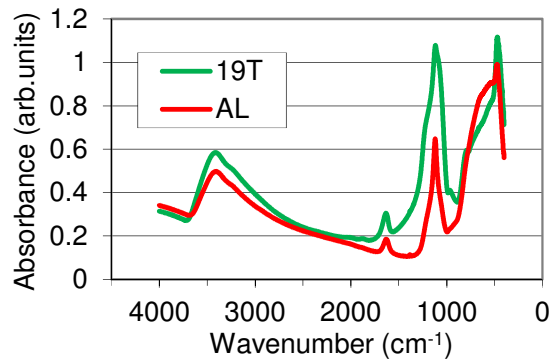


Figure 15: FT-IR spectra of 19T and P25-PC500 AL powders scratched from ceramic substrates.

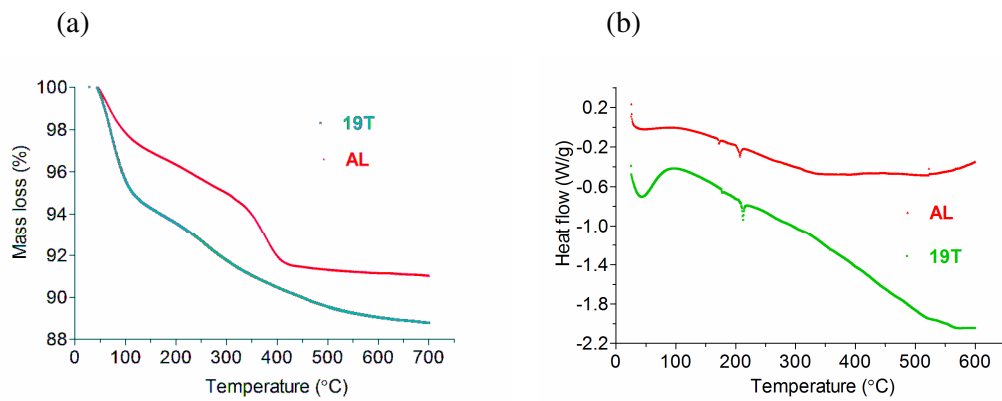


Figure 16: TG (a) and DSC curves (b) for 19T and P25-PC500 AL samples (measured by R. Cerc Korošec (University of Ljubljana, Slovenia)).

Table 6: Overview of the main properties of TiO₂-SiO₂ materials tested as self-disinfecting films. Characteristics of Pilkington Activ™ are taken from Mills et al. (2003b). Characteristics of VPC10 were partly obtained from Kete et al. (2013).

Samples→ Characteristics↓	19T	P25-PC500 AL	Pilkington Activ™	VPC10
crystalline phase, doping	anatase	anatase mostly, partly rutile	anatase	anatase, N-doped
Si/Ti ratio	1.9	2.0	/	/
crystallite size (nm)	14	41	30	/
BET surface (m ² / g)	217	175	/	85
thickness (μm)	1	20-25	0.045	5-6
band gap (eV)	3.36	3.42	3.44	3.15
appearance	smooth transparent microcracks	white rough microcracks	smooth transparent	white rough microcracks
hydroxylation	good	good	/	/

5.1.2 Coatings for water disinfection

Four different photocatalytic coatings on two different supports were used in this study; in addition to two self-disinfecting coatings P25-PC500 AL film and nitrogen-doped VPC10, also carbon-doped KRONOcLean 7000 and PC10, undoped analogue of VPC10, were tested in two different reactors for water disinfection, CTP and ncCTP (Chapter 4.1.2). Slightly modified preparation of patented photocatalyst P25-PC500 AL and its modified counterparts are described in Chapter 4.2.2. Modified procedure resulted in adequately adhered sufficiently thick films with preserved activity during five cycles of use. However, after five cycles the photocatalysts lost from 8% (PC10) up to 15% (P25-PC500) of their initial mass. This could be explained by the removal of surface photocatalytic material from supporting glass slides as a consequence of insufficient adhesion for water disinfection application.

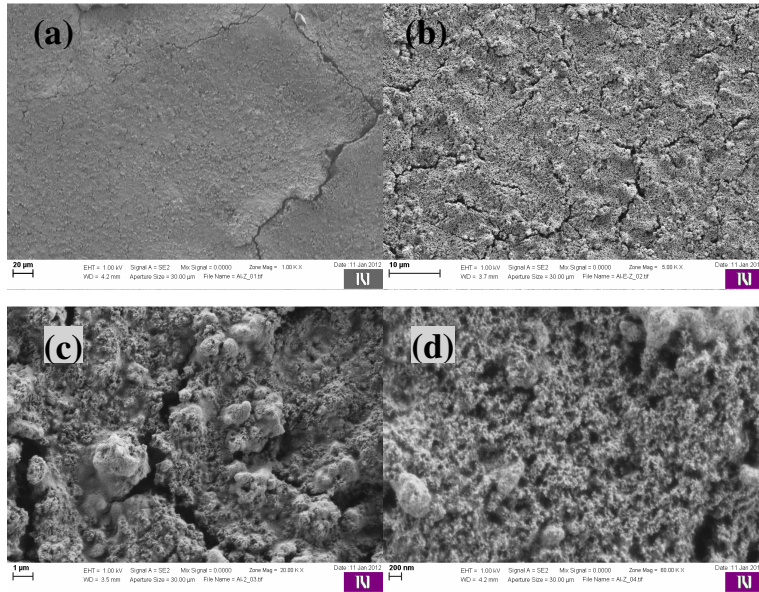


Figure 17: SEM corresponding to the photocatalytic coating P25-PC500 deposited on soda-lime glass, at different magnifications. Scale at the bottom left of micrographs is: 20 μm (a), 10 μm (b), 1 μm (c), 200 nm (d).

SEM indicated similar surface morphology of P25-PC500 (Figure 17) as compared to P25-PC500 AL (Figure 11) prepared on ceramics (see Chapter 5.1.1). Change of the substrate from ceramics to soda-lime glass obviously didn't influence surface structure of the film.

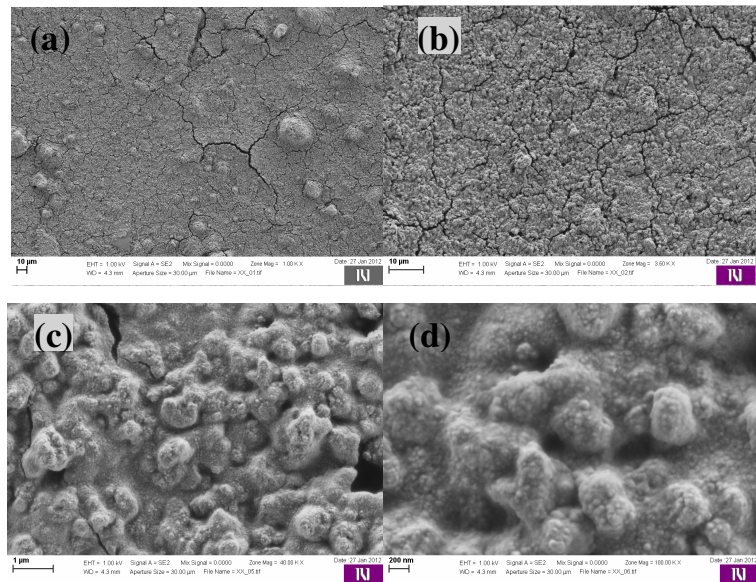


Figure 18: SEM corresponding to the nitrogen-doped photocatalytic coating VPC10 deposited on a soda-lime glass, at different magnifications. Scales at the bottom left of micrographs is: 10 μm (a), 10 μm (b), 1 μm (c), 200 nm (d).

From SEM we also estimated thickness of the coating, which was 5-9 μm . Like for P25-PC500 AL on ceramics (Figure 14), XRD pattern of P25-PC500 (Figure 21) indicates prevailing presence of anatase, but also rutile is visible (Reyes-Coronado 2008). The grain size was measured to be in average 22.1 nm. FT-IR analysis (Figure 22) indicated similar composition of P25-PC500, VPC10 and PC10 photocatalysts, only PC500 material exhibited much higher hydroxylation (explanation in Chapter 5.1.1). However, PC500 was observed to be inactive as a photocatalysts (not shown), which could be a consequence of its low crystallinity as indicated by XRD pattern (Figure 21). VPC10 also had a similar surface structure as its counterparts, deposited on aluminum (Figure 12 and 18). Also thickness of the film was observed to be the same, 5-6 μm . Average grain size was 14.2 nm. XPS analysis (Table 7) indicated slightly higher content of nitrogen in VPC10 than in P25-PC500 or PC10 films. However, PC500 contained the highest amount of nitrogen (1 atomic %). The main properties of materials, including nitrogen content, obtained by XPS analysis is shown in Table 8. Besides intentional N-doping of VPC10, nitrogen from air could incorporate into materials during preparation procedure in air (Subhayan et al. 2008).

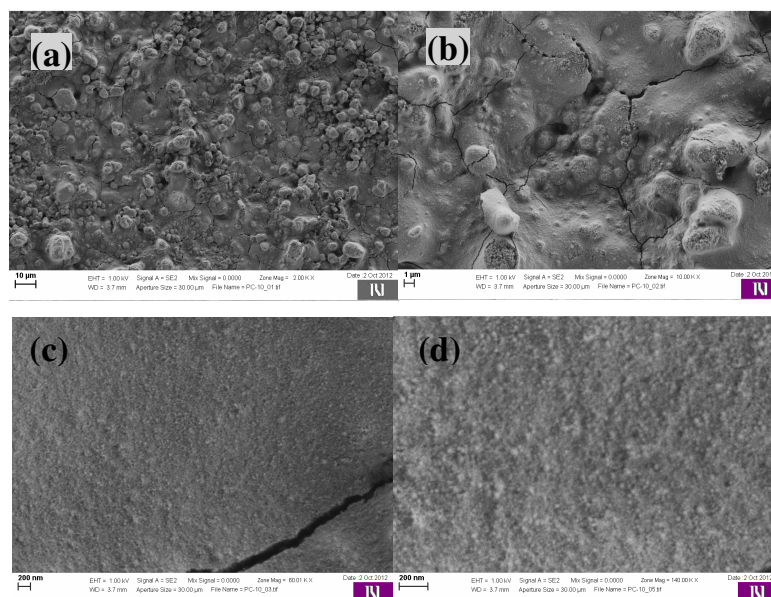


Figure 19: SEM corresponding to the undoped PC10 analogue of nitrogen-doped VPC10, photocatalytic coating deposited on a soda-lime glass, at different magnifications. Scales at the bottom left of micrographs is: 10 μm (a), 10 μm (b), 200 nm (c), 200 nm (d).

Structure of PC500 seems to be the most appropriate for nitrogen incorporation, and high nitrogen incorporation could also be the reason for decreased crystallinity of the material (Subhayan et al. 2008). Only N 1s peak was found in all four photocatalysts and has been assigned to interstitial N-doping (Ti–O–N species) (Rengifo-Herrera et al. 2009) and band gaps calculated were similar for all materials tested (Table 8). SEM indicated more compact and smoother surface of PC10 (Figure 19). Thickness of the coating was also consequently lower compared to other films, 2-5 μm . PC10 had the highest amount of silicon, originating from a silica binder (Table 7). However, according to study of Guan (2005), Si content of all films, i.e. 10-20 mol%, provides optimum photocatalytic character to the materials. Average size of crystal grains, 24.5 nm, was the highest from all the materials tested. Therefore we presume the lowest surface area for PC10, but also smaller density of crystalline defects. In the opposite, PC500 had the lowest average size of crystal grains, 4.6 nm, what could repress its activity (Chapter 5.1.1.).

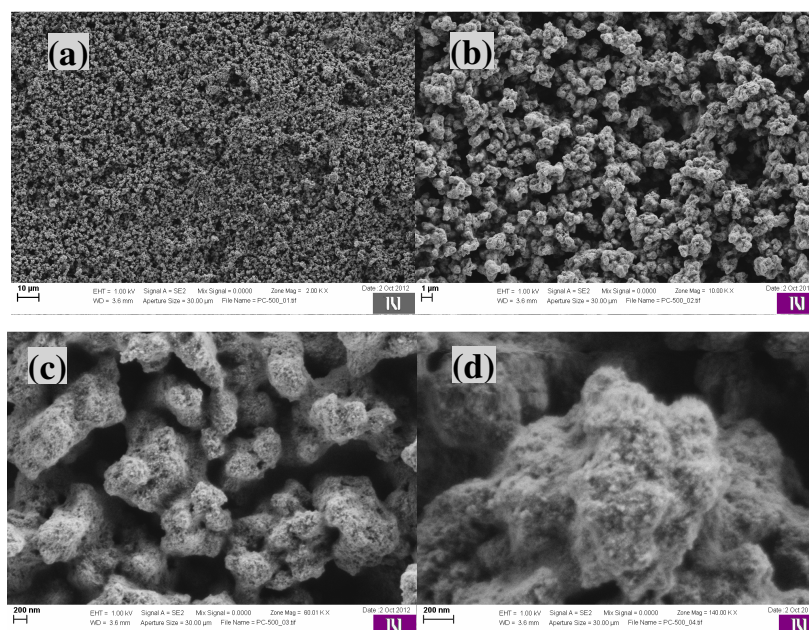


Figure 20: SEM corresponding to photocatalytic coating PC500 deposited on a soda-lime glass, at different magnifications. Scales at the bottom left of micrographs is: 10 μm (a), 1 μm (b), 200 nm (c), 200 nm (d).

In addition, SEM of PC500 showed 5-8 μm film with surface pores spacious enough to trap *E. coli* inside (Figure 20), what could also be one explanation for the observed inactivity of

PC500 film (data not shown). Another explanation could be an excessive capacity of the material for water adsorption, which could result in excess electron-hole recombination (Park et al. 1999). As carbon-doped KRONOcLean 7000 shown no antibacterial activity at all in preliminary tests in ncCTP using daylight and lower activity than P25-PC500 when using UVA, it was not characterized further on (Figure 28). The main properties of coatings tested for water disinfection are listed in Table 8.

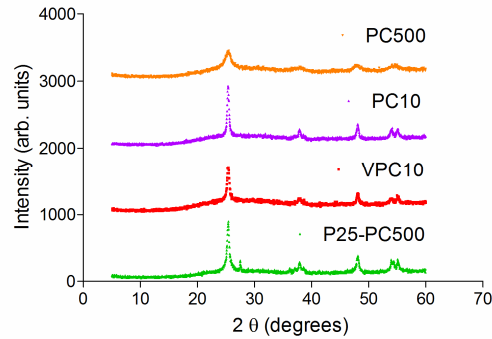


Figure 21: XRD patterns of TiO₂ materials P25-PC500, VPC10, PC10 and PC500 scratched from soda-lime slides, prepared for disinfection tests in CTP reactor.

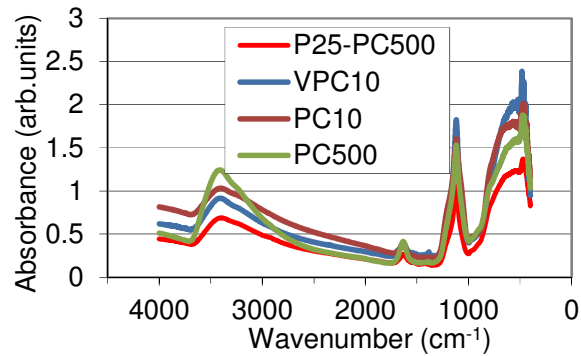


Figure 22: FT-IR spectra of P25-PC500, VPC10, PC10 and PC500 powders scratched from soda-lime slides, prepared for disinfection tests in CTP reactor.

Table 7: Elemental composition of photocatalysts used in water disinfection tests in CTP. Atomic percentages of the elements are reported, as obtained by XPS analysis (measured by S. Gross (University of Padova, Italy))

Samples	Elements (atomic %)									Si/Ti Ratio
	O	C	Si	Ti	Na	N	S	Ca	Cl	
P25-PC500	45.6	20.6	15.1	12.0	0.0	0.3	6.3	0.0	0.1	1.3
VPC10	53.1	18.0	16.7	8.5	2.7	0.7	0.2	0.0	0.0	2.0
PC10	55.7	15.3	19.4	7.3	2.0	0.4	0.0	0.0	0.1	2.7

Table 8: Overview of the main properties of TiO₂-SiO₂ coatings tested as materials for water disinfection.

Samples→ Characteristics↓	P25-PC500	VPC10	PC10	PC500
crystalline phase, doping	anatase mostly, partly rutile	anatase, N- doped	anatase	anatase, amorphous
N content (atomic %)	0.3	0.7	0.4	1.0
crystals size (nm)	22.1	14.2	24.5	4.6
BET surface (m ² / g)	144	116	/	274
thickness (μm)	5-9	5-6	2-5	5-8
band gap (eV)	3.24	3.24	3.16	3.31
appearance	white rough microcracks	white rough microcracks	white compact microcracks	white rough microcracs
hydroxylation	good	good	good	extreme

5.2 Assessment of antibacterial activity of photocatalytic materials

5.2.1 Preliminary evaluation of self-disinfecting coatings by fluorescence microscopy

Fluorescence microscopy is mainly used for the assessment of physiological states of microorganisms after being exposed to photocatalysis (Josset et al. 2007; Dunlop et al. 2010; Pablos et al. 2011; Cai et al. 2013). Preliminary evaluation of LIVE/DEAD[®] BacLight™ Bacterial Viability Kit L7012 with fluorescent microscopy confirmed its usability for evaluation of the bacterial samples, exposed to photocatalysis (Figure 23). PI and SYTO 9 are two nucleic acid dyes, which are the major constituents of LIVE/DEAD[®] BacLight™ Bacterial Viability Kit. SYTO 9 is a green fluorescent nucleic acid dye, which generally labels all bacteria in a population, those with intact membranes and those with damaged membranes. On the other hand, PI could penetrate only bacteria with damaged cytoplasmic membranes, causing a reduction in fluorescence of the SYTO 9 dye, by replacement of SYTO 9 in binding sites because of its higher affinity towards nucleic acids, and through fluorescence resonance energy transfer (FRET) from SYTO 9 to PI when both dyes bind in close vicinity.

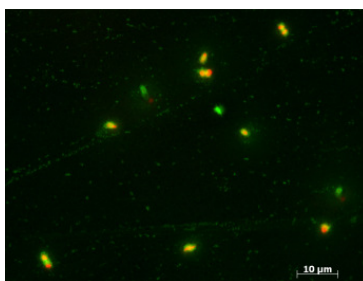


Figure 23: Fluorescence image of stained *E. coli* after photocatalysis. Bacterial cells were exposed on photocatalytic film, under UVA (20 W/m^2), for 4 h, collected from surface, stained by BacLight (Life Technologies) and analysed by fluorescent microscope. Green cells have preserved integrity of their membranes, i.e. are alive, red cells lost membrane integrity, i.e. are dead, and red-green bacteria are somewhere between the two boundary physiological states (Image acquired by E. Fabbretti).

Thus, with an appropriate mixture of the SYTO 9 and PI, bacteria with intact cell membranes are fluorescent green, whereas microbes with damaged membranes are fluorescent red

(probes.invitrogen.com/media/pis/mp07007.pdf; probes.invitrogen.com/media/pis/mp34952.pdf; Stock 2004; Berney et al. 2007b). From our result it is evident that *BacLight* can detect differently impaired *E. coli* cells after UVA-photocatalytic treatment. In Figure 23 one could clearly see still alive green cells and co-localization of green and red signals in different amounts as a consequence of differently impaired membranes' integrity of bacteria.

5.2.2 Antibacterial evaluation of self-disinfecting coatings by microplate-based spectrofluorimetric assays

First, we tested the capability of *E. coli* to grow in nutrient medium (biomass increase) and the metabolic activity (XTT assay) after being exposed to surfaces coated with photocatalytically active films in the presence of UVA. Bacterial growth was followed by gradual biomass increase in ca. 16 hours post-exposure (Figure 24, left panels). In parallel, the transformation of XTT into formazan was quantified in order to assess the reducing activity of bacteria (Figure 24, right panels). Bacterial growth was inhibited by all photocatalytic treatments in comparison to the negative control. Both, longer exposure time and higher specific photo-oxidative efficacy of the different surfaces prolonged the initial lag phase. The curves corresponding to the XTT conversion into formazan confirm the bacterial metabolism inhibition. UVA treatment in the absence of photoactive coating causes inhibition in the bacterial growth and metabolic activity (Figure 24g and h), but this effect is not time-dependent since longer exposure times had almost no additional effect, probably as a consequence of the *E. coli* adaptive responses to UVA (Hoerter et al. 2005). After the initial inactivation of proportion of bacteria, antioxidant defense and repair mechanisms allow the remaining bacteria to adapt and restart growing. It is more likely that initial growth arrest of the photocatalytically treated bacterial samples reflects photolytic activity of UVA irradiation alone, while longer exposure times clearly showed photocatalyst-dependent growth inhibition, which was observed as a prolongation of the initial lag phase of growth and metabolic activity curves. In agreement with previous reports, the contact of bacteria with TiO₂-structured films in the dark had no effect on the bacterial viability. Both bacterial growth and XTT conversion are almost identical in control and treated bacteria, which were maintained in the dark (Figure 24a-f). This observation also suggests a complete removal of *E. coli* bacteria from photocatalytic films (also from more hydrophilic UVA-activated) by simple pipet washing with nutrient media. Three tested TiO₂-coatings used for the method development (P25-PC500 AL, 19T and Pilkington Activ™) inhibited bacterial growth and

metabolic activity in accordance to their predicted photocatalytic potential. Gogniat et al. (2006) showed that the rate of adsorption of cells onto TiO₂ is positively correlated with its bactericidal effect. Better inactivation of *E. coli* as a consequence of a better adhesion between the bacteria and the photocatalyst was also observed by Guillard et al. (2008), where the effect was strongly related to the larger surface area of photocatalyst. Rough morphology of thicker P25-PC500 AL films observed in SEM images could therefore improve adsorption capacity of the catalyst and could explain the higher P25-PC500 AL photocatalysis efficiency. Also, nitrogen-doped photocatalyst surface morphology is believed to improve bacterial adsorption on material and, therefore, its antibacterial activity. Both microplate-based assays showed rather similar patterns of inhibition for all photocatalysts and controls, indicating that metabolic impairment inevitably results in a growth delay, and giving the possibility that either of them is selected alone for the antibacterial evaluation of photocatalytic coatings.

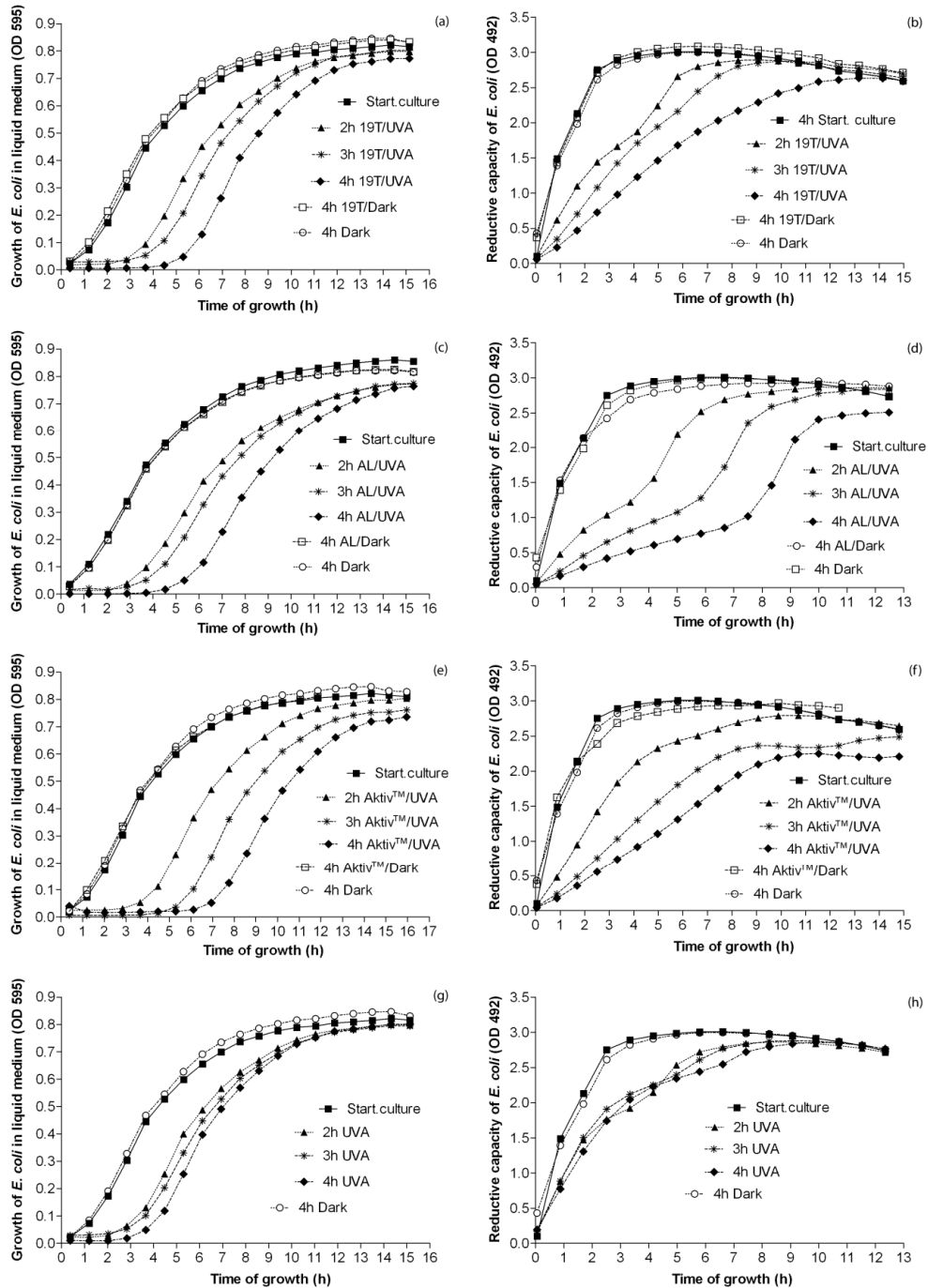


Figure 24: Growth and metabolic activity of *E. coli* exposed to UVA-activated photocatalytic coatings. Curves show the increase in bacterial biomass (absorbance at OD 595; left panels) and metabolic reduction of XTT into a formazan compound (absorbance at OD 492; right panels) up to 16 hours after the exposure. Bacterial samples were exposed to photocatalysts 19T (a and b), P25-PC500 AL (c and d), Pilkington Aktiv™ (e and f) or UVA alone (g and h). Empty substrates (Dark) and all photocatalytic samples (e.g., AL/Dark) kept in dark for 4 hours were negative controls. Initial bacterial density was 1×10^9 *E. coli*/mL (4×10^8 CFU/mL). Exposure times were 2, 3 and 4 hours (to

ca. 20 W/m²). Starting bacterial cultures (Start. culture) represent bacterial suspension prior exposure to any of the photocatalysts or ceramic substrate. Results of one representative experiment of at least three performed by microplate-based XTT and growth assay are presented.

Some concerns have been raised also by Cai et al. (2013) that *BacLight* may not be applicable for the assessment of antimicrobial effects following UV-induced photocatalytic exposure due to its tendency to show higher viability as compared to other methods. Based on the calibration curve (Figure 5) and by attribution of 100% viability to the negative control (Dark), P25-PC500 AL-exposed bacterial samples consisted of approximately 75% viable cells after 4-hours of treatment. No significant effect on viability could be observed also for other photocatalytically treated samples and control samples when using UVA irradiation (Figure 25). Previous studies reported the use of *BacLight* in the assessment of UVA related and UVA photocatalysis related alterations in bacterial membrane permeability, although the analyses were based on fluorescence microscopy (Pigeot-Remy et al. 2012) or flow cytometry (Berney et al. 2007a). However, Berney et al. (2007b) detected intermediate cellular states, characterized by different intracellular concentration of SYTO 9 and PI, and linked them to different extent of outer and cytoplasmic membranes injuries in UVA-irradiated *E. coli*.

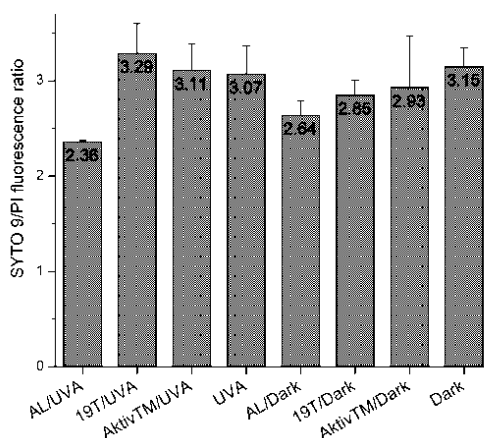


Figure 25: Effect of UVA-activated photocatalytic coatings on *E. coli* membrane integrity. Photocatalysts tested were P25-PC500 AL (AL), 19T and Pilkington Aktiv™ (AktivTM), while non-activated coatings in dark and UVA alone were used as negative controls. Initial bacterial density was 5×10^8 *E. coli*/mL (4×10^8 CFU/mL). Exposure lasted for 4 hours (to ca. 20 W/m²). Data were obtained by using microplate-based *BacLight* assay (Life Technologies). Lower SYTO 9/PI fluorescence ratio corresponds to more compromised bacterial membranes. Bars show mean values (n=2) and SD.

Outer membrane damages enhance membrane permeability for SYTO 9, while PI entrance into bacteria also requires a damaged cytoplasmic membrane. They concluded that these intermediate states could lead to difficulties in the result interpretations that are based on simplified green – live and red – dead partitioning of examined cells by epifluorescence microscopy. We assumed that the occurrence of different intermediate cellular states after UVA or UVA/photocatalyst treatment resulted in low differentiation capability of the *BacLight* assay when measuring the average fluorescence of the cell population in a microplate reader as well as in the inconsistency of the observed cell damages in comparison to the cell impairments detected by microplate-based XTT and growth assays. However, further experiments would be required to determine in more detail what degree of membrane damage corresponds to specific color intensity and how UVA and photocatalysis of different strength could affect the whole population read-out of the *BacLight* assay in antibacterial evaluation of photocatalytic coatings.

5.2.3 Comparison of microplate-based spectrometric growth and XTT assays and colony count

Next, we performed a quantitative analysis of the results from growth and XTT microplate-based assays and compared them to the colony count. To this end, we used the growth- and XTT-generated data and determined at what times post-treatment *E. coli* cultures reach the set threshold values in the middle of exponential phases; absorbance 0.3 at 595 nm for growth assay and 1.5 at 492 nm for XTT assay. Data are collected in Table 9, where they are compared to the conventional colony count assay. Although all three assays showed similar general pattern of photocatalytic effects on bacteria, both microplate-based assays exerted higher sensitivity and reliability as compared to the colony count, clearly distinguishing photocatalyst with different activity and giving reproducible data in repeated experiments. It became evident that photo-exposure caused injuries which are not lethal but inhibit bacterial metabolism and the successive growth and division, which was clearly seen in growth and XTT assays. Regardless there is a mixture of two quite different TiO₂ particles (P25 and PC500) in P25-PC500 AL, which could make the photocatalytic properties of the resulting films not so reproducible for different batches, we didn't observe very high SD for AL photocatalysts (prepared in more batches) compared to other two photocatalyst in the study. Nevertheless, a slightly higher SD for AL, which were attributed to higher activity of these

photocatalysts as SD increased with antimicrobial strength of materials, were reduced with few more repeats (Table 9).

Table 9: Comparison of two microplate-based assays and the colony count method for the antibacterial evaluation of photocatalytic coatings. The antibacterial effect of three photocatalytic coatings (P25-PC500 AL, 19T and Pilkington Activ™) were tested after UVA exposure (ca. 20 W/m²) of 2, 3 and 4 hours. The initial bacterial density was of 1 x 10⁹ E. coli/mL (4 x 10⁸ CFU/mL). Data were obtained by microplate-based XTT and growth assays and colony count assay. Table shows time periods in which bacteria reached the threshold value 1.5 (at OD 492) in the XTT assay and the threshold value 0.3 (at OD 595) in the growth assay. Colony count column shows the number of colonies detected on the solid nutrient agar plates 24 hours after plating. All three assays were performed in parallel. Starting bacterial cultures (Start. culture) represent bacteria solutions prior exposure to any of the photocatalysts or ceramic substrate. UVA and Dark only bacteria samples were exposed to UVA or kept in dark on empty ceramic substrate. Other negative controls include E. coli, kept on the photocatalysts in dark. Tests were repeated three or more times, but colony count did not always result in countable plates (n values lower than 3). Mean values and SD are displayed.

UVA SAMPLES	Microplate-based						Colony count		
	XTT assay			Growth assay			mean values (CFU/mL)	SD (CFU/mL)	n
	mean values (h)	SD (h)	n	mean values (h)	SD (h)	n			
2 h AL/UVA	4.11	0.33	8	5.25	0.25	8	2.27 x 10 ⁸	1.44 x 10 ⁸	4
3 h AL/UVA	5.69	0.99	7	6.63	0.55	7	6.44 x 10 ⁷	6.30 x 10 ⁷	5
4 h AL/UVA	8.15	2.01	6	8.25	1.49	6	7.85 x 10 ⁷	2.80 x 10 ⁷	3
2 h 19T/UVA	2.52	0.82	4	4.97	0.24	4	3.27 x 10 ⁸	1.09 x 10 ⁸	3
3 h 19T/UVA	3.22	0.60	4	5.66	0.79	4	2.09 x 10 ⁸	5.73 x 10 ⁷	2
4 h 19T/UVA	4.81	0.92	5	7.02	0.45	5	1.47 x 10 ⁸	5.50 x 10 ⁷	3
2h Akt/UVA	2.15	0.51	6	5.78	0.60	6	2.12 x 10 ⁸	5.34 x 10 ⁷	5
3 h Akt/UVA	3.24	1.39	7	6.80	0.59	7	1.46 x 10 ⁸	2.07 x 10 ⁷	6
4 h Akt/UVA	5.08	1.58	7	7.88	0.70	7	8.48 x 10 ⁷	4.97 x 10 ⁷	4

Table 9 continues to the next page↓

2 h UVA	1.56	0.34	4	4.58	0.21	4	3.73×10^8	8.48×10^7	4
3 h UVA	1.58	0.31	3	5.07	0.11	3	3.12×10^8	1.95×10^7	3
4 h UVA	1.78	0.45	4	5.53	0.52	4	3.14×10^8	8.11×10^7	3
CONTROLS									
4 h AL/Dark	0.93	0.17	6	2.61	0.12	6	5.40×10^8	--	1
4 h 19T/Dark	1.03	0.11	3	2.45	0.11	3	3.36×10^8	8.49×10^6	2
4 h Akt/Dark	0.68	0.12	5	2.49	0.07	5	2.44×10^8	--	1
4 h Dark	1.01	0.18	6	2.66	0.12	6	4.16×10^8	5.74×10^7	3
Start.cult.	0.86	0.15	8	2.64	0.33	8	3.89×10^8	5.61×10^7	4

With P25-PC500 AL photocatalyst having the most pronounced inhibitory effect, the time necessary for reaching $OD_{595} = 0.3$ in growth assay and $OD_{492} = 1.5$ in XTT assay increases from 2.64 ± 0.33 to 8.25 ± 1.49 h and from 0.86 ± 0.15 to 8.15 ± 2.01 h after 4-hour exposure, respectively (Table 9). Next important characteristic is the dynamic range of the assay, defined as a range of densities over which the method performs in a linear manner with an acceptable level of accuracy and precision. Dynamic range of the microplate-based methods was observed to be high (Figure 6), and thus enabling simple detection of any inhibition in growth or metabolic activity. The same applies to the colony count method. However, labor- and material-intensive serial dilutions are needed to obtain countable plates within the useful range of 30-300 colonies, and great care must be taken during dilution and plating to ensure accuracy of results (Koch 1994). In contrary, sensitivity of colony count was observed to be low, differently from microplate-based growth and XTT assays, both of which exhibit a high sensitivity, where either difference in bacterial densities or growth/metabolic inhibition can be detected.

Images of bacterial colonies grown on the solid nutrient medium in Figure 26 demonstrate that the exposure to activated photocatalysts (Figure 26a-c) and to UVA alone (Figure 26d) resulted in heterogeneous bacterial colonies as compared to the non-irradiated controls (Figure 26e-f), which most likely reflects metabolism impairments and growth delay. As a result, the number of colony alone is not informative enough, as exemplified by the case of bacterial cultures exposed to UVA only. While growth assay clearly showed a growth inhibition after the 2-hour irradiation, colony count did not detect any noticeable effect of UVA 24 hours after irradiation as concluded from the number of colonies. Bacteria were attenuated, but alive and able to recover, however colony count was not able to detect this

effect of the treatment. Robertson et al. (2005) noticed that after the UVA-treatment of drinking water, slow-growing bacterial phenotypes, SCV, appeared on nutrient plates. It is interesting that they did not observe SCV in the UVA/TiO₂ system, while in our study we detected the strongest appearance of SCV in samples exposed to UVA-irradiated Pilkington Activ™ (Figure 26c). Comparison between microplate-based growth assay and colony count assay also shows that they do not always provide the same information; like for time-dependent efficiency of P25-PC500 AL film and the effect of photolysis (Table 9). We observed that the colony count method lacks sensitivity and accuracy which are highly desirable in evaluation of photocatalysts where differences in the activity are not very high and in the photocatalytic materials development. High inter- and intra-experimental variability severely affects the capability of colony count to differentiate between closely related photocatalysts. Sensitivity of colony count is lower because the method itself gives only the number of viable cells, which were able to form colonies, and provide no information about the potential cell impairments that manifest in the growth delay, that is in smaller colonies. Indeed, we observed heterogeneous colonies in photocatalyst/UVA-treated bacteria, most likely reflecting sublethal radical attack that could result in SCV (Ede et al. 2012).

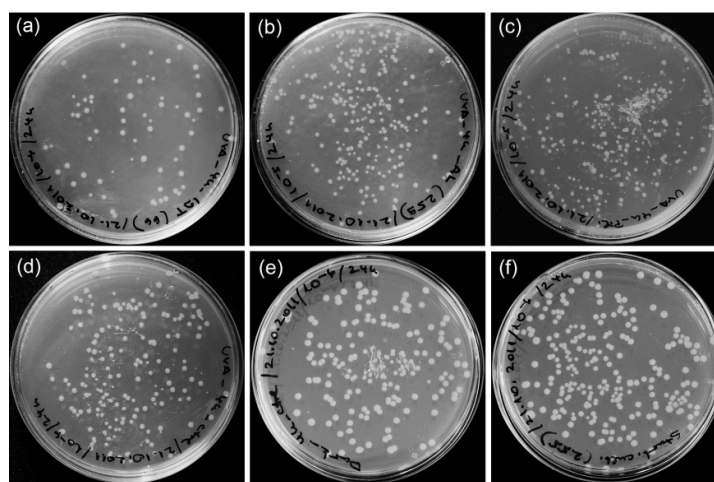


Figure 26: Effect of photocatalysis and photolysis on *E. coli* colony size. Representative images show bacterial colonies on solid nutrient medium evolved from bacteria exposed to UVA-activated photocatalytic films P25-PC500 AL (a), 19T (b), or Pilkington Activ™ (c), UVA-irradiated pure ceramic substrate (d), non-irradiated ceramic substrate (e) and the control non-treated bacteria (f). Bacterial samples at the density of 1×10^9 *E. coli*/mL (4×10^8 CFU/mL) were exposed to treatment for four hours. Images were obtained after 24 hours of growth at 37 °C. One representative experiment of at least two performed is shown.

In contrast to colony count method, microplate-based XTT, and growth assays were also able to detect sublethal changes, which resulted in the reduced metabolism and growth delay. Based on our observations, we believe that the examined photocatalytic coatings affect bacteria at two levels. To some extent they reduce the number of viable bacteria in the exposed samples, affecting the most susceptible bacteria. This can be observed by the colony count. However, it is evident that they also cause injuries which are not lethal but inhibit bacterial metabolism and the successive growth and division, which was clearly seen in growth and XTT assays. Inhibitory effects increase when longer exposure times or stronger photocatalysts are applied. Regardless of its disadvantages, colony count is often the method of choice in quantitative evaluation of antibacterial properties of different photocatalysts (Robertson et al. 2005; Wong et al. 2006; Gogniat et al. 2006; Guillard et al. 2008; Ditta et al. 2008; Ede et al. 2012), and therefore enables comparison of results among different research studies.

5.2.4 Validation of UVA-tested microplate-based assays by visible light-induced photocatalytic coatings

We further applied microplate-based XTT and growth assay as well as *BacLight* assay to *E. coli* exposed to Vis (daylight)-activated photocatalytic films, P25-PC500 AL coating and its VPC10 nitrogen-doped analogue. Vis (Figure 27) alone did not have any significant effect on bacterial growth or metabolic activity as observed from growth and XTT assay (Figure 27a and b). However, both photocatalytic coatings showed strong reduction in the *E. coli* growth and, even more, in the XTT transformation when activated with Vis. Interestingly, it appeared that in both assays the VPC10 N-doped TiO₂ is more effective at high bacterial densities (5×10^8 *E. coli*/mL), and P25-PC500 AL photocatalyst at low bacterial density (5×10^6 *E. coli*/mL). In strong contrast to UVA-irradiated photocatalysts, *BacLight* assay proved to be very sensitive and capable to discriminate among different experimental conditions, namely two bacterial densities and two photocatalysts, after 4-hour exposition to the Vis (Figure 27c). Results demonstrate strong negative influence of photocatalysis on *E. coli* membranes integrity. Additionally, there is no significant difference between SYTO 9/PI fluorescence ratios of bacteria kept on empty ceramics in dark and bacteria exposed to visible lamp only, suggesting that the Vis alone (at this intensity) has rather small effect on bacterial membrane integrity. VPC10 nitrogen-doped TiO₂ photocatalyst had stronger effect than its

P25-PC500 AL analogue and diluted bacteria (5×10^6 *E. coli*/mL) were more sensitive than concentrated cultures to membrane damages promoted by photocatalysis.

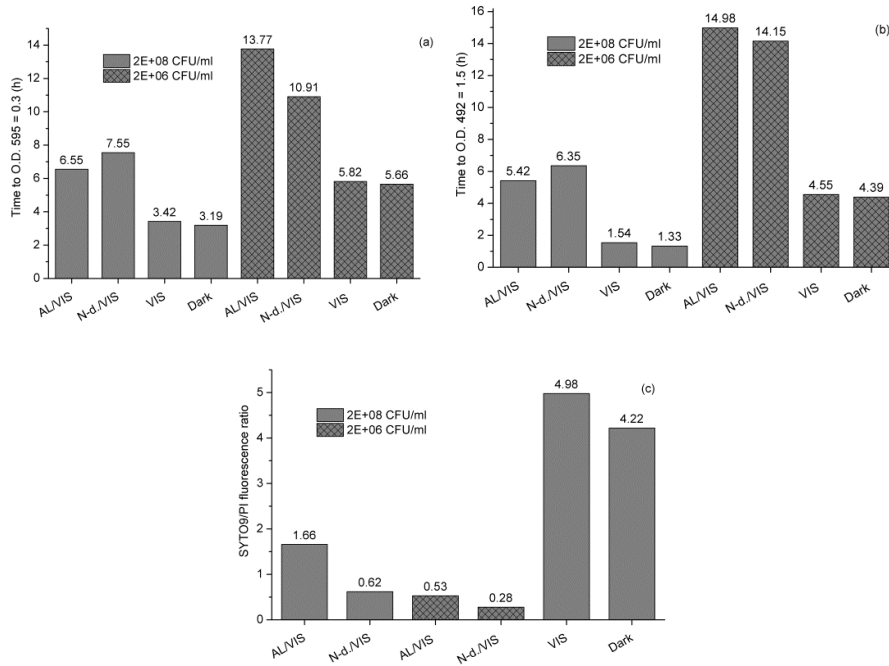


Figure 27: Validation of microplate-based assays in the antibacterial evaluation of Vis-activated photocatalytic coatings. XTT, growth and BacLight assays were performed on *E. coli* exposed to P25-PC500 AL and VPC10 N-doped AL photocatalysts for 4 hours. Two *E. coli* densities were tested: 5×10^8 (plain) and 5×10^6 (grid) per mL. Bars show time periods in which bacteria reach the value 0.3 (OD 595) in the growth assay (a) and the value 1.5 (OD 492) in the XTT assay (b). Higher threshold values correspond to more impaired bacterial growth (a) or metabolic activity (b). Note that lower bacterial densities result in higher starting threshold values (grid bars in graphs a and b). Lower SYTO 9/PI fluorescence ratio corresponds to more compromised bacterial membranes (c). Bacterial samples kept on empty ceramics in dark (Dark) or under interior daylight (Vis) were used as controls. Experiment was performed only once.

5.2.5 *E. coli* inactivation in simplified water disinfection process

5.2.5.1 Disinfection by a prototype ncCTP

Experiments were performed as part of characterization of a prototype photocatalytic system – ncCTP reactor designed for Electrolux Italia s.p.a. (Kete et al. 2012). Bacteria in saline

were exposed to UVA activated P25-PC500 and carbon-doped KRONOcLean 7000 films, to UVA alone and to Vis-activated carbon-doped KRONOcLean 7000 photocatalysts and were then assessed with microplate-based assays and colony count assay, similar to self-disinfecting photocatalytic coatings (Chapter 5.2.2). Saturation of solution with oxygen varied from 86-100% (6.9-9.1 mg/L) obtained by mild oxygen bubbling, which was sufficient to mix water to prevent precipitation of microorganisms and to enable sufficient mass transfer during disinfection.

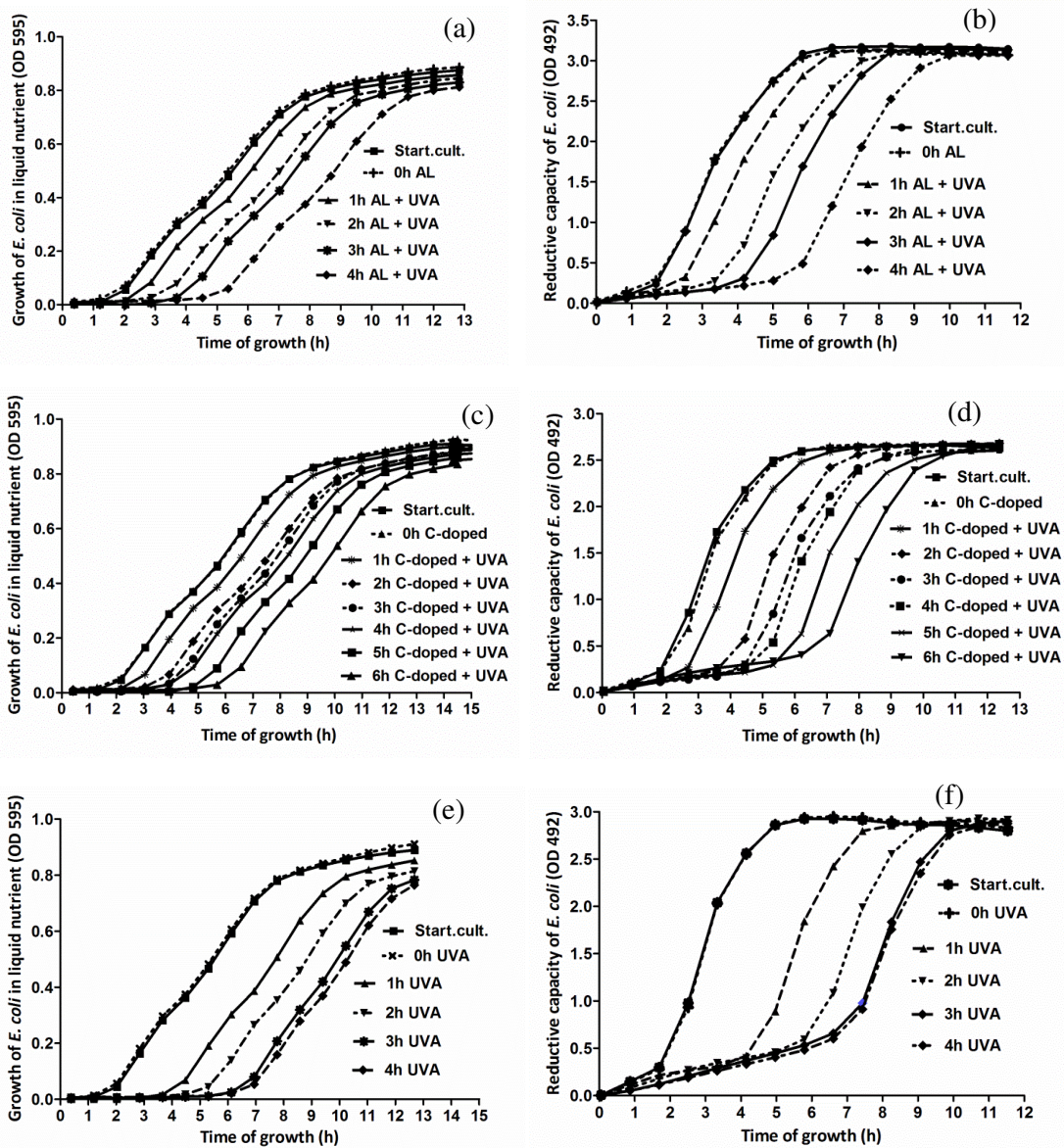


Figure 28 continues to the next page ↓

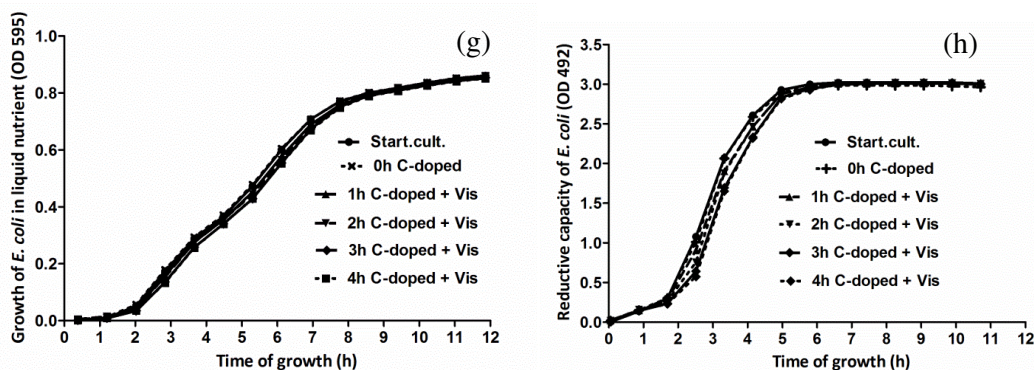


Figure 28: Growth and metabolic activity of *E. coli* exposed to UVA- and Vis-activated photocatalysts in prototype ncCTP reactor. Curves show the increase in bacterial biomass (absorbance at OD 595; left panels) and metabolic reduction of XTT into a formazan compound (absorbance at OD 492; right panels) up to 13 hours after the exposure. Bacterial samples were exposed to UVA-activated P25-PC500 AL and carbon-doped KRONOcClean 7000 films (a-d), UVA alone (e and f) and to Vis-activated carbon-doped films (g and h). Initial bacterial density in reactor was $2-4 \times 10^8$ *E. coli*/mL ($5-9 \times 10^7$ CFU/mL). Exposure times were up to 6 hours. Starting bacterial cultures (Start.cult.) were not introduced into reactor. Analyzed bacteria were sampled before photocatalytic treatment (0 h), and after 1, 2, 3, 4 and, exceptioanally, 6 hours of exposure. Experiment was performed only once.

The temperature increased from the room temperature – ca. 25 °C to maximum 32 °C at the end of the 4-6 hours tests, which is not considered as a temperature that could affect photocatalytic disinfection (Chapter 2.6.2.2). pH dropped starting from 5.5-6.0 to 5.2-5.5 at the end of experiments and could be attributed to the compounds generated during photocatalysis. These pH values represent appropriate conditions for good contact between negatively charged bacteria and positively charged photocatalyst, therefore efficient disinfection could be achieved (Chapter 2.6.2.3; Sichel et al. 2007; Foster et al. 2011). In contrast to the results from self-disinfecting coatings assessment, UVA/photocatalytic systems showed lower antibacterial activity than UVA lamps alone (photolysis) (Figure 28a-f). This was explained by different, more light-concentrating space in an empty reactor tube, which predominates photocatalytic conditions achieved in the same reactor tube with inserted photocatalytic plates. Additional experiments would be needed with the reactor tube filled with blank plates in order to obtain the same conformation and light distribution as in photocatalytic experiments. However, regarding microplate-based growth and XTT assay, activity of photocatalytic systems continued to increase with the irradiation time (Figure 28a-

d), while disinfection ability of UVA alone was stopped at three hours. Sample exposed to UVA alone for four hours behaved similarly as three hours sample (Figure 28e and f). The same was observed in evaluating self-disinfecting coatings (Figure 24) and was explained in Chapter 5.2.2. Therefore, with prolonged exposure time or improved activity of the photocatalytic systems antimicrobial trends are expected to be different, i.e. efficiency of the photocatalysis would overcome the effect of UVA photolysis, as it is generally observed (Chapter 2.5.1). Carbon-doped KRONOcLean 7000 TiO₂ sample expected to work under Vis (Chapter 2.4), did not show any activity on *E. coli* during four hours of exposure (Figure 28g and h). Quantitative outcome of photocatalytic tests performed in ncCTP reactor is presented in Table 10. Differently from previous experiments with self-disinfecting coatings (Chapter 5.2.3), slow-growing bacterial phenotypes recovered on solid nutrient media (colony count assay) only from bacteria exposed to UVA alone for three and four hours (longer exposure), in agreement with results of Robertson et al. (2005). In terms of size, photocatalysis did not result in heterogenous colony population (Figure 29).

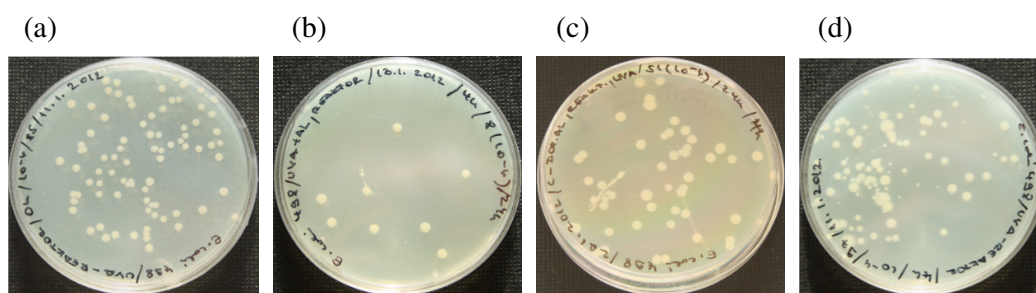


Figure 29: Effect of photocatalysis and photolysis on *E. coli* colony size. All water disinfecting conditions were studied in ncCTP. Representative images show bacterial colonies on solid nutrient medium evolved from bacteria; before illumination (a), exposed to UVA-activated photocatalytic films P25-PC500 AL (b), UVA-activated carbon-doped photocatalysts (c) and UVA photolysis (d). Bacterial samples at the density of $2-4 \times 10^8$ *E. coli*/mL were exposed to treatment for four hours. Images were obtained after 20 hours of growth at 37 °C. Experiment was performed only once.

It is worth mentioning here that generation of SCV in drinking water could be a possible health hazard as numerous studies, mostly with staphylococci, indicated an association between SCV and persistent, recurrent and antibiotic-resistant infections (reviewed in Proctor 2006).

Table 10: Quantitative outcome of photocatalytic tests performed in ncCTP reactor. The antibacterial effects of three different photocatalytic conditions, UVA-activated P25-PC500 and UVA- and Vis-activated carbon-doped KRONOcLean 7000 photocatalysts, in addition to UVA alone up to 6 h exposure are listed. The initial bacterial density in reactor was 2.4×10^8 *E. coli*/mL. Data were obtained by microplate-based XTT and growth assays and colony count assay. Table shows time periods in which bacteria reached the threshold value 1.5 (at OD 492) in the XTT assay and the threshold value 0.3 (at OD 595) in the growth assay. Colony count column shows the number of colonies detected on the solid nutrient agar plates 24 hours after plating. All three assays were performed in parallel. Starting bacterial cultures (Start.cult.) represent bacteria solutions that were not introduced into reactor, while 0 h samples represent bacteria samples taken from reactor prior the illumination. For microplate-based XTT and growth assay threshold values were compared with the thresholds values for the standard bacterial samples (Figure 7) and corresponding densities for treated samples were calculated (e.g. 4 hours P25-PC500 sample behaved regarding metabolic activity as 3.36×10^5 untreated *E. coli* and grew as 5.49×10^5 untreated *E. coli*). Experiment was performed only once.

SAMPLES	Microplate-based assays				
	XTT assay OD 492=1.5 (h)	Density (<i>E. coli</i> /mL)	Growth assay OD 595=0.3 (h)	Density (<i>E. coli</i> /mL)	Colony count (CFU/mL)
P25-PC500 /UVA					
0 h	3.08	2.15×10^8	3.63	2.29×10^8	6.50×10^7
1 h	4.20	3.41×10^7	4.39	6.16×10^7	5.50×10^7
2 h	4.93	1.03×10^7	5.29	1.30×10^7	4.00×10^7
3 h	5.65	3.14×10^6	5.91	4.45×10^6	2.15×10^7
4 h	7.01	3.36×10^5	7.12	5.49×10^5	8.00×10^6
C-doped /UVA					
0 h	3.21	1.53×10^8	3.76	1.70×10^8	4.80×10^7
1 h	3.91	4.40×10^7	4.42	5.69×10^7	3.50×10^7
2 h	5.00	6.92×10^6	5.28	1.37×10^7	2.96×10^7
3 h	5.63	3.00×10^6	5.73	6.47×10^6	3.80×10^7
4 h	5.93	1.88×10^6	5.94	4.56×10^6	3.81×10^7
5 h	6.60	6.60×10^5	6.70	1.29×10^6	4.05×10^7
6 h	7.57	1.45×10^5	7.54	3.20×10^5	3.60×10^7

Table 10 continues to the next page↓

UVA alone					
0 h	2.93	1.93×10^8	3.69	1.76×10^8	8.50×10^7
1 h	5.49	2.24×10^6	6.10	2.29×10^6	4.80×10^7
2 h	6.99	2.65×10^5	7.26	2.84×10^5	2.94×10^7
3 h	7.93	3.21×10^4	8.44	3.39×10^4	2.03×10^7
4 h	8.00	2.84×10^4	8.77	1.87×10^4	9.70×10^5
C-doped /Vis					
0 h	2.89	1.53×10^8	3.74	1.76×10^8	8.70×10^7
1 h	3.00	1.82×10^8	3.91	1.33×10^8	8.80×10^7
2 h	3.05	1.69×10^8	3.92	1.31×10^8	/
3 h	3.18	1.38×10^8	4.09	9.84×10^7	3.98×10^7
4 h	3.21	1.31×10^8	4.09	9.84×10^7	7.50×10^7
5 h	3.34	1.07×10^8	4.33	6.61×10^7	7.80×10^7
6 h	3.35	1.06×10^8	4.24	7.67×10^7	/
Start.cult.	3.11	2.05×10^8	3.75	1.86×10^8	6.52×10^7

Comparing influence of UVA alone or photocatalysis on bacterial metabolic activity and biomass formation, i.e. bacterial growth (and division) in liquid medium, the same pattern is detected (Figure 28a-f). Results from colony count however, are following a different trend, with the highest effect being observed for UVA between three and four hour exposure (Table 8), indicating impairments of photo-treated cells at the beginning of exposure, which could eventually lead to cell disability to grow on nutrient plates after longer exposure times, i.e. by long-lasting UVA disinfection. *BacLight* again, like for UVA/self-disinfecting coatings (Chapter 5.2.2) did not detect any remarkable effect on cell wall integrity of *E. coli*, exposed to photocatalysis or UVA-photolysis (not shown).

5.2.5.2 Improved disinfection in CTP reactor

As preliminary experiments done in prototype ncCTP revealed a need for further optimization, further water disinfection studies were performed in CTP reactor. CTP configuration was already optimized (Cernigoj et al. 2006). In addition, it needs ca. 7-times less testing bacterial solution than ncCTP. For the experiments, we used TiO₂-SiO₂ photocatalysts P25-PC500, nitrogen-doped VPC10 and its undoped analogue PC10, which differ in the type of commercial titania powder that they contain. The temperature increased from the room temperature – ca. 25 °C to maximum 34 °C at the end of tests (different from

the previous one, this photocatalytic system lacks a sampling point for continuous measurements of e.g. temperature, pH and conc. of O₂ during experiments). Photocatalysts were observed to be active under Vis (ca. 6 W/m² UVA intensity) (Figure 30a-f) and UVA illumination (ca. 60 W/m² UVA intensity) (Figure 31a-f). All photocatalysts in this study highly increased photo-oxidative disinfection rate, in comparison to both, Vis or UVA lights alone (Figure 30 and 31). P25-PC500 was the most active photocatalysts under UVA and Vis (Table 9a and b). Nitrogen-doped VPC10 and its undoped analogue PC10 showed similar activity under Vis and UVA (Table 11a and b), suggesting that doping did not influence TiO₂ particles photocatalytic performance in coatings. Consistent with previous tests too, longer exposures were more damaging for bacteria (Chapters 5.2.2 and 5.2.5.1). Daylight lamps (visible lamps) emits also some UVA irradiation (ca. 6 W/m²), which was more likely to be responsible for the observed activity of all photocatalysts under the Vis (daylight). Therefore, to improve disinfection rate, which is important in water disinfection processes, next experiments were performed with UVA lamps (60 W/m²). This way we also came closer to UV intensities found in the sunlight (20-40 W/m², UV spectra is different from our UVA lamps). Increased UVA intensity enhanced photocatalytic killing. UVA lamps alone were also more detrimental for bacteria than visible lamps (daylight). Therefore, both, photocatalysis and photolysis contribute to disinfection (Chapter 2.6.2.1). In addition photocatalysis and photolysis under UVA and Vis resulted in the formation of SCV on nutrient plates (Chapters 2.8.1, 5.2.3 and 5.2.5.1) (Figure 33). Dark conditions, using either different photocatalysts or bare glass plates placed in the reactor, did not affect bacterial viability (Figure 32 and Table 11c), like in the previous experiments with self-cleaning films and in the ncCTP reactor. XTT and growth assay proved again as very sensitive assays. In addition, and differently from the previous milder photocatalytic conditions in the photocatalytic chamber and ncCTP, colony count and *BacLight* were able to show progression of the photocatalytic killing. However, microplate-based growth and XTT assay were also capable of indicating small injuries at the beginning of disinfection or cell impairments in less harmful conditions, e.g. when visible lamp was the only disinfection agent in the study (Table 11). Therefore, when more stringent photolytic and photocatalytic conditions are used in an antibacterial activity evaluation, any of the assays tested, i.e. standard colony count assay, *BacLight* assay or XTT and growth assay, could be used as detection methods, at least as far as laboratory strain of the *E. coli* is concerned. Differently, less stringent disinfection conditions require more sensitive assays, like microplate-based XTT and growth assays tested in our study. This part of the study also demonstrated

capability of photocatalytic water disinfection for real application; we succeeded in complete removal of microorganisms from water, what was proved by different detection methods. For UVA/P25-PC500 combination we achieved almost complete disinfection as early as 1 hour after exposure (Figure 31a-b). In addition, when harsh disinfection conditions are employed, as in the case of experiments performed in CTP, active bacterial populations may continue to decrease also in the dark, as it has been already shown (Rincon and Pulgarin 2004c). Therefore, it is possible that total disinfection in CTP may require even shorter time of the photocatalytic exposure.

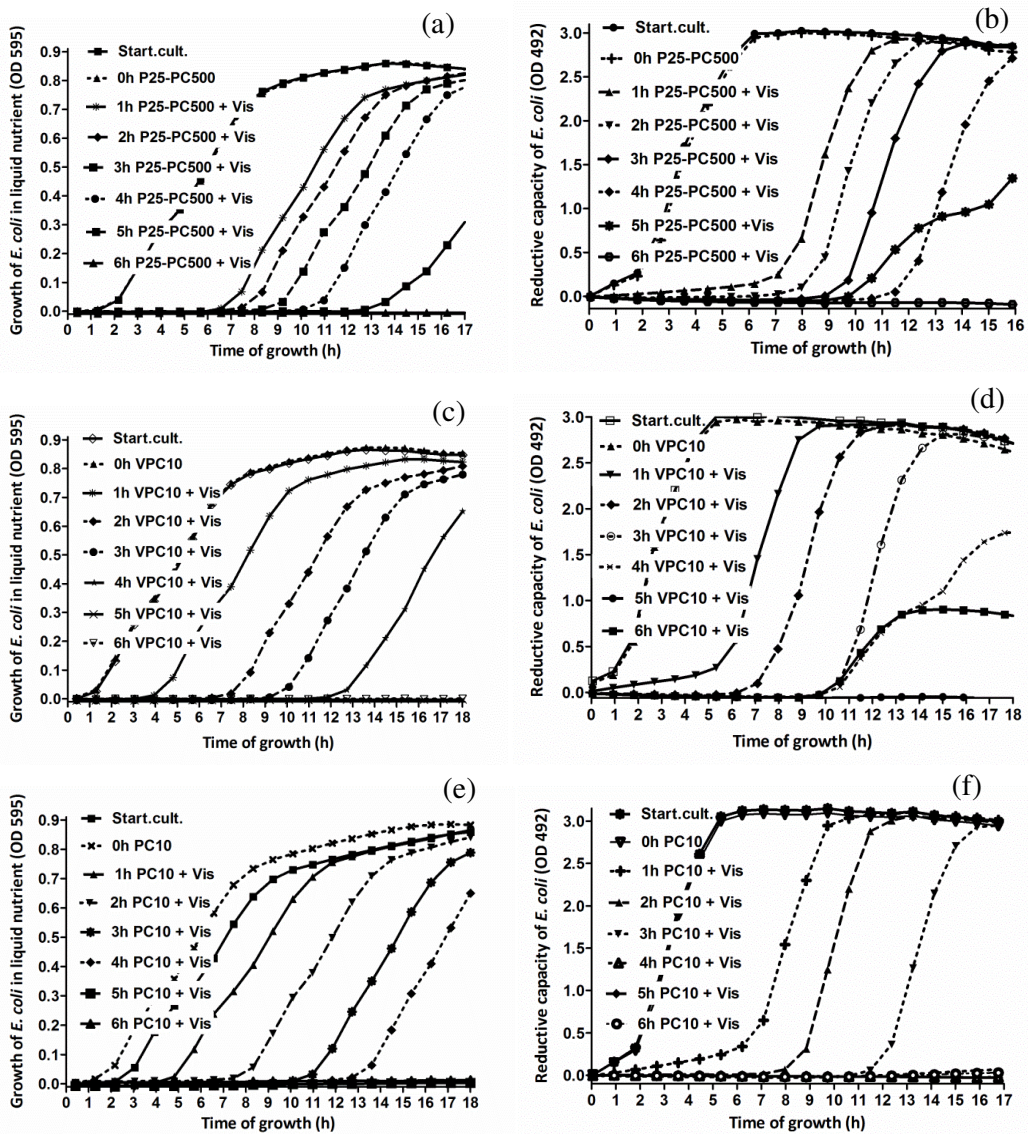


Figure 30 continues to the next page ↓

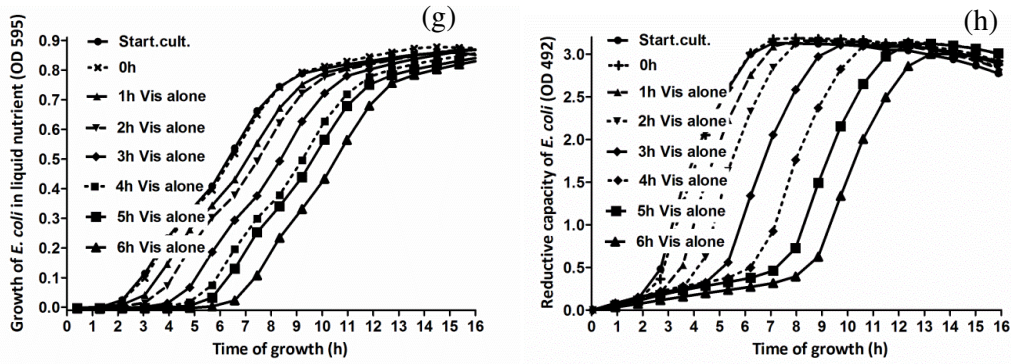


Figure 30: Growth and metabolic activity of *E. coli* exposed to Vis and Vis-activated photocatalysts in CTP reactor. Curves show the increase in bacterial biomass (absorbance at OD 595; left panels) and metabolic reduction of XTT into a formazan compound (absorbance at OD 492; right panels) up to 18 hours after the exposure. Bacterial samples were exposed to Vis-activated P25-PC500 films (a and b), nitrogen-doped VPC10 films (c and d), PC10 films (e and f) and to Vis alone (g and h). Initial bacterial density in the reactor was $1-2 \times 10^8$ *E. coli*/mL ($2-5 \times 10^7$ CFU/mL). Exposure lasted up to 6 hours. Starting bacterial cultures (Start.cult.) were not introduced into the reactor. Analyzed bacteria were sampled before photocatalytic treatment (0 h), and after 1, 2, 3, 4, 5 and 6 hours of exposure. Results of one experiment out of two or more performed by microplate-based XTT and growth assay are presented.

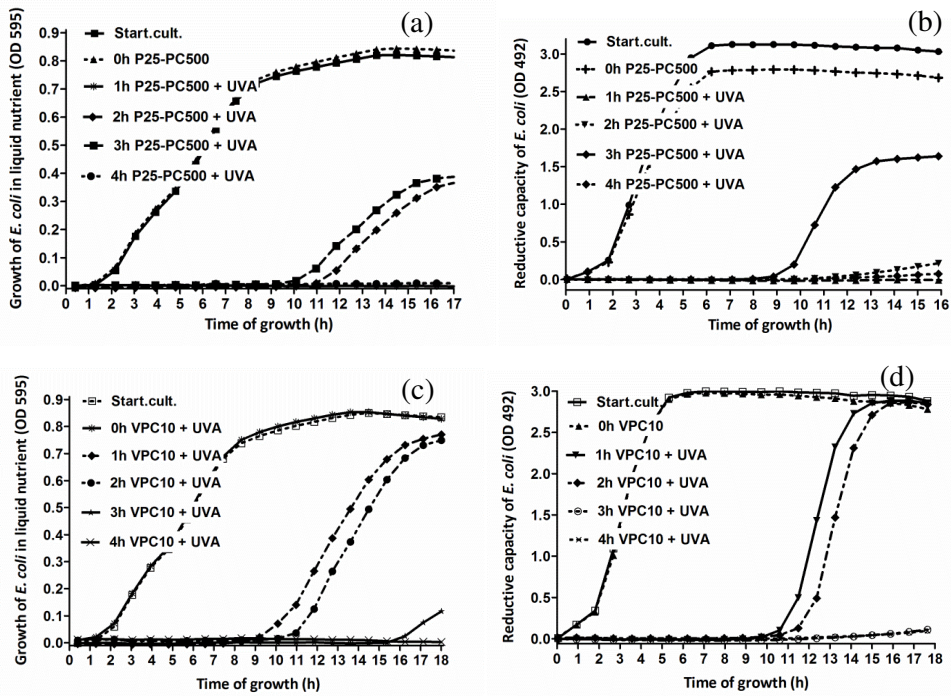


Figure 31 continues to the next page ↓

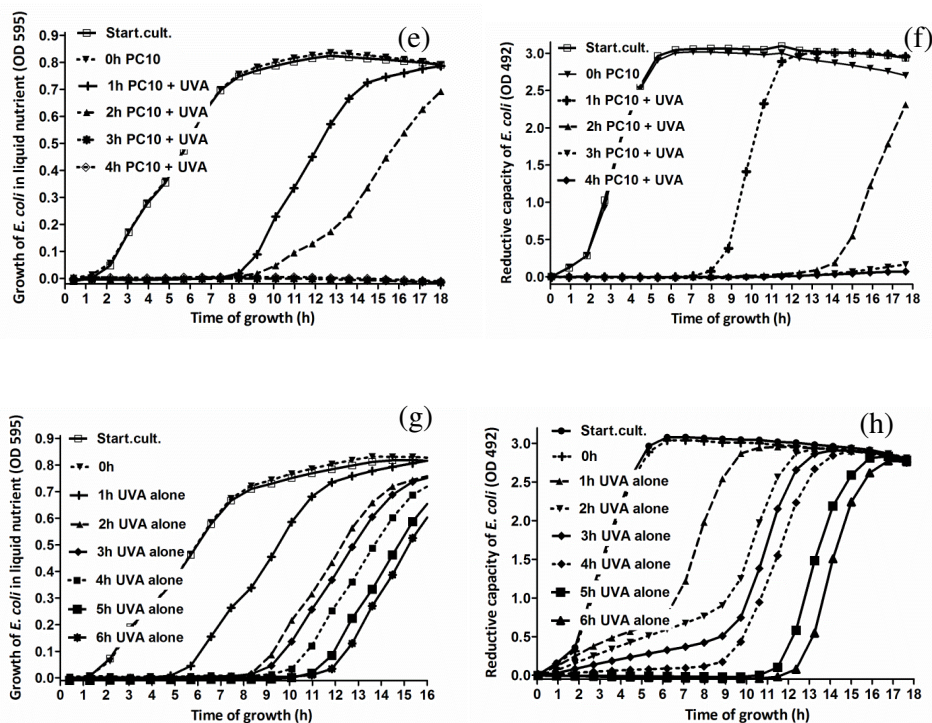


Figure 31: Growth and metabolic activity of *E. coli* exposed to UVA and UVA-activated photocatalysts in CTP reactor. Curves show the increase in bacterial biomass (absorbance at OD 595; left panels) and metabolic reduction of XTT into a formazan compound (absorbance at OD 492; right panels) up to 18 hours after the exposure. Bacterial samples were exposed to UVA-activated P25-PC500 films (a and b), nitrogen-doped VPC10 films (c and d), PC10 films (e and f) and to UVA alone (g and h). Initial bacterial density in the reactor was $1-2 \times 10^8$ *E. coli*/mL ($2-5 \times 10^7$ CFU/mL). Exposure lasted up to 6 hours. Starting bacterial cultures (Start.cult.) were not introduced into the reactor. Analyzed bacteria were sampled before photocatalytic treatment (0 h), and every whole hour up to 6 hours of exposure. One representative experiment of at least two performed is shown.

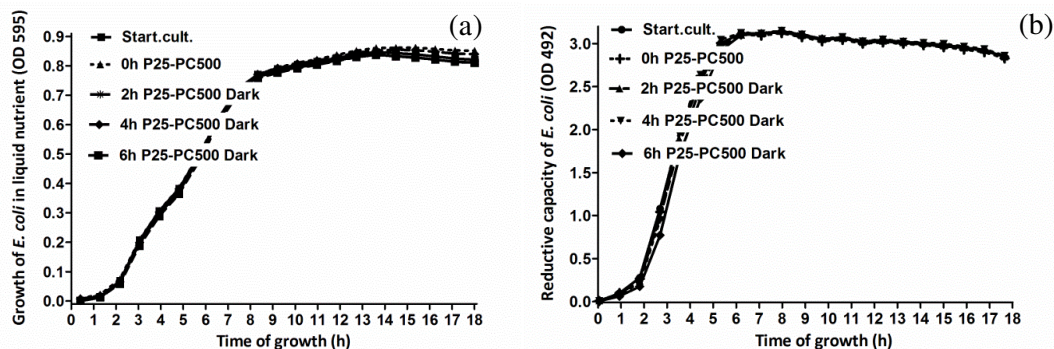


Figure 32: Growth and metabolic activity of *E. coli* exposed in dark to photocatalytic plates P25-PC500 in CTP reactor. Curves show the increase in bacterial biomass (absorbance at OD 595; left

panels) and metabolic reduction of XTT into a formazan compound (absorbance at OD 492; right panels) up to 18 hours after the exposure. Initial bacterial density in reactor was $1-2 \times 10^8$ *E. coli*/mL ($2-5 \times 10^7$ CFU/mL). Exposure lasted up to 6 hours. Starting bacterial cultures (Start.cult.) were not introduced into the reactor. Analyzed bacteria were sampled before photocatalytic treatment (0 h), and after 2, 4 and 6 hours of exposure.

Table 11: Quantitative evaluation of photocatalytic tests performed in CTP reactor. The antibacterial effect of three different photocatalytic films: P25-PC500, nitrogen-doped VPC10 and its undoped analogue were tested for its water disinfection efficiency by using daylight (Vis) (a) and UVA (b) for activation. Exposure lasted up to 6 hours. The initial bacterial density in the reactor was $1-2 \times 10^8$ *E. coli*/mL. Data were obtained by microplate-based XTT, growth and BacLight assays and colony count assay. Tables (a-c) show time periods in which bacteria reached the threshold value 1.5 at OD 492 in the XTT assay and the threshold value 0.3 at OD 595 in the growth assay. Regarding BacLight assay, fluorescence ratios of the SYTO 9 and PI fluorescence were calculated for bacterial samples. Colony count column shows the number of colonies detected on the solid nutrient agar plates 20 hours after plating. All assays were performed in parallel. Starting bacterial cultures (Start. cult.) represent bacteria solutions that were not introduced into the reactor, while 0 h sample represents bacteria samples in reactor prior illumination. Other four control experiments were performed in dark, with all three photocatalysts and with bare glass substrate (c). Higher values in the microplate-based XTT and growth assays correspond to bacterial populations with lower metabolic capacity or with lower ability for biomass formation in liquid nutrient. Lower SYTO 9/PI fluorescence ratio corresponds to more compromised bacterial membranes. ND^x (x = 1, 2) indicates bacterial viabilities in analysed sample, which are below detection limits of assays (non-detectable). Numbers in superscript give numbers of measurements, from which mean values were calculate.

(a)

Vis samples	Microplate-based assays						Colony count (CFU/mL)	
	XTT assay		Growth assay		BacLight assay			
	OD 492=1.5 (h)		OD 595=0.3 (h)		SYTO9/PI fluor.ratio		mean	SD
P25-PC500	mean	SD	mean	SD	mean	SD	mean	SD
1 h	10.66 ³	3.03	10.80 ³	2.67	2.73 ⁴	1.64	--	--
2 h	10.70 ² /ND ²	1.26	10.63 ² /ND ¹	1.05	2.31 ³	1.93	ND ¹	--
3 h	11.18/ND ²	--	11.21 ³ /ND ¹	4.62	1.14 ²	1.00	ND ¹	--
4 h	13.61/ND ²	--	13.76 ² /ND ¹	1.46	2.15 ³	1.81	ND ²	--
5 h	16.49/ND ²	--	16.91/ND ²	--	0.83 ²	0.78	--	--

Table 11 continues to the next page↓

6 h	ND ³	--	ND ³	--	0.35 ²	0.20	ND ²	--
VPC10								
1 h	7.11 ²	0.06	6.20 ²	0.42	2.78 ³	0.37	3.48x10 ⁷⁽³⁾	--
2 h	9.57 ³	0.52	9.49 ³	0.30	2.94 ⁴	0.53	6.73x10 ⁵⁽²⁾	2.43x10 ⁵
3 h	10.99 ³	1.16	11.05 ³	1.04	2.24 ⁴	1.18	2.50x10 ⁴	--
4 h	14.22 ³	1.90	13.61 ³	1.61	1.56 ⁴	1.27	7.26x10 ³⁽⁴⁾	8.10x10 ³
5 h	14.62 ²	0.35	15.05 ²	0.40	1.67 ³	1.37	--	--
6 h	20.64 ²	0.19	16.06 ²	0.04	1.56 ²	2.09	57/ND ²	--
PC10								
1 h	7.04 ²	1.27	6.41 ²	1.22	3.60 ²	0.56	8.33x10 ⁶⁽²⁾	1.03x10 ⁷
2 h	9.30 ²	0.94	9.53 ²	0.88	2.19 ²	0.13	5.80x10 ³	--
3 h	12.04 ²	2.04	11.78 ²	1.99	0.46 ²	0.01	4.80x10 ²	--
4 h	10.79/ND ¹	--	14.33 ²	1.39	0.29 ²	0.01	1.50x10 ¹⁽²⁾	0.00x10 ⁰
5 h	ND ²	--	14.91/ND ¹	--	0.19 ²	0.00	ND ²	--
6 h	ND ²	--	ND ²	--	0.18 ²	0.04	ND ²	--
Vis alone								
1 h	4.17 ³	0.29	4.93 ³	0.27	3.38 ²	1.10	3.48x10 ⁷⁽³⁾	1.03x10 ⁷
2 h	5.06 ³	0.14	5.61 ³	0.06	3.05 ²	0.32	2.37x10 ⁷⁽³⁾	5.53x10 ⁶
3 h	6.08 ³	0.32	6.57 ³	0.13	2.87 ²	0.81	1.39x10 ⁷⁽³⁾	3.39x10 ⁶
4 h	6.74 ³	0.83	7.14 ³	0.30	2.70 ²	0.72	1.53x10 ⁷⁽³⁾	5.34x10 ⁶
5 h	6.89 ²	2.79	6.70 ²	1.74	4.20 ²	0.67	6.24x10 ⁷⁽²⁾	6.88x10 ⁷
6 h	7.00 ²	2.74	7.29 ²	2.32	3.53 ²	0.33	1.42x10 ⁷⁽²⁾	7.71x10 ⁶

(b)

UVA samples	Microplate-based assays						Colony count (CFU/mL)	
	XTT assay		Growth assay		<i>BacLight</i> assay			
	OD 492=1.5 (h)		OD 595=0.3 (h)		SYTO9/PI fluor.ratio			
P25-PC500	mean	SD	mean	SD	mean	SD	mean	SD
1 h	ND ²	--	ND ²	--	0.51 ²	0.11	20	--
2 h	ND ²	--	15.17/ND ¹	--	0.37 ²	0.02	ND ²	--
3 h	16.4 ²	5.32	14.12/NA ¹	--	0.37 ²	0.06	ND ²	--
4 h	ND ²	--	ND ²	--	0.60 ²	0.23	ND ²	--
VPC10								
1 h	11.03 ²	2.00	11.16 ²	1.33	3.25 ²	0.83	4.32x10 ⁴⁽²⁾	5.78x10 ⁴

Table II continues to the next page

2 h	14.27 ²	1.40	13.62 ²	0.85	0.56 ²	0.45	8.30x10 ²	--
3 h	18.91/ND ¹	--	20.08/ND ¹	--	0.27 ²	0.04	ND ²	--
4 h	16.85/ND ¹	--	ND ²	--	0.20 ²	0.07	ND ²	--
PC10								
1 h	10.13 ²	0.40	10.42 ²	0.49	4.03 ²	0.07	1.06x10 ⁴ (2)	1.41x10 ²
2 h	16.63/ND ¹	--	13.73 ²	0.64	1.25 ²	0.57	1.70x10 ²	--
3 h	ND ²	--	ND ²	--	0.29 ²	0.11	ND ¹	--
4 h	ND ²	--	ND ²	--	0.25 ²	0.06	ND ²	--
UVA alone								
1 h	7.18 ²	0.34	7.63 ²	0.34	3.99 ²	0.33	3.04x10 ⁷ (2)	1.36x10 ⁷
2 h	10.3 ³	0.35	10.48 ²	0.50	4.84 ²	0.23	6.60x10 ⁶ (2)	2.83x10 ⁶
3 h	11.51 ²	1.07	11.75 ²	0.61	4.52 ²	1.52	4.84x10 ⁵ (2)	5.89x10 ⁵
4 h	12.39 ²	1.37	11.92 ²	0.46	4.14 ²	1.20	5.50x10 ⁴ (2)	5.94x10 ⁴
5 h	12.46 ²	1.15	12.73 ²	0.87	3.85 ²	1.11	5.57x10 ³ (2)	2.74x10 ³
6 h	13.06 ²	1.51	13.64 ²	0.28	3.48 ²	1.07	1.41x10 ³ (2)	4.81x10 ²

(c)

Control samples	Microplate-based assays						Colony count (CFU/mL)	
	XTT assay		Growth assay		<i>BacLight</i> assay		mean	SD
	OD 492=1.5 (h)		OD 595=0.3 (h)		SYTO9/PI fluor.ratio			
	mean	SD	mean	SD	mean	SD		
0 h	3.43 ¹⁸	0.27	4.19 ²⁰	0.22	3.12 ¹²	0.44	5.24x10 ⁷ (22)	1.64x10 ⁷
Start.cult.	3.32 ²⁰	0.25	4.23 ¹⁸	0.26	3.12 ¹²	0.44	--	--
6h Dark								
P25-PC500	3.36	--	4.07	--	3.21	--	5.30x10 ⁷	--
VPC10	3.56	--	--	--	3.44	--	1.12x10 ⁷	--
PC10	3.29	--	3.62	--	3.18	--	1.22x10 ⁷	--
Dark alone	3.40	--	3.99	--	2.59	--	3.50x10 ⁷	--

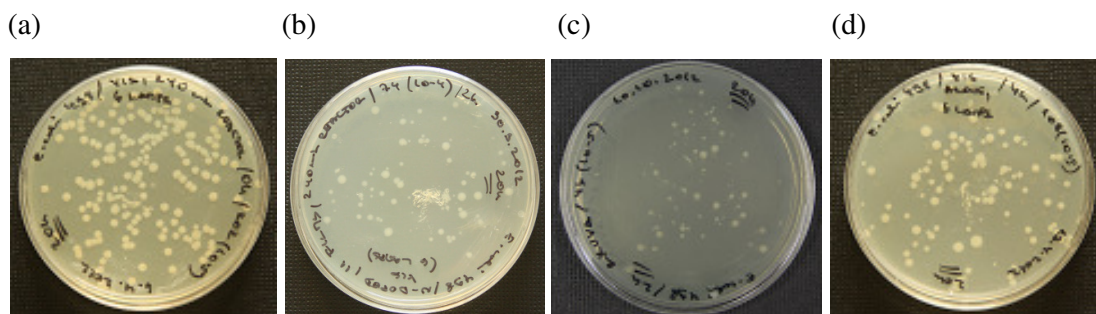


Figure 33: Effect of photocatalysis, Vis and UVA light photolysis on *E. coli* colony size. All water disinfecting conditions were studied in CTP reactor. Representative images show bacterial colonies on solid nutrient medium evolved from bacteria before illumination (a), exposed 2 h to Vis-activated photocatalytic films VPC10 (b), 2 h to UVA alone (c) and 6 h to Vis alone (d). Initial bacterial density in reactor was $1-2 \times 10^8$ *E. coli*/mL. Images were obtained after 20 hours of growth at 37 °C. One representative experiment of at least two performed is shown.

5.2.6 Flow cytometry assays for the evaluation of antibacterial activity of photocatalytic coatings

Cell wall and membranes protect and stabilize cells against external stress, and are the first target of photocatalytically produced ROS (Foster et al. 2011). Compromised membranes also suggest impairments of cell metabolism. Consequently, assays that evaluate membranes integrity are valuable indicators of cell viability of bacteria being challenged with photocatalysis (Gogniat et al. 2006). In the final step, we tried to evaluate antibacterial activity of different photocatalytic coatings, designed for self-cleaning surfaces or water disinfection, by flow cytometry using a combination of different fluorescent dyes (Chapter 2.8.2). In this way, we were able to evaluate antibacterial activity of different photocatalysts at the single cell level. Membrane integrity was assessed with PI in combination with SYTO 9, TO or SYBR Safe or by single dye staining employing all dyes from the pairs stated above (Chapter 2.8.2). Among nucleic acids-binding dyes tested, TO-PI, SYTO 9-PI pairs and SYTO 9 alone seems the most promising to distinguish between differently active photocatalytic coatings (Figure 34, 35 and 38a).

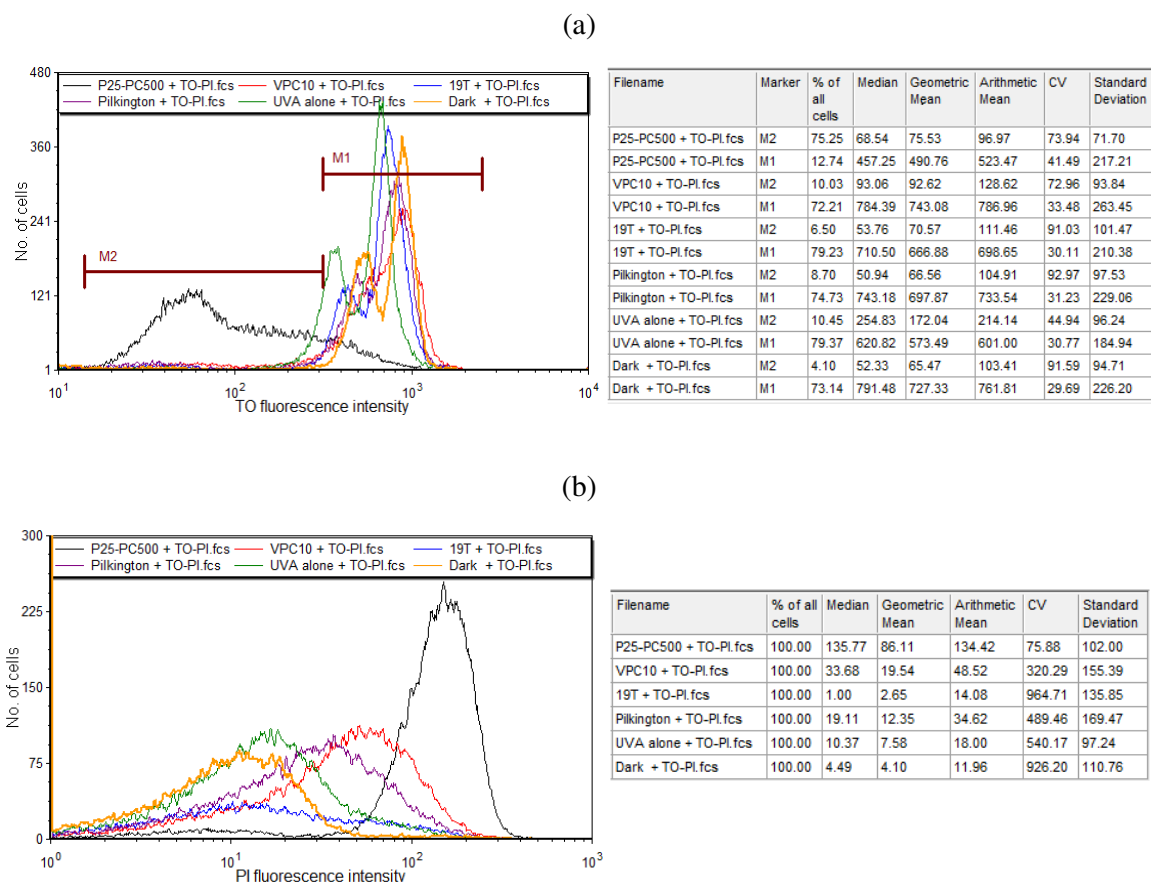
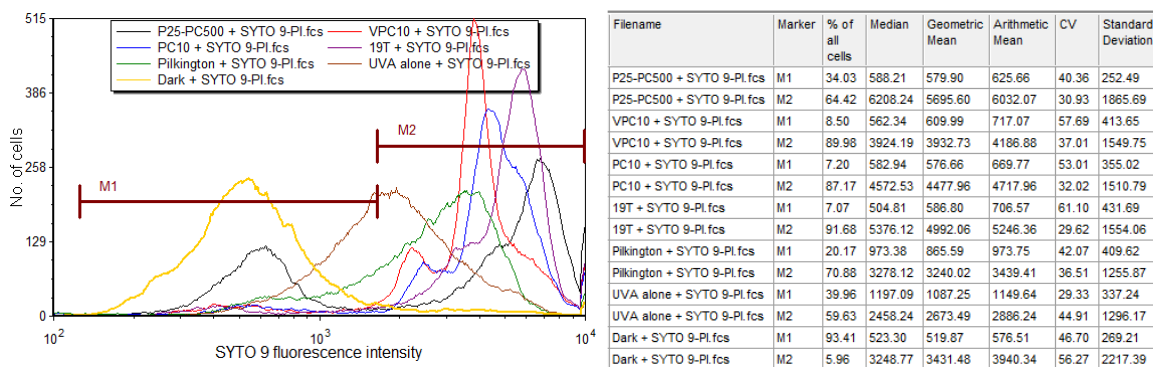


Figure 34: Membrane integrity of *E. coli* exposed to photocatalysis, as indicated by double TO-PI staining. TO fluorescence (a) and PI fluorescence (b) from cells exposed to photocatalytic coatings P25-PC500, VPC10, 19T and Pilkington self-cleaning glass irradiated by UVA, and to uncoated glass under UVA and in dark is shown in graphs and tables. Markers (M) distinguish between cells with damaged (M2) and intact (M1) cell membranes. Results of one representative experiment out of two or three performed are presented.

For more active materials (most evident for P25-PC500) TO fluorescence decreased, while PI fluorescence increased as compared to the negative control (Dark) and it could be explained like suggested by Stock (2004) for the *BacLight* assay, i.e., by the combinational effect of the displacement of TO by PI and FRET emission of light from TO to PI, when both dyes are present in injured cells (Chapter 5.2.1). Fluorescence shift is less significant for less active materials (VPC10 and Pilkington) or UVA photolysis. Nevertheless, as fluorescence shifts occur in opposite directions (TO decreases and PI increases), TO/PI fluorescence ratios (like for *BacLight* assay), provides a good and sensitive read-out for the comparison of different photocatalysts. Surprisingly, when using SYTO 9-PI staining, fluorescence intensities of both

stains increased after photocatalytic treatment as compared to the control sample in dark (Figure 35).

(a)



(b)

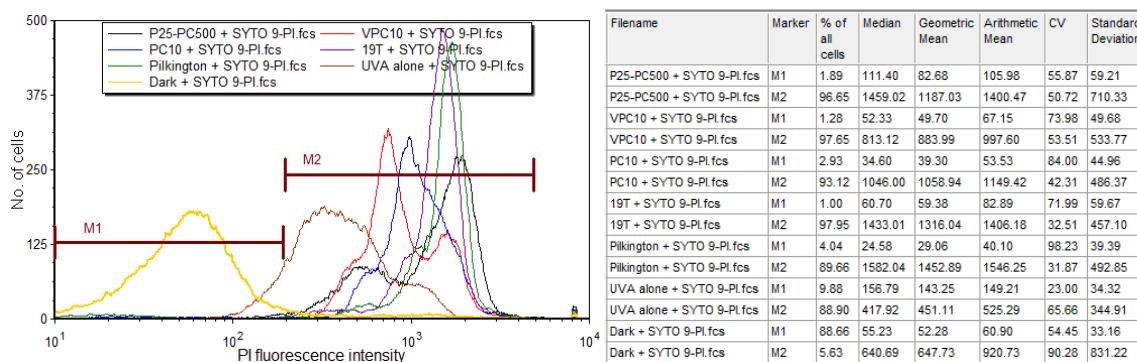
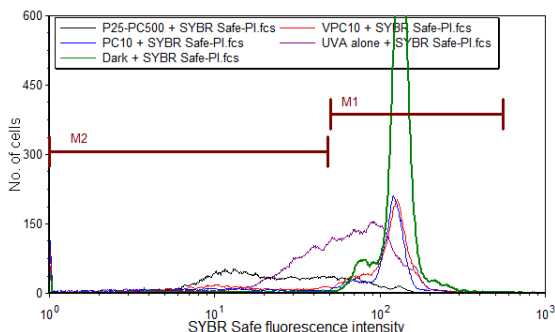


Figure 35: Membrane integrity of *E. coli* exposed to photocatalysis, as indicated by double SYTO 9-PI staining. SYTO 9 fluorescence (a) and PI fluorescence (b) from cells exposed to photocatalytic coatings P25-PC500, VPC10, PC10, 19T and Pilkington irradiated by UVA, and to uncoated glass under UVA and in dark is shown in graphs and tables. Markers (M) distinguish between cells with damaged (M1) and intact (M2) cell membranes. Results of one representative experiment out of two or three performed are presented.

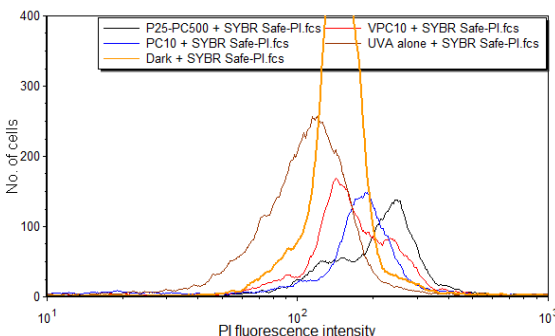
This indicates that SYTO 9-PI staining is not working as expected, according to the BacLight assay. Cells with damaged or absent outer membrane, which is also the first target of photocatalysis, became more permeable for SYTO 9 (Berney et al. 2007b). Nevertheless, the staining buffer used for all samples contained ethylenediaminetetraacetic acid (EDTA), which should facilitate bacterial outer membrane disintegration. However, it seems that in our experimental setting SYTO 9 uptake is additionally triggered by the photocatalytic treatment

and that the steady-state level of SYTO 9 uptake in non-damaged cell does not reach the intracellular saturation point. This observation could serve also for an explanation of inability of *BacLight* assay to differentiate among milder photocatalytic conditions, like in antibacterial evaluation of self-disinfecting coatings, where *BacLight* showed only a slight decrease of SYTO 9/PI fluorescence ratio for the most active P25-PC500 AL sample (positive control) as compared to all other samples (Figure 25).

(a)



(b)



Filename	Marker	% of all cells	Median	Geometric Mean	Arithmetic Mean	CV	Standard Deviation
P25-PC500 + SYBR Safe-Pl.fcs	M1	23.33	75.67	83.48	93.37	63.98	59.73
P25-PC500 + SYBR Safe-Pl.fcs	M2	74.97	14.72	13.37	18.22	67.38	12.28
VPC10 + SYBR Safe-Pl.fcs	M1	72.08	121.88	116.08	122.46	36.08	44.18
VPC10 + SYBR Safe-Pl.fcs	M2	27.00	9.82	8.04	13.68	92.29	12.63
PC10 + SYBR Safe-Pl.fcs	M1	68.28	119.71	115.33	121.01	35.91	43.45
PC10 + SYBR Safe-Pl.fcs	M2	30.64	4.45	4.55	9.36	119.24	11.16
UVA alone + SYBR Safe-Pl.fcs	M1	60.53	88.17	90.07	96.95	44.47	43.11
UVA alone + SYBR Safe-Pl.fcs	M2	37.41	29.69	18.22	26.70	54.97	14.68
Dark + SYBR Safe-Pl.fcs	M1	96.11	132.16	129.11	133.24	28.06	37.39
Dark + SYBR Safe-Pl.fcs	M2	3.51	4.00	4.26	9.67	124.44	12.04

Figure 36: Membrane integrity of *E. coli* exposed to photocatalysis, as indicated by double SYBR Safe-PI staining. SYBR Safe fluorescence (a) and PI fluorescence (b) from cells exposed to photocatalytic coatings P25-PC500, VPC10, PC10 and Pilkington irradiated by UVA, and to uncoated glass under UVA and in dark is shown in graphs and tables. Markers (M) distinguish between cells with damaged (M1) and intact (M2) cell membranes. Results of one representative experiment out of two or three performed are presented.

The combination of PI with SYBR Safe was tested (Figure 36), because SYBR Safe (i) is already present in many laboratories as a safer replacement of ethidium bromide in the routine DNA labelling and (ii) is similar to SYBR Green I, which was already used in flow cytometric analysis of microbial samples (Barbesti et al. 2000; Berney et al. 2008), also in

combination with PI (Berney et al. 2008), including photocatalysis evaluation (Gogniat et al. 2006). In contrast to the previous dye combinations used, SYBR Safe-PI showed lower potential for the antibacterial evaluation of photocatalytic materials. However, in accordance to previous two assays, SYBR Safe fluorescence was decreasing in accordance to the antibacterial treatment applied and more significantly for the strongest photocatalyst P25-PC500. In contrary, PI fluorescence of the photocatalysis-exposed samples was increasing gradually from the least to the most active photocatalysts, but only to a minor extends, as compared to dark- and UVA-treated samples. In order to determine if a single dyes could be used instead of the dye combinations, what is especially attractive for the cheap PI staining, we further on performed single stain assays with TO, SYBR Safe, SYTO 9 and PI dyes (Figure 37 and 38).

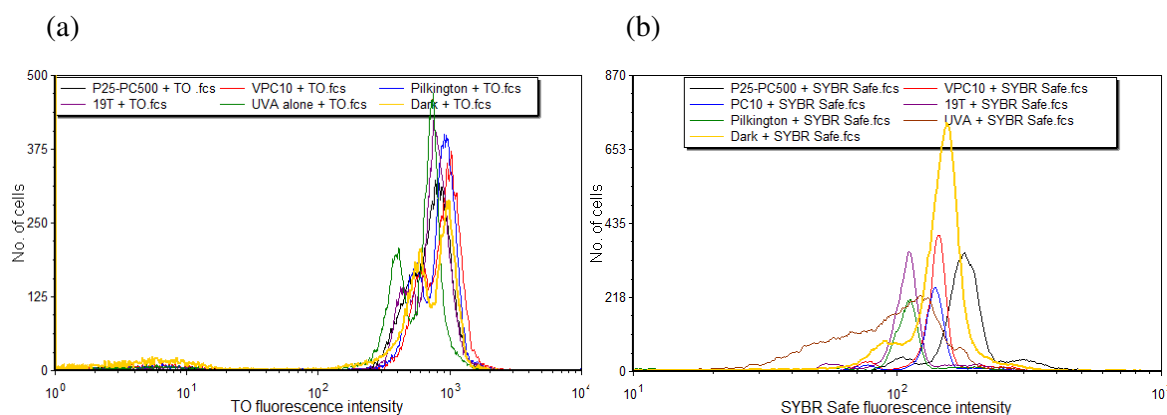


Figure 37: Membrane integrity of *E. coli* exposed to photocatalysis, as indicated by single TO (a) and SYBR Safe (b) staining. TO fluorescence (a) and SYBR Safe fluorescence (b) from cells exposed to photocatalytic coatings P25-PC500, VPC10, PC10, 19T and Pilkington, and to uncoated glass under UVA and in dark is shown. Results of one representative experiment out of two or three performed are presented.

TO and SYBR Safe fluorescence was completely insensitive in detecting different cell membrane integrity of the photocatalysis- and photolysis-treated samples as compared to controls. Therefore, TO and SYBR Safe as a single dye are not suitable for the evaluation of bacterial membrane integrity after the photocatalytic treatment. Similar to the SYTO 9 in the combination with PI, also SYTO 9 alone was very efficient in distinguishing control and different photocatalytic samples (Figure 38a). Sequence of the SYTO 9 fluorescence shifts coincided with the expectations, with Dark control having less permeable cell wall, followed by UVA samples, and photocatalytically treated samples. Sensitivity of PI assay was again

lower than in combination with other dyes, i.e. with TO (Figure 34) or SYTO 9 (Figure 35) or SYBR Safe (Figure 36). PI alone was able to distinguish only the bacteria treated with the strongest photocatalyst P25-PC500, while the fluorescence stayed at the control level for all the rest of the conditions used (Figure 38b).

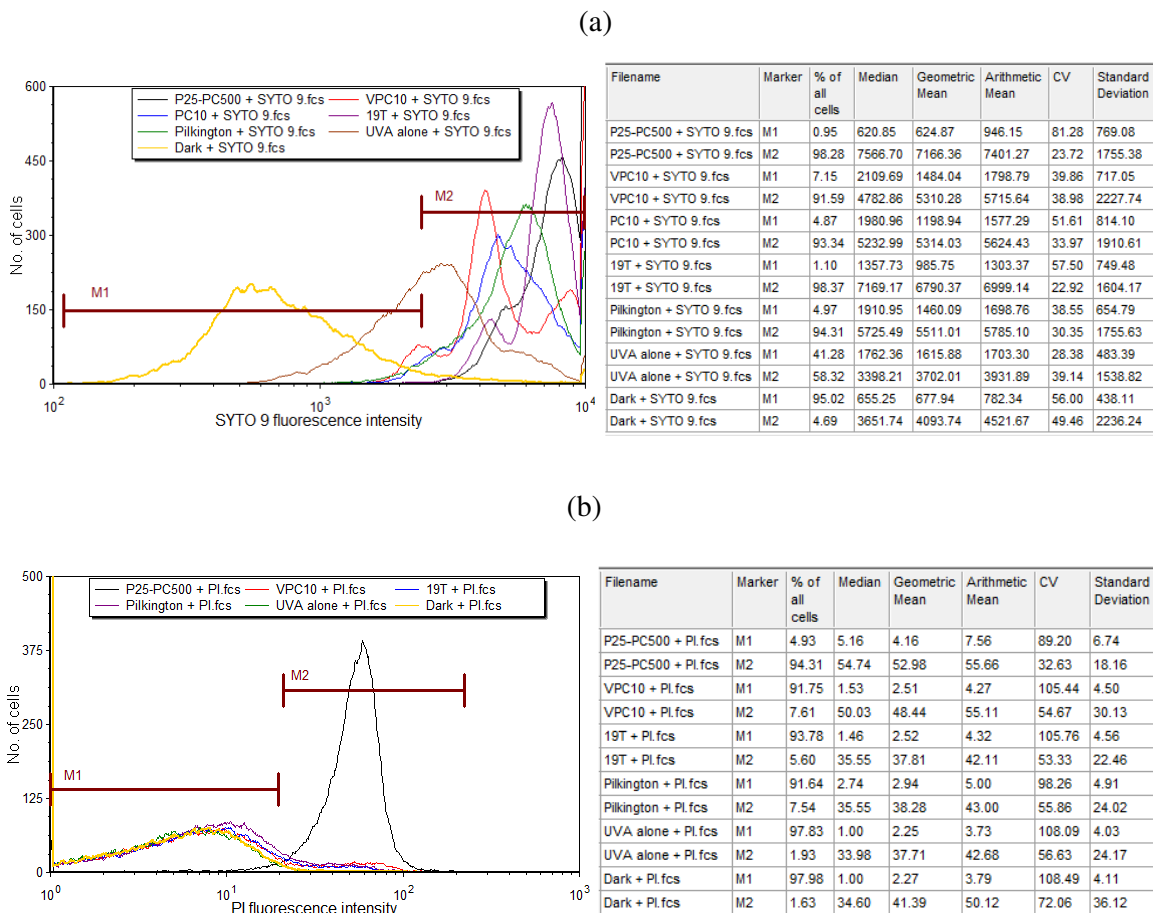


Figure 38: Membrane integrity of *E. coli* exposed to photocatalysis, as indicated by single stain SYTO 9 and PI staining. SYTO 9 fluorescence (a) and PI fluorescence (b) from cells exposed to photocatalytic coatings P25-PC500, VPC10, PC10, 19T and Pilkington, and to uncoated glass under UVA and in dark is shown in graphs and tables. Markers (M) distinguish between cells with damaged (M1) and intact (M2) cell membranes. Results of one representative experiment out of two or three performed are presented.

Based on the results presented above, we concluded in this part of the study that DNA-labeling dye combinations TO-PI and SYTO 9-PI, or even SYTO 9 alone, are very suitable for the evaluation of antimicrobial activity of different photocatalytic coatings by flow cytometry (Figure 34, 35 and 38a). In order to obtain more complete information on

physiological status of the bacteria exposed to photocatalytically active surfaces, DiBAC4(3) was used in the next step for the evaluation of membrane potential of cells. DiBAC4(3) is one of the preferred probes for determination of cellular inner membrane (IM) potential. Membrane potential is an important parameter in the cell life, as it has a key role in cell physiological processes, e.g., ATP generation and substance transport. Membrane potential reflects membrane integrity and energy status as well as cell viability in general (Strauber and Muller 2010). DiBAC4(3) enters depolarized cells, binds to intracellular proteins or membrane and exhibits enhanced fluorescence and a red spectral shift (manufacturer's instructions). DiBAC4(3) was a very useful viability indicator also in our study. Photocatalytically treated samples clearly showed higher DiBAC4(3) fluorescence as compared to the control Dark sample and UVA-treated sample (Figure 39).

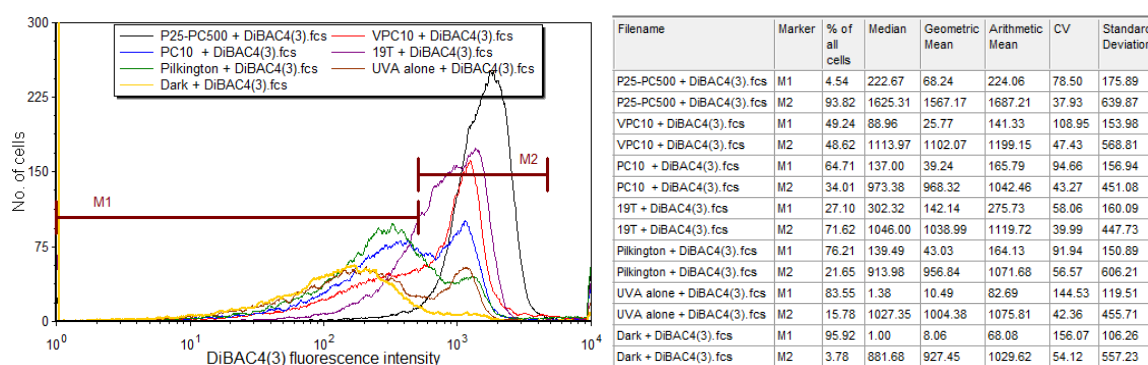


Figure 39: Depolarization of *E. coli* membranes as indicated by DiBAC4(3) staining. DiBAC4(3) fluorescence from bacteria exposed to photocatalytic coatings P25-PC500, VPC10, PC10, 19T and Pilkington, and to uncoated glass under UVA and in dark is shown in graph and table. Markers distinguish between cells with impaired (M2) and preserved (M1) membrane potential. Results of one representative experiment out of two or three performed are presented.

Staining bacteria with esterified fluorogenic substrates is another staining that enable rapid detection of metabolically active bacteria (Hoefel et al. 2003). According to the manufacturer, carboxyfluorescein diacetate (CFDA) is cell-permeant, enzymatically cleaved to fluorescent product carboxyfluorescein (CF) that is retained in cells with intact membranes (<http://www.lifetechnologies.com/order/catalog/product/C195>). Nevertheless, the attempt to follow bacterial metabolic activity through conversion of fluorogenic substrate CFDA by esterases was not successful in our experimental setting (Figure 40). Experiments of the CFDA staining using different amounts of EDTA in the staining buffer are shown, i.e. 1 mM

(Figure 40a) and 5 mM (Figure 40b). EDTA was increased in order to enhance disruption of bacterial outer membrane for an improved staining, because outer membrane of some gram-negative bacteria was recognized as a barrier for certain stains (e.g., DiBAC4(3) or SYTO 9) (Berney et al. 2007b; Berney et al. 2008). We also prolonged the staining period, from 20 min up to 1 hour, with no effect on the CF fluorescence intensity (data not shown). In the preliminary method calibration experiments, we used some standard methods for bacterial cell wall disruption and denaturation of the cell components, including esterases (followed by CFDA staining). We used EtOH, EtOH combined with heating at 60 °C and iPrOH (Hoefel et al. 2003; <http://tools.lifetechnologies.com/content/sfs/manuals/mp34856.pdf>). Unfortunately, we did not observe any difference between treated and untreated samples when using CFDA staining (results with isopropanol (iPrOH) are shown in Figure 9). Therefore, despite all our efforts, metabolic activity indicator CFDA, which is a cell-permeable substrate for cell esterase, was in our hands not performing well in terms of antibacterial evaluation of different photocatalytic coating, not even when using a modified and potentially stronger staining protocol (Figure 40).

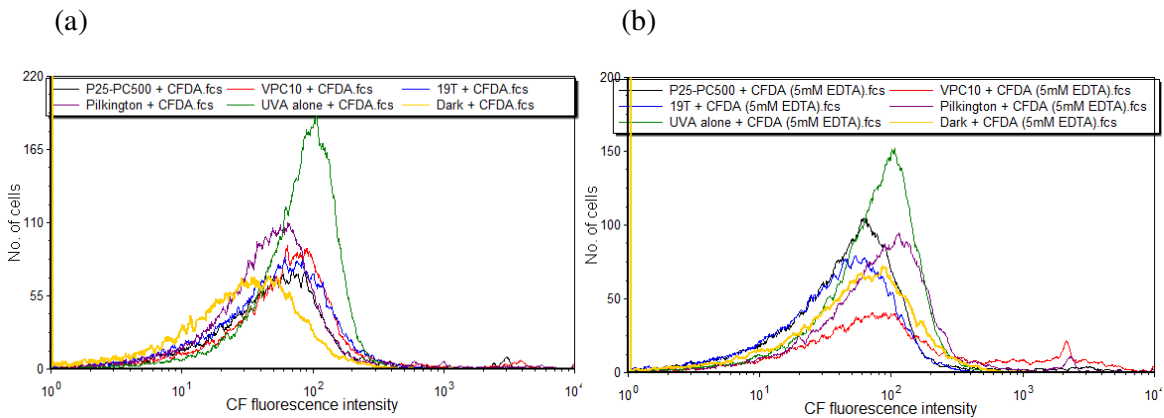


Figure 40: Metabolic activity of *E. coli* exposed to photocatalysis, as indicated by esterase substrate CFDA. CFDA is hydrolyzed and retained inside viable cells as fluorescent CF. CF fluorescence of bacteria exposed to photocatalytic coatings P25-PC500, VPC10, 19T and Pilkington self-cleaning glass irradiated by UVA, and to uncoated glass under UVA and in dark is shown in graphs. CFDA staining was performed in 1 mM (a) and 5 mM (b) PBS buffer. Results of one representative experiment out of two or three performed are presented.

Difficult discrimination between active and inactive (heated in ethanol) *E. coli* was observed also by Hoefel et al. (2003). Further optimization of the CFDA staining is needed, most likely

considering also flow-cytometric measurements. For instance, Berney et al. (2008) achieved optimal signal-to-noise discrimination on the green fluorescence versus red fluorescence dot plot, while we measured only green fluorescence. Also, samples lysates could be analysed instead of intact cells as it is used for ATP detection (Hammes et al. 2010). Fluorimeter in the format of a microtiter plate reader would enable evaluation of many samples at the same time. It was recommended to use more than one viability indicator for the analysis, and to find the best stain combination for any research question involved (Berney et al. 2007b; Hammes et. al 2010).

6 Conclusions

Antimicrobial evaluation of photocatalytic materials requires an interdisciplinary approach, bringing together material and life sciences. Sufficient understanding of specific characteristics and physiological requirement of the microorganisms and characteristics of photocatalytic materials included in these studies is of great importance for a reliable evaluation of photocatalytic materials. Experimental conditions need to be carefully decided also to design the most appropriate testing protocol for certain photocatalytic application. Ongoing standardisation efforts can provide additional guidelines and increase comparability and practical value of antibacterial testing. Standard testing parameters and introduction of appropriate controls is one of the major future challenges in the field of photocatalytic materials with antimicrobial applications.

A highly important part is the selection of an appropriate detection method. Although plate count is currently still the most frequently used method, antimicrobial testing could benefit from the implementation of fluorescence or colorimetric methods, or at least by implementation of more high-throughput growth-based assays, for the assessment of microbial viability and physiological status of exposed microorganisms. Plate count technique is also not sensitive enough to detect intermediate states like cell injuries and it can observe bacterial death only in retrospect. Contrary to this, fluorescent and colored indicators enable determination of different levels of cellular integrity and functionality, i.e. viability immediately the after photocatalytic exposure, without cell culturing, and also a single cell level analysis. However, indicators must be carefully selected and methods optimized for certain photocatalytic applications.

Critical parameters for an assay include the sensitivity, the reproducibility, and the dynamic range. The time needed to collect data and analyse results is another important factor and the assay platforms that can deliver reliable results in a shorter period of time are highly desirable. We demonstrated the suitability and high degree of accuracy for XTT, growth and *BacLight* assays performed in 96-well microplates and developed for testing the bacterial physiological status, after being exposed to photocatalytic surfaces. The methodology can be easily adapted to 384-well format and allows automatic analysis by means of a microtiter plate reader. Acquisition and evaluation of the results is simple as the device enables on-line computer processing of the data, including data collection, statistical calculations and report

generation. Specifically, we showed that microplate-based XTT and growth assays are sensitive tools for evaluating the antibacterial effect of different photocatalytic coatings.

BacLight was the third assay performed in a microplate format. Although other assays performed in parallel clearly showed reduction in at least the size of colonies (colony count) or quite substantial decrease in the overall metabolism and growth in the population of UVA/photocatalyst treated bacteria (XTT and growth assay), *BacLight* assay showed almost no difference between control and treated self-disinfecting samples, tested under UVA. In the context of Vis-induced photocatalysts, however, *BacLight* assay clearly detected photocatalysis-related changes in the membrane permeability, and was therefore able to distinguish between different photocatalytic conditions. *BacLight* assay was on the other hand very appropriate for water disinfection studies employing photocatalytic films, where more harmful photocatalytic conditions occurred than in testing conditions for self-disinfecting coatings. Results obtained coincide with results of microplate-based XTT and growth assay, and also of colony count. Moreover, *BacLight* derived information is obtained immediately after the treatment. When evaluating harsher photocatalytic conditions, widely used and immediate *BacLight* assay could therefore also predict the results of standard colony count, obtained 24 hours after the treatment, and thus saving time and consumables.

Pilkington Glass Activ™ (Activ™) photocatalytic glass was observed to be suitable standard material in our antibacterial studies, specially for thin self-disinfecting films as it holds similar antibacterial activity. For studying modified enhanced sunlight- and daylight-photoactive TiO₂ or materials adjusted for certain application, e.g. for air filters, additional reference materials have to be discussed, and could be selected among successful commercial photocatalyst, similiary as P25 was selected among different titania powders.

By incorporating N-doped or C-doped titania commercial powder into our TiO₂-SiO₂ sol formulation (comprising colloidal titania and silica as a binder) we did not succeed to prepare an efficient visible light-active material. Mixture of P25 and PC500 of equal mass was consistently giving the most active photocatalyst. However, different powders resulted in films with different structure; for example PC10 gave more compact and well-adhered reinforced coating.

As indicated by preliminary flow cytometry measurements, TO-PI, SYTO 9-PI or SYTO 9 assays were observed to be the most promising indicator of *E. coli* membrane integrity after being exposed to UVA activated photocatalytic coatings, designed to be self-cleaning surfaces or water disinfection materials, and tested according to the set-up for self-disinfecting films. TO-PI showed to be more sensitive than more frequently used *BacLight* (PI-SYTO 9) assay. Membrane depolarization indicator DiBAC4(3) also proved to be very useful for antibacterial evaluation in photocatalytic disinfection research, while metabolic activity evaluation by using esterase substrate CFDA was unsuccessful in our hands.

Parts of the dissertation have been so far published in:

- 1) Zvab U, Bergant Marusic M, Lavrencic Stangar U (2012) Microplate-based assays for the evaluation of antibacterial effects of photocatalytic coatings. *Appl Microbiol Biotechnol* 96:1341-1351.
- 2) Zvab U, Lavrencic Stangar U, Bergant Marusic M (2014) Methodologies for the analysis of antimicrobial effects of immobilized photocatalytic materials. *Appl Microbiol Biotechnol* doi:10.1007/s00253-013-5464-y
- 3) Kete M, Zvab U, Tasbihi M, Lavrencic Stangar U (2012) Technical report of the prototype photoreactor design, its realization and water purification performance assessment: Confidential report for Electrolux Italia s.p.a., University of Nova Gorica, Slovenia.

7 References

- Akhavan O (2009) Lasting antibacterial activities of Ag-TiO₂/Ag/a-TiO₂ nanocomposite thin film photocatalysts under solar light irradiation. *J Colloid Interf Sci* 336:117-124.
- Alakomi HL, Matto J, Virkajarvi I, Saarela M (2005) Application of a microplate scale fluorochrome staining assay for the assessment of viability of probiotic preparations. *J Microbiol Methods* 62:25-35.
- Alrousan DMA, Dunlop PSM, McMurray TA, Byrne JA (2009) Photocatalytic inactivation of *E. coli* in surface water using immobilised nanoparticle TiO₂ films. *Water Res* 43:47-54.
- Arslan I, Balcioglu IA, Bahnemann DW (2000) Heterogeneous photocatalytic treatment of simulated dyehouse effluents using novel TiO₂-photocatalysts. *Appl Catal B* 26:193-206.
- Andreozzi R, Caprio V, Insola A, Marotta R (1999) Advanced oxidation processes (AOP) for water purification and recovery. *Catal Today* 53:51-59.
- Apel K, Hirt H (2004) Reactive oxygen species: metabolism, oxidative stress, and signal transduction. *Annu Rev Plant Biol* 55:373-399.
- Asahi R, Morikawa T, Ohwaki T, Aoki K, Taga Y (2001) Visible-light photocatalysis in nitrogen doped titanium oxides. *Science* 293:269-271.
- Bahnemann D (2004) Photocatalytic water treatment: solar energy applications. *Photocatalysis* 77:445-459.
- Bahnemann DW, Friedmann D, Mendive CB (2010) Mechanisms of photocatalytic reactions. Proceedings of the 6th European meeting on solar chemistry & photocatalysis: environmental applications, Prague, pp 26-28
- Baram N, Starosvetky D, Starosvetsky J, Epshtein M, Armon R, Ein-Eli Y (2007) Enhanced photo-efficiency of immobilized TiO₂ catalyst via intense anodic bias. *Electrochem commun* 9:1684-1688.
- Baram N, Starosvetky D, Starosvetsky J, Epshtein M, Armon R, Ein-Eli Y (2011) Photocatalytic inactivation of microorganisms using nanotubular TiO₂. *Appl Catal B* 101:212-219.
- Barbesti S, Citterio S, Labra M, Baroni MD, Neri MG, Sgorbati S (2000) Two and three-color fluorescence flow cytometric analysis of immunoidentified viable bacteria. *Cytometry* 40:214-218.

- Battin TJ, Kammer FVD, Weilhartner A, Ottofuelling S, Hofmann T (2009) Nanostructured TiO₂: transport behavior and effects on aquatic microbial communities under environmental conditions. *Environ Sci Technol* 43:8098-8104.
- Beckman EM, Kawaguchi TG, Chandler T, Decho AW (2008) Development of a microplate-based fluorescence immunoassay using quantum dot streptavidin conjugates for enumeration of putative marine bacteria, *Alteromonas* sp., associated with a benthic harpacticoid copepod. *J Microbiol Methods* 75:441-444.
- Belhacova L, Krysa J, Geryk J, Jirkovsky J (1999) Inactivation of microorganisms in a flow-through photoreactor with an immobilized layer TiO₂. *J Chem Technol Biotechnol* 74:149-154.
- Benabbou AK, Derriche Z, Felix C, Lejeune P, Guillard C (2007) Photocatalytic inactivation of *Escherichia coli*. Effect of concentration of TiO₂ and microorganism, nature, and intensity of UV irradiation. *Appl Catal B* 76:257-263.
- Beranek R, Kisch H (2008) Tuning the optical and photoelectrochemical properties of surface-modified TiO₂. *Photochem Photobiol Sci* 7:40-48.
- Berney M, Weilenmann HU, Egli T (2007a) Adaptation to UVA radiation of *E. coli* growing in continuous culture. *J Photochem Photobiol B Biol* 86:149-159. *Water Res*
- Berney M, Hammes F, Bosshard F, Weilenmann HU, Egli T (2007b) Assessment and interpretation of bacterial viability by using the LIVE/DEAD *BacLight* kit in combination with flow cytometry. *Appl Environ Microbiol* 73:3283-3290.
- Berney M, Vital M, Hulshoff I, Weilenmann HU, Egli T, Hammes F (2008) Rapid, cultivation-independent assessment of microbial viability in drinking water. *Water Res* 42:4010-4018.
- Bickley RI, Gonzales-Carreno T, Lees JS, Palmisano L, Tilley RJD (1991) A structural investigation of titanium dioxide photocatalysts. *J Solid State Chem* 92:178-190.
- Blake DM, Maness P, Huang Z, Wolfrum EJ, Huang J (1999) Application of the photocatalytic chemistry of titanium dioxide to disinfection and the killing of cancer cells. *Separ Purif Method* 28:1-50.
- Blake MD (2001) Bibliography of work on the photocatalytic removal of hazardous compounds from water and air. National renewable energy laboratory. <http://www.nrel.gov/docs/fy02osti/31319.pdf>. Accessed 19 August 2013
- Blanco-Galvez J, Fernández-Ibanez P, Malato S (2007) Solar photocatalytic detoxification and disinfection of water: recent overview. *J Solar Energy Eng* 129:4-15.

- Boelsterli UA (2007) Xenobiotic-induced oxidative stress. In: Mechanistic toxicology, 2nd edn. CRC Press, Boca Raton, pp 117-175
- Bui TH, Felix C, Pigeot-Remy S, Herrmann JM, Lejeune P, Guillard C (2008) Photocatalytic inactivation of wild and hyper-adherent *E. coli* strains in presence of suspended or supported TiO₂. Influence of the isoelectric point of the particle size and of the adsorptive properties of titania. *J Adv Oxid Technol* 11:510-518.
- Burton JG, Jauniaux E (2011) Oxidative stress. *Best Pract Res Clin Obstet Gynaecol* 25:287-299.
- Caballero L, Whitehead AK, Allen SN, Verran J (2009) Inactivation of *Escherichia coli* on immobilized TiO₂ using fluorescent light. *J Photochem Photobiol A Chem* 202:92-98.
- Cai Y, Stromme M, Welch K (2013) Bacteria viability assessment after photocatalytic treatment. *3 Biotech* (in press) doi: 10.1007/s13205-013-0137-1
- Cao S, Yeung KL, Kwan JKC, To PMT, Yu SCT (2009) An investigation of the performance of catalytic aerogel filters. *Appl Catal B* 86:127-136.
- Carp O, Huisman CL, Reller A (2004) Photoinduced reactivity of titanium dioxide. *Prog Solid State Chem* 32:33-177.
- CEN <http://esearch.cen.eu/esearch/extendedsearch.aspx> Accessed 23 July 2013
- Cernigoj U, Lavrencic Stangar U, Trebse P (2006) Evaluation of a novel Carberry type photoreactor for the degradation of organic pollutants in water. *J Photochem Photobiol A Chem* 188:169-176.
- Cernigoj U, Lavrencic Stangar U (2009) Preparation of TiO₂/SiO₂ sols and use thereof for deposition of self-cleaning anti-fogging coatings. International application number PCT/SI2009/000052, international publication number WO 2010/053459 A1, European Patent Office, Munich.
- Cernigoj U, Kete M, Lavrencic Stangar U (2010) Development of of a fluorescence-based method for evaluation of self-cleaning properties of photocatalytic layers. *Catal Today* 151:46-52.
- Chapman D, Kimstach V (1996) Chapter 3 – Selection of water quality variables. In: Chapman D (ed) *Water Quality Assessments - a guide to use of biota, sediments and water in environmental monitoring*. 2nd edn. Published on behalf of WHO by F & FN Spon.
- Chawengkijwanich C, Hayata Y (2008) Development of TiO₂ powder-coated food packaging film and its ability to inactivate *Escherichia coli* in vitro and in actual tests. *Int J Food Microbiol* 123:288-292.

- Chen F, Yang X, Wu Q (2009a) Antifungal capability of TiO₂ coated film on moist wood. *Build Environ* 44:1088-1093.
- Chen F, Yang X, Wu Q (2009b) Photocatalytic oxidation of *Escherichia coli*, *Aspergillus niger*, and formaldehyde under different ultraviolet irradiation conditions. *Environ Sci Technol* 43:4606-4611.
- Chen F, Yang X, Wu Q (2009c) Antifungal capability of TiO₂ coated film on moist wood. *Build Environ* 44:1088-1093.
- Chen F, Yang X, Mak KCH, Chan WTD (2010) Photocatalytic oxidation for antimicrobial control in built environment: a brief literature overview. *Building and Environment* 45:1747-1754.
- Cheng S, Tsai SJ, Lee YF (1995) Photocatalytic decomposition of phenol over titanium oxide of various structures. *Catal Today* 26:87-96.
- Cheng TC, Yao KS, Yeh N, Chang CI, Hsu HC, Gonzales F, Chang CY (2011) Bactericidal effect of blue LED light irradiated TiO₂/Fe₃O₄ particles on fish pathogen in seawater. *Thin Solid Films* 519:5002-5006.
- Cho M, Chung H, Choi W, Yoon J (2004) Linear correlation between inactivation of *E. coli* and OH radical concentration in TiO₂ photocatalytic disinfection. *Water Res* 38:1069-1077.
- Cho M, Cates EL, Kim J (2011) Inactivation and surface interactions of MS-2 bacteriophage in a TiO₂ photoelectrocatalytic reactor. *Water Res* 45:2104-2110.
- Chollet GF, Josset S., Keller N, Keller V, Lett MC (2009) Monitoring the bactericidal effect of UV-A photocatalysis: A first approach through 1D and 2D protein electrophoresis. *Catal Today* 147:169-172.
- Clementi EA, Marks LR, Duffey ME, Hakansson AP (2012) A novel initiation mechanism of death in *Streptococcus pneumoniae* induced by the human milk protein-lipid complex HAMLET and activated during physiological death. *J Biol Chem* 287:27168-27182.
- Cushnie TPT, Robertson PKJ, Officer S, Pollard PM, McCullagh C, Robertson MCR (2009) Variables to be considered when assessing the photocatalytic destruction of bacterial pathogens. *Chemosphere* 74:1374-1378.
- Cushnie TPT, Robertson PKJ, Officer S, Pollard PM, Prabhu R, McCullagh C, Robertson JMC (2010) Photobactericidal effects of TiO₂ thin films at low temperatures—A preliminary study. *J Photochem Photobiol A Chem* 216:290-294.
- Datye AK, Riegel G, Bolton JR, Huang M, Prairie MR (1995) Microstructural characterization of a fumed titanium dioxide photocatalyst 115:236-239.

- Davey HM (2011) Life, death, and in-between: meanings and methods in microbiology, minireview. *Appl Environ Microbiol* 77:5571-5576.
- Ditta IB, Steele A, Liptrot C, Tobin J, Tyler H, Yates HM, Shell DW, Foster HA (2008) Photocatalytic antimicrobial activity of thin surface films of TiO₂, CuO and TiO₂/CuO dual layers on *Escherichia coli* and bacteriophage T4. *Appl Microbiol Biotechnol* 79:127-133.
- Di Valentin C, Pacchioni G, Selloni A, Livraghi S, Giamello E (2005) Characterization of paramagnetic species in N-doped TiO₂ powders by EPR spectroscopy and DFT calculations. *J Phys Chem Lett* 109:11414-11419.
- Downes A, Blunt TP (1877) Researches on the effect of light upon bacteria and other organisms. *Proc. R. Soc. London*, 26:488-500.
- Dunlop PSM, Byrne JA, Manga N, Eggins BR (2002) The photocatalytic removal of bacterial pollutants from drinking water. *J Photochem Photobiol A Chem* 148:355-363.
- Dunlop PSM, McMurray TA, Hamilton JWJ, Byrne JA (2008) Photocatalytic inactivation of *Clostridium perfringens* spores on TiO₂ electrodes. *J Photochem Photobiol A Chem* 196:113-119.
- Dunlop PMS, Sheeran CP, Byrne JA, McMahon MAS, Boyle MA, McGuigan KG (2010) Inactivation of clinically relevant pathogens by photocatalytic coatings. *J Photochem Photobiol A Chem* 216:303-310.
- Ede S, Hafner L, Dunlop P, Byrne J, Will G (2012) Photocatalytic disinfection of bacterial pollutants using suspended and immobilized TiO₂ powders. *Photochem Photobiol* 88:728-35.
- Elguezabal N, Bastida F, Sevilla IA, González N, Molina E, Garrido JM, Juste RA (2011) Estimation of *Mycobacterium avium* subsp. paratuberculosis growth parameters: strain characterization and comparison of methods. *Appl Environ Microbiol* 77:8615-24.
- EPA <http://water.epa.gov/drink/contaminants/index.cfm>. Accessed 12 October 2013
- Fallani M, Young D, Scott J, Norin E, Amarri S, Adam R, Aguilera M, Khanna S, Gil A, Edwards CA, Dore J; Other Members of the INFABIO Team (2010) Intestinal microbiota of 6-week-old infants across Europe: geographic influence beyond delivery mode, breast-feeding, and antibiotics. *J Pediatr Gastroenterol Nutr* 51:77-84.
- Federici G, Shaw BJ, Handy RD (2007) Toxicity of titanium dioxide nanoparticles to rainbow trout (*Oncorhynchus mykiss*): gill injury, oxidative stress, and other physiological effects. *Aquat Toxicol* 2011:1444-1452.

- Fisher MB, Keane DA, Fernandez P, Colreavy J, Hinder SJ, McGuigan KG, Pillai SC (2013) Nitrogen and copper doped solar light active TiO₂ photocatalysts for water decontamination. *Appl Catal B* 130-131:8-13.
- Foster HA, Ditta IB, Varghese S, Steele A (2011) Photocatalytic disinfection using titanium dioxide: spectrum and mechanism of antimicrobial activity. *Appl Microbial Biotechnol* 90:1847-1868. doi: 10.1002/cvde.201106978
- Foster HA, Sheel DW, Evans P, Sheel P, Varghese S, Elfakhri SO, Hodgkinson JL, Yates HM (2012). Antimicrobial activity against hospital-related pathogens of dual layer CuO/TiO₂ coatings prepared by CVD. *Chem Vap Depos* 18:140-146.
- Fox MA, Dulay MT (1993) Heterogeneous photocatalysis. *Chem Rev* 93:341-357.
- Fresno F, Suaarez S, Portela S, Coronado JM (2014) Photocatalytic materials: recent achievements and near future trends. *J Mater Chem A* (in press) doi: 10.1039/C3TA13793G10
- Fujishima A, Zhang X, Tryk DA (2008) TiO₂ photocatalysis and related surface phenomena. *Surf Sci Rep* 63:515-582.
- Fujioka SR, Yoneyama SB (2002) Sunlight inactivation of human enteric viruses and fecal bacteria. *Water Sci Technol* 46:291-295.
- Fuller ME, Streger SH, Rothmel RK, Mailloux BJ, Hall JA, Onstott TC, Fredrickson JK, Balkwill DL, DeFlaun MF (2000) Development of a vital fluorescent staining method for monitoring bacterial transport in subsurface environments. *Appl Environ Microbiol* 66:4486-4496.
- Gao Y, Masuda Y, Seo WS, Ohta H, Koumoto K (2004) TiO₂ nanoparticles prepared using an aqueous peroxotitanate solution. *Ceram Int* 30:1365-1368.
- Gannon CJ (2000) The global infectious disease threat and its implications for the United States. NIE 99-17D. <http://www.fas.org/irp/threat/nie99-17d.htm>. Accessed 7 December 2013
- Gelover S, Gomez LA, Reyes K, Leal MT (2006) A practical demonstration of water disinfection using TiO₂ films and sunlight. *Water Res* 40:3274-3280.
- Gerlach D, Reichardt W, Vettermann S (1998) Extracellular superoxide dismutase from *Streptococcus pyogenes* type 12 strain is manganese-dependent. *FEMS Microbiol Lett* 160:217-224.
- Ghosh M, Bandyopadhyay M, Mukherje A (2010) Genotoxicity of titanium dioxide (TiO₂) nanoparticles at two trophic levels: plant and human lymphocytes. *Chemosphere* 81:1253-1262.

- Gogniat G, Thyssen M, Denis M, Pulgarin C, Dukan S (2006) The bactericidal effect of TiO₂ photocatalysis involves adsorption onto catalyst and the loss of membrane integrity. *FEMS Microbiol Lett* 258:18-24.
- Gomes AI, Vilar VJP, Boaventura RAR (2009) Synthetic and natural waters disinfection using natural solar radiation in a pilot plant with CPCs. *Catal Today* 144:55-61.
- Goswami DY, Trivedi DM, Block SS (1997) Photocatalytic disinfection of indoor air. *J Sol Energ Eng* 119:92-96.
- Graziani L, Quagliarini E, Osimani A, Aquilanti L, Clementi F, Yepremian C, Lariccia V, Amoroso S, D'Orazio M (2013) Evaluation of inhibitory effect of TiO₂ nanocoatings against microalgal growth on clay brick façades under weak UV exposure conditions. *Build Environ* 64:38-45.
- Grieken R, Marugan J, Pablos C, Furones L, Lopez A (2010) Comparison between the photocatalytic inactivation of Gram-positive *E. faecalis* and Gram-negative *E. coli* faecal contamination indicator microorganisms. *Appl Catal B* 100:212-220.
- Guan K (2005) Relationship between photocatalytic activity, hydrophilicity and self-cleaning effect of TiO₂/SiO₂ films. *Surf Coat Technol* 191:155-160.
- Guillard C, Bui TH, Felix C, Moules V, Lina B, Lejeune P (2008) Microbiological disinfection of water and air by photocatalysis. *C R Chim* 11:107-113.
- Gumy D, Rincon AG, Hajdu R, Pulgarin C (2006) Solar photocatalysis for detoxification and disinfection of water: Different types of suspended and fixed TiO₂ catalysts study. *Sol Energy* 80:1376-1381.
- Hammes F, Berney M, Wang Y, Vital M, Koster O, Egli T (2008) Flow-cytometric total bacterial cell counts as a descriptive microbiological parameter for drinking water treatment processes. *Water Res* 44:3915-23.
- Hammes F, Goldschmidt F, Vital M, Wang Y, Egli T (2010) Measurement and interpretation of microbial adenosine tri-phosphate (ATP) in aquatic environments. *Water Res* 44:3915-3923.
- Hara-Kudo Y, Segawa Y, Kimura K (2006) Sanitation of seawater effluent from seaweed processing plants using a photo-catalytic TiO₂ oxidation. *Chemosphere* 62:149-154.
- Hargesheimer EE, Watson SB (1996) Drinking water treatment options for taste and odor control. *Water Res* 30:1423-1430.
- Hashimoto K, Irie H, Fujishima A (2005) TiO₂ photocatalysis: a historical overview and future prospects. *Jpn J Appl Phys* 44:8269-8285.

- He C, Li X, Xiong Y, Zhu X, Liu S (2005) The enhanced PC and PEC oxidation of formic acid in aqueous solution using a Cu-TiO₂/ITO film. *Chemosphere* 58:381-389.
- Heaselgrave W, Patel N, Kilvington S, Kehoe SC, McGuigan KG (2006) Solar disinfection of poliovirus and *Acanthamoeba polyphaga* cysts in water - a laboratory study using simulated sunlight. *Lett Appl Microbiol.* 43:125-130.
- Hermann JM (2005) Heterogeneous photocatalysis: state of the art and present applications. *Top Catal* 34:49-65.
- Herrera Melian JA, Dona Rodriguez JM, Viera Suarez A, Tello Rendon E, Valdes do Campo C, Arana J, Perez Pena P (2000) The photocatalytic disinfection of urban waste waters. *Chemosphere* 41:323-327.
- Hijnen WA, Beerendonk EF, Medema GJ (2006) Inactivation credit of UV radiation for viruses, bacteria and protozoan (oo)cysts in water: a review. *Water Res* 40:3-22.
- Hoerter JD, Arnold AA, Kuczynska DA, Shibuya A, Ward CS, Sauer MG, Gizachew A, Hotchkiss TM, Fleming TJ, Johnson S (2005) Effects of sublethal UVA irradiation on activity levels of oxidative defense enzymes and protein oxidation in *Escherichia coli*. *J Photochem Photobiol B Biol* 81:171-180.
- Hoefel D, Grooby WL, Monis PT, Andrews S, Saint CP (2003) A comparative study of carboxyfluorescein diacetate and carboxyfluorescein diacetate succinimidyl ester as indicators of bacterial activity. *J Microbiol Methods* 52:379-388.
- Hong J, Ma H, Otaki M (2005) Controlling algal growth in photo-dependent decolorant sludge by photocatalysis. *J Biosci Bioeng* 99:592-597.
- Hu S, Li F, Fan Z (2012) Preparation of SiO₂-coated TiO₂ composite materials with enhanced photocatalytic activity under UV light. *Bull Korean Chem Soc* 33:1895-1899.
- Hurum DC, Agrios AG, Gray KA, Rajh T, Thurnauer MC (2003) Explaining the enhanced photocatalytic activity of Degussa P25 mixed-phase TiO₂ using EPR. *J Phys Chem B* 107:4545-4549.
- IARC (2010) Volume 93 – Carbon black, titanium dioxide and talc. In: IARC monographs. <http://monographs.iarc.fr/ENG/Monographs/vol93/mono93.pdf>. Accessed 19 August 2013
- Ingo GM, Riccucci C, Bultrini G, Dire S, Chiozzini G (2001) Thermal and microchemical characterization of sol-gel SiO₂, TiO₂, and xSiO₂-(1-x)TiO₂ ceramic materials. *J Therm Anal Calorim* 66:37-46.
- Ireland JC, Klostermann P, Rice EW, Clark RM (1993) Inactivation of *Escherichia coli* by titanium dioxide photocatalytic oxidation. *Appl Environ Microbiol* 59:1668-1670.

ISO

http://www.iso.org/iso/home/search.htm?qt=photocatalytic&published=on&active_tab=standards&sort_by=rel. Accessed 22 August 2013

- Jacoby WA, Maness PC, Wolfrum EJ, Blake DM, Fennell JA (1998) Mineralization of bacterial cell mass on a photocatalytic surface in air. *Environ Sci Technol* 32:2650-2653.
- Jepras RI, Carter J, Pearson SC, Paul FE, Wilkinson MJ (1995) Development of a robust flow cytometric assay for determining numbers of viable bacteria. *Appl Environ Microbiol* 61:2696-2701.
- JIS <http://www.webstore.jsa.or.jp/webstore/JIS/FlowControl.jsp> Accessed 22 August 2013
- Jones RG, Thompson CB (2009) Tumor suppressors and cell metabolism: a recipe for cancer growth. *Genes & Dev* 23:537-548.
- Josset S, Taranto J, Keller N, Keller V, Lett M, Ledoux MJ, Bonnet V, Rougeau S (2007) UV-A photocatalytic treatment of high flow rate air contaminated with *Legionella pneumophila*. *Catal Today* 129:215-222.
- Karunakaran C, Abiramasubdari G, Gomathisankar P, Manikandan G, Anandi V (2011) Preparation and characterization of ZnO–TiO₂ nanocomposite for photocatalytic disinfection of bacteria and detoxification of cyanide under visible light. *Mater Res Bull* 46:1586-1592.
- Kaur J, Karthikeyan R, Smith R (2013) Assessment of *Escherichia coli* reactivation after photocatalytic water disinfection using flow cytometry: comparison with a culture-based method. *Wa Sci Technol* 13:816-825.
- Kete M, Zvab U, Tasbihi M, Lavrencic Stangar U (2012) Technical report of the prototype photoreactor design, its realization and water purification performance assessment: Confidential report for Electrolux Italia s.p.a, University of Nova Gorica, Slovenia.
- Kete M, Pavlica E, Fresno F, Bratina G, Lavrencic Stangar U (2014) Photocatalytic coatings containing commercial TiO₂ nanoparticles. *Chem Eng J* (submitted).
- Khaengraeng R, Reed RH (2005) Oxygen and photoinactivation of *Escherichia coli* in UVA and sunlight. *J Appl Microbiol* 99:39-50.
- Khan JS, Reed HR, Rasul GM (2012a) Thin-film fixed-bed reactor (TFFBR) for solar photocatalytic inactivation of aquaculture pathogen *Aeromonas hydrophila*. *BMC Microbiol* 12:5.

- Khan JS, Reed HR, Rasul GM (2012b) Thin-film fixed-bed reactor for solar photocatalytic inactivation of *Aeromonas hydrophila*: influence of water quality. *BMC Microbiol* 12:258.
- Kim YJ, Park C, Yoon J (2008) Developing a testing method for antimicrobial efficacy on TiO₂ photocatalytic products. *Environ Eng Res* 13:136-140.
- Kim S, Ghafoor K, Lee J, Feng M, Hong J, Lee D-U, Park J (2013) Bacterial inactivation in water, DNA strand breaking, and membrane damage induced by ultraviolet-assisted titanium dioxide photocatalysis. *Water Res* 47:4403-4411.
- Klug HP, Alexander LE (1973) *X-ray Diffraction Procedures*. 2nd edn. John Wiley and Sons, Hoboken, pp 687-708.
- Ko G, First MW, Burge HA (2000) Influence of relative humidity on particle size and UV sensitivity of *Serratia marcescens* and *Mycobacterium bovis* BCG aerosols. *Tuber Lung Dis* 80:217-218.
- Koch AC (1994) Growth measurements. In: Gerhardt P, Murray RGE, Wood WA, Krieg NR (eds) *Methods for general and molecular bacteriology*, ASM Press, Washington DC, pp 254-257
- Koizumi Y, Taya M (2002) Photocatalytic inactivation of phage MS2 in titanium dioxide suspensions containing various ionic species. *Biotechnol Lett* 24:459-462.
- Kuhn KP, Chaberny IF, Massholder K, Stickler M, Benz VW, Sonntag H-G, Erdinger L (2003a) Disinfection of surfaces by photocatalytic oxidation with titanium dioxide and UVA light. *Chemosphere* 53:71-77.
- Kuhn DM, Balkis M, Chandra J, Muherjee PK, Ghannoum MA (2003b) Uses and limitations of the XTT assay in studies of *Candida* growth and metabolism. *J Clin Microbiol* 41:506-508.
- Kumar A, Pandey AK, Singh SS, Shanker R, Dhawan A (2011) Engineered ZnO and TiO₂ nanoparticles induce oxidative stress and DNA damage leading to reduced viability of *Escherichia coli*. *Free Radic Biol Med* 51:1872-1881.
- Lee JH, Kang M, Choung SJ, Ogino K, Miyata S, Kim MS, Park JY, Kim JB (2004) The preparation of TiO₂ nanometer photocatalyst film by a hydrothermal method and its sterilization performance for *Giardia lamblia*. *Water Res* 38:713-719.
- Levy IK, Mizrahi M, Ruano G, Zampieri G, Requejo FG, Litter MI (2012) TiO₂-photocatalytic reduction of pentavalent and trivalent arsenic: production of elemental arsenic and arsine. *Environ Sci Technol* 46:2299-308.

- Li S, Zhu R, Zhu H, Xue M, Sun X, Yao S, Wang S (2008) Nanotoxicity of TiO₂ nanoparticles to erythrocyte in vitro. *Food Chem Toxicol* 46:3626-3631.
- Li H, Cui Q, Feng B, Wang J, Lu X, Weng J (2013) Antibacterial activity of TiO₂ nanotubes: influence of crystal phase, morphology and Ag deposition. *Appl Surf Sci* (In Press) doi: 10.1016/j.apsusc.2013.07.076
- Lin C, Lee J, Chang C, Chang Y, Lee Y, Hwa M (2010) Novel TiO₂ thin films/glass fiber photocatalytic reactors in the removal of bioaerosols. *Surf Coat Technol* 205:S341-S344.
- Li Puma G, Bono A, Krishnaiah D, Collin JG (2008) Preparation of titanium dioxide photocatalyst loaded onto activated carbon support using chemical vapor deposition: A review paper. *J Hazard Mater* 157:209-219.
- Liu L, John B, Yeung KL, Si G (2007) Non-UV based germicidal activity of metal-doped TiO₂ coating on solid surfaces. 19:745-750.
- Liu Y, Wang X, Yang F, Yang X (2008) Excellent antimicrobial properties of mesoporous anatase TiO₂ and Ag/TiO₂ composite films. *Microporous Mesoporous Mater* 114:431-439.
- Lonnen J, Kilvington S, Kehoe SC, Al-Touati F, McGuigan KG (2005) Solar and photocatalytic disinfection of protozoan, fungal and bacterial microbes in drinking water. *Water Res* 39:877-883.
- Lowdin E, Odenholt-Tornqvist I, Bengtsson S, Cars O (1993) A new method to determine postantibiotic effects of subinhibitory antibiotic concentration. *Antimicrob Agents Chemother* 37:2200-2205.
- Madigan TM, Martinko MJ, Parker J (2003) Chapter 21: Human-microbe interactions. In: *Brock biology of microorganisms*, 10th edn. Pearson Education Inc, Upper Saddle River, pp 727-754.
- Malato S, Fernandez-Ibanez P, Maldonado MI, Blanco-Galvez J, Gernjak W (2009) Decontamination and disinfection of water by solar photocatalysis: recent overview and trends. *Catal Today* 147:1-59.
- Malato S, Fernandez-Ibanez P, Maldonado MI, Oller I, Polo-Lopez I (2013) Solar photocatalytic pilot plants: commercially available reactors. In: Pichat P (ed) *Photocatalysis and water purification: from fundamentals to recent applications*, Wiley-VCH, Weinheim, pp 377-397

- Maness P, Smolinski S, Blake DM, Huang Z, Wolfrum EJ, Jacoby WA (1999) Bactericidal activity of photocatalytic TiO₂ reaction: toward an understanding of its killing mechanism. *Appl Environ Microbiol* 65:4094-4098.
- Marinescu C, Sofronia A, Rusti C, Piticescu R, Badilita V, Vasile E, Baies R, Tanasescu S (2011) DSC investigation of nanocrystalline TiO₂ powder. *J Therm Anal Calorim* 103:49-57.
- Marugan J, Grieken R, Pablos C, Sordo C (2010) Analogies and differences between photocatalytic oxidation of chemicals and photocatalytic inactivation of microorganisms. *Water Res* 44:789-796.
- Matsunaga T, Tomoda R, Nakajima T, Wake H (1985) Photoelectrochemical sterilization of microbial cells by semiconductor powders. *FEMS Microbiol Lett* 29:211-214.
- Matsunaga T, Tomoda R, Nakajima T, Nakamura N, Komine T (1988) Continuous-sterilization system that uses photosemiconductor powders. *Appl Environ Microbiol* 54:1330-1333.
- McCullagh C, Robertson JMC, Bahnemann DW, Robertson PKJ (2007) The application of TiO₂ photocatalysis for disinfection of water contaminated with pathogenic microorganisms: a review. *Res Chem Intermed* 33(3-5):359-375.
- McCullagh C, Skillen N, Adams M, Robertson PKJ (2011) Photocatalytic reactors for environmental remediation: a review. *J Chem Technol Biotechnol* 86:1002-1017.
- McHugh IO, Tucker AL (2007) Flow cytometry for the rapid detection of bacteria in cell culture production medium. *Cytometry A* 71:1019-1026.
- McLoughlin OA, Kehoe SC, McGuigan KG, Duffy EF, Touati FA, Gernjak W, Alberola IO, Malato S, Gill LW (2004) Solar disinfection of contaminated water: a comparison of three small-scale reactors. *Sol Energy* 77:657-664.
- Melemi M, Stamatakis D, Xekoukoulotakis NP, Mantzavinos D, Kalogerakis N (2009) Disinfection of municipal wastewater by TiO₂ photocatalysis with UV-A, visible and solar irradiation and BDD electrolysis. *Global Nest J* 11:357-363.
- McHugh IO, Tucker AL (2007) Flow cytometry for the rapid detection of bacteria in cell culture production medium. *Cytometry A* 71:1019-26.
- Miller RJ, Bennett S, Keller AA, Pease S, Lenihan HS (2012) TiO₂ nanoparticles are phototoxic to marine phytoplankton. *PLoS ONE* 7(1):e30321.
- Mills A, Lee S (2002) A web-based overview of semiconductor photochemistry-based current commercial applications. *J Photochem Photobiol A Chem* 152:233-247.

- Mills A, Hill G, Bhopal S, Parkin PI, O'Neill AS (2003a) Thick titanium dioxide films for semiconductor photocatalysis. *J Photochem Photobiol A* 160:185-194.
- Mills A, Lepre A, Elliott N, Bhopal S, Parkin IP, O'Neill SA (2003b) Characterisation of the photocatalyst Pilkington Activ™: a reference film photocatalyst?. *J Photochem Photobiol A Chem* 160:213-224.
- Mills A, Hill C, Robertson PKJ (2012) Overview of the current ISO tests for photocatalytic materials. *J Photochem Photobiol A Chem* 237:7-23.
- Mizunoe Y, Wai SN, Takade A, Yoshida S (1999) Restoration of culturability of starvation-stressed and low-temperature stressed *Escherichia coli* O157 cells by using H₂O₂-degrading compounds. *Arch Microbiol* 172:63-67.
- Modesto O, Hammer P, Nogueira RFP (2013) Gas phase photocatalytic bacteria inactivation using metal modified TiO₂ catalysts. *J Photochem Photobiol A Chem* 253:38-44.
- Morales AE, Sanchez Mora E, Pal U (2007) Use of diffuse reflectance spectroscopy for optical characterization of un-supported nanostructures. *Rev Mex Fis S* 5:18:22.
- Muranyi P, Schraml C, Wunderlich J (2010) Antimicrobial efficiency of titanium dioxide-coated surfaces. *J Appl Microbiol* 108:1966-1973.
- Muszkat L, Feigelson L, Bir L, Muszkat KA, Teitel M, Dornay I, Kirchner B, Kritzman (2005) Solar photo-inactivation of phytopathogens by trace level hydrogen peroxide and titanium dioxide photocatalysis. *Phytoparasitica* 33:267-274.
- Nadtochenko AV, Rincon GA, Stanca ES, Kiwi J (2005) Dynamics of *E. coli* membrane cell peroxidation during TiO₂ photocatalysis studied by ATR-FTIR spectroscopy and AFM microscopy. *J Photochem Photobiol A: Chem*, 169:131–137.
- Nakata K, Fujishima A (2012) TiO₂ photocatalysis: design and applications. *J Photochem Photobiol C* 13:169-189.
- Nakayama N, Hayashi T (2008) Preparation of TiO₂ nanoparticles surface-modified by both carboxylic acid and amine: dispersibility and stabilization in organic solvents. *Colloids Surf A Physicochem Eng Asp* 317:543-550.
- Naito K, Tachikawa T, Cui CS, Sugimoto A, Fujitsuka M, Majima T (2006) Single-molecule detection of airborne singlet oxygen. *J Am Chem Soc* 128:16430-16431.
- Nhung LTT, Nagata H, Takahashi A, Aihara M, Okamoto T, Shimohata T, Mawatari K, Akutagawa M, Kinouchi Y, Haraguchi M (2012) Sterilization effect of UV light on *Bacillus* spores using TiO₂ films depends on wavelength. *J Med Invest* 59:53-58.
- Nowakowska J, Oliver JD (2013) Resistance to environmental stresses by *Vibrio vulnificus* in the viable but nonculturable state. *FEMS Microbiol Ecol* 84:213-22.

- Ochiai T, Fukuda T, Nakata K, Murakami T, Tryk DA, Koide Y, Fujishima A (2010) Photocatalytic inactivation and removal of algae with TiO₂-coated materials. *J Appl Electrochem* 40:1737-1742.
- Ohtani B, Prieto-Mahaney OO, Li D, Abe R (2010) What is Degussa (Evonik) P25? Crystalline composition analysis, reconstruction from isolated pure particles and photocatalytic activity test. *J Photochem Photobiol A Chem* 216:179-182.
- Ohko Y, Hashimoto K, Fujishima A (1997) Kinetics of photocatalytic reactions under extremely low-intensity UV illumination on titanium dioxide thin films. *J Phys Chem A* 101:8057-8062.
- Oliver DJ (2010) Recent findings on the viable but nonculturable state in pathogenic bacteria. *FEMS Microbiol Rev* 34:415-425.
- Pablos C, Grieken R, Marugan J, Moreno B (2011) Photocatalytic inactivation of bacteria in a fixed-bed reactor: Mechanistic insights by epifluorescence microscopy. *Catal Today* 161:133-139.
- Pal A, Pehkonen OS, Yu EL, Ray BM (2008) Photocatalytic inactivation of airborne in a continuous-flow reactor. *Ind Eng Res* 47:7580-7585.
- Paleologou A, Marakas H, Xekoukoulotakis N, Moya A, Vergara Y, Kalogerakis N, Gikas P, Mantzavinos D (2007) Disinfection of water and wastewater by TiO₂ photocatalysis, sonolysis and UV-C irradiation. *Catal Today* 129:136-142.
- Park DR, Zhang J, Ikeue K, Yamashita H, Anpo M (1999) Photocatalytic oxidation of ethylene to CO₂ and H₂O on ultrafine powdered TiO₂ photocatalysts in the presence of O₂ and H₂O. *J Catal* 185:114-119.
- Paz Y (2009) Photocatalytic treatment of air: from basic aspects to reactors. In: Lasa HI, Rosales BS (Eds) *Advances in Chemical Engineering*, 36:289-336.
- Paz Y (2010) Application of TiO₂ photocatalysis for air treatment: Patents' overview. *Appl Catal B* 99:448-460.
- Pelczar MR, Microbiology. In: *Encyclopædia Britannica*. <http://www.britannica.com/EBchecked/topic/380246/microbiology>. Accessed 7 September 2013
- Pera-Titus M, Garcia-Molina V, Banos AM, Gimenez J, Esplugas S (2004) Degradation of chlorophenols by means of advanced oxidation processes: a general review. *Appl Catal B* 47:219-256.

- Petkovic J, Kuzma T, Rade K, Novak S, Filipic M (2011) Pre-irradiation of anatase TiO₂ particles with UV enhances their cytotoxic and genotoxic potential in human hepatoma HepG2 cells. *J Hazard Mater* 196:145-152.
- Pettit RK, Weber CA, Kean MJ, Hoffmann H, Pettit GR, Tan R, Franks KS, Horton ML (2005) Microplate alamar blue for *Staphylococcus epidermis* biofilm susceptibility testing. *Antimicrob Agents Chemother* 49: 2612-2617.
- Pichat P, Cermenati L, Albini A, Mas D, Delprat H, Guillard C (2000) Degradation processes of organic compounds over UV-irradiated TiO₂. Effect of ozone. *Res Chem Intermed* 26:161-170.
- Pigeot-Remy S, Simonet F, Atlan D, Lazzaroni JC, Guillard (2012) Bactericidal efficiency and mode of action: a comparative study of photochemistry and photocatalysis. *Water Res* 46:3208-2218.
- Pizzaro P, Guillard C, Perol N, Herrmann JM (2005) Photocatalytic degradation of imazapyr in water: comparison of activities of different supported and unsupported TiO₂-based catalysts. *Catal Today* 101:211-218.
- Polo A, Diamant MV, Bjarnsholt T, Hoiby N, Villa F, Pedferri MP, Cappitelli F (2011) Effects of photoactivated titanium dioxide nanopowders and coating on planktonic and biofilm growth of *Pseudomonas aeruginosa*. *Photochem Photobiol* 87:1387-1394.
- Priya DN, Modak JM, Trebse P, Zabar R, Raichur AM (2011) Photocatalytic degradation of dimethoate using LbL fabricated TiO₂/polymer hybrid films. *J Hazard Mater* 195:214-222.
- Proctor RA, von Eiff C, Kahl BC, Becker K, McNamara P, Herrmann M, Peters G (2006) Small colony variants: a pathogenic form of bacteria that facilitates persistent and recurrent infections. *Nat Rev Microbiol* 4:295-305.
- Quek PH, Hu J (2008) Indicators for photoreactivation and dark repair studies following ultraviolet disinfection. *J Ind Microbiol Biotechnol* 35:533-541.
- Rachel A, Sarakha M, Subrahmanyam M, Boule P (2002) Comparison of several titanium dioxides for the photocatalytic degradation of benzenesulfonic acids. *Appl Catal B* 37:293-300.
- Ramier J, Costa ND, Plummer CJG, Leterrier Y, Manson JE, Eckert R, Gaudiana R (2008) Cohesion and adhesion of nanoporous TiO₂ coatings on titanium wires for photovoltaic applications. *Thin Solid Films* 516:1913-1919.
- Reddy MP, Venugopal A, Subrahmanyam M (2007) Hydroxyapatite-supported Ag-TiO₂ as *Escherichia coli* disinfection photocatalyst. *Water Res* 41:379-386.

- Rengifo-Herrera JA, Pierzhala K, Sienkiewicz A, Forro L, Kiwi J, Pulgarin C (2009) Abatement of organics and *Escherichia coli* by N, S co-doped TiO₂ under UV and visible light. Implications of the formation of singlet oxygen (¹O₂) under visible light. *Appl Catal B* 88:398-406.
- Reyes-Coronado D, Gattorno-Rodriguez G, Pesqueira-Epinosa ME, Cab C, Coss R, Oskam G (2008) Phase-pure TiO₂ nanoparticles: anatase, brookite and rutile. *Nanotechnology* 19:145605-15.
- Rincon AG, Pulgarin C (2003) Photocatalytical inactivation of *E. coli*: effect of (continuous–intermittent) light intensity and of (suspended–fixed) TiO₂ concentration. *Appl Catal B* 44:263-284.
- Rincon AG, Pulgarin C (2004a) Field solar *E. coli* inactivation in the absence and presence of TiO₂: is UV solar dose an appropriate parameter for standardization of water solar disinfection? *Sol Energy* 77:635-648.
- Rincon AG, Pulgarin C (2004b) Effect of pH, inorganic ions, organic matter and H₂O₂ on *E. coli* K12 photocatalytic inactivation by TiO₂: implications in solar water disinfection. *Appl Catal B* 51:283-302.
- Rincon AG, Pulgarin C (2004c) Bactericidal action of illuminated TiO₂ on pure *Escherichia coli* and natural bacterial consortia: post-irradiation events in the dark and assessment of the effective disinfection time. *Appl Catal B* 49:99-112.
- Robertson JMC, Lawton LA, Robertson PKJ (2005) A comparison of the effectiveness of TiO₂ photocatalysis and UVA photolysis for the destruction of three pathogenic micro-organisms. *J Photochem Photobiol A Chem* 175:51-56.
- Rodriguez CP, Zioli RL, Guimaraes JR (2007) Inactivation of *Escherichia coli* in water by TiO₂-assisted disinfection using solar light. *J Braz Chem Soc* 18:126-134.
- Rothschild L (2002) Life in extreme environments. *Ad Astra* 14:1. <http://www.nss.org/adastra/volume14/rothschild.html>. Accessed 5 January 2014
- Sakthivel S, Shankar MV, Palanichamy M, Arabindoo B, Bahnemann DW, Murugesan V (2004) Enhancement of photocatalytic activity by metal deposition: characterisation and photonic efficiency of Pt, Au and Pd deposited on TiO₂ catalyst. *Water Res* 38:3001-3008.
- Sanchez B, Sanchez M, Munoz M, Cobas G, Portela R, Suarez S, Gonzalez AE, Rodriguez N, Amils R (2012) Photocatalytic elimination of indoor air biological and chemical pollution in realistic conditions. *Chemosphere* 87:625-630.

- Sawada D, Ohmasa M, Fukuda M, Masuno K, Koide H, Tsunoda S, Nakamura K (2005) Disinfection of some pathogens of mushroom cultivation by photocatalytic treatment. *Mycoscience* 46:54-60.
- Schwegmann H, Ruppert J, Frimmel FH (2013) Influence of the pH-value on the photocatalytic disinfection of bacteria with TiO₂ – Explanation by DLVO and XDLVO theory. *Water Res* 47:1503-1511.
- Shang C, Cheung LM, Ho C, Zeng M (2009) Repression of photoreactivation and dark repair of coliform bacteria by TiO₂-modified UV-C disinfection. *Appl Catal B* 89:536-542.
- Shlaes DM, Sahm D, Opiela C, Spellberg B (2013) Commentary: The FDA Reboot of Antibiotic Development. *Antimicrob Agents Chemother* doi: 10.1128/AAC.01277-13.
- Sichel C, Cara M, Tello J, Blanco J, Fernandez P (2007) Solar photocatalytic disinfection of agricultural pathogenic fungi: *Fusarium* species. *Appl Catal B* 74:152-160.
- Smit MAL, Spaan S, Heederik D (2005) Endotoxin exposure and symptoms in wastewater treatment workers. *Am J Ind Med* 48:30-39.
- Sommer R, Lhotsky M, Haider T, Cabaj A (2000) UV inactivation, liquid-holding recovery, and photoreactivation of *Escherichia coli* O157 and other pathogenic *Escherichia coli* strains in water. *J Food Prot* 63:1015-1020.
- Sordo C, Grieken R, Marugan J, Fernandez P (2010) Solar photocatalytic disinfection with immobilised TiO₂ at pilot-plant scale. *Water Sci Technol* 61:507-512.
- Sousa VM, Manaia CM, Mendes A, Nunes OC (2013) Photoinactivation of various antibiotic resistant strains of *Escherichia coli* using a paint coat. *J Photochem Photobiol A Chem* 251:148-153.
- Stock SM (2004) Mechanism and use of the commercially available viability stain, *BacLight*. *Cytometry A* 61A:189-195.
- Straka PR, Stokes LJ (1956) Rapid destruction of bacteria in commonly used diluents and its elimination. *Appl Microbiol.* 5:21-25.
- Strauber H, Muller S (2010) Viability states of bacteria-specific mechanisms of selected probes. *Cytometry Part A* 77A:623-634.
- Subhayan B, Takayuki N, Faruk HM, Takakazu T (2008) Correlation of structural, optical and surface morphological properties of N-doped TiO₂ thin films prepared by facing targets sputtering technique. *J Phys: Conf Ser* 100 082015.
- Suligoj A, Cernigoj U, Lavrencic Stangar U (2010) Preparation procedure of durable titania coatings on metal supports for photocatalytic cleaning applications. National

- application number P-201000432, The Slovenian Intellectual Property Office, Ljubljana.
- Subrahmanyam M, Boule P, Kumari VD, Kumar DN, Sancelme M, Rachel A (2008) Pumice stone supported titanium dioxide for removal of pathogen in drinking water and recalcitrant in wastewater. *Sol Energy* 82:1099-1106.
- Sunada K, Kikuchi Y, Hashimoto K, Fujishima A (1998) Bactericidal and detoxification effects of TiO₂ thin film photocatalysts. *Environ Sci Technol* 32:726-728.
- Sunada K, Watanabe T, Hashimoto K (2003) Studies on photokilling of bacteria on TiO₂ thin film. *J Photochem Photobiol A Chem* 156:227-233.
- Taranto J, Frochet D, Pichat P (2009) Photocatalytic treatment of air: comparison of various TiO₂, coating methods, and supports using methanol or n-octane as test pollutant. *Ind Eng Chem Res* 48:6229-6236.
- Tasbihi M, Ngah CR, Aziz N, Mansor A, Abdullah AZ, Teong LK, Mohamed AR (2007) Lifetime and regeneration studies of various supported TiO₂ photocatalysts for the degradation of phenol under UV-C light in a batch reactor. *Ind Eng Chem Res* 46:9006-9014.
- Tatsuma T, Tachibana S, Fujishima A (2001) Remote oxidation of organic compounds by UV-irradiated TiO₂ via the gas phase. *J Phys Chem B* 29:6987-6992.
- Tiller JC (2008) Coatings for prevention or deactivation of biological decontamination. In: Kohli R and Mittal KL (eds) *Developments in surface contamination and cleaning*, William Andrew Inc, New York, pp 1013-1065
- Trevors JT (2003) Fluorescent probes for bacterial cytoplasmic membrane research. *J Biochem Biophys Methods* 57:87-103.
- Valant J, Drobne D, Novak S (2012) Effect of ingested titanium dioxide nanoparticles on the digestive gland cell membrane of terrestrial isopods. *Chemosphere* 87:19-25.
- Vamanu CI, Cimpan MR, Hol PJ, Sornes S, Lie SA, Gjerdet NR (2008) Induction of cell death by TiO₂ nanoparticles: Studies on a human monoblastoid cell line. *Toxicol In Vitro* 22:1689-1696.
- Villarino A, Bouvet O, Regnault B, Martin-Delautre S, Grimont PA (2000) Exploring the frontier between life and death in *Escherichia coli*: evaluation of different viability markers in live and heat- or UV-killed cells. *Res Microbiol* 151:755-768.
- Vohra A, Goswami DY, Deshpande DA, Block SS (2006) Enhanced photocatalytic disinfection of indoor air. *Appl Catal B* 64:57-65.

- Wegelin M, Canonica S, Mechsner K, Fleischmann T, Pesaro F, Metzler A (1994) Solar water disinfection: scope of the process and analysis of radiation experiments. *J Water SRT-Aqua* 43:154-169.
- WHO (2011) Guidelines for drinking-water quality, 4th edn.. http://whqlibdoc.who.int/publications/2011/9789241548151_eng.pdf. Accessed 19 July 2013.
- Wong MS, Chu WS, Sun DS, Huang HS, Chen JH, Tsai PJ, Lin NT, Yu MS, Hsu SF, Wang SL, Chang HH (2006) Visible-light-induced bactericidal activity of a nitrogen-doped titanium photocatalyst against human pathogens. *Appl Environ Microbiol* 72:6111-6116.
- Wu CS (2005) Synthesis of polyethylene-octene elastomer/SiO₂-TiO₂ nanocomposites via in situ polymerization: properties and characterization of the hybrid. *J Polym Sci A Polym Chem* 43:1690-1701.
- Wu D, You H, Jin D, Li X (2011) Enhanced inactivation of *Escherichia coli* with Ag-coated TiO₂ thin film under UV-C irradiation. *J Photochem Photobiol A Chem* 217:177-183.
- Wu Q, Wang W, Li Y, Li Y, Ye B, Tang M, Wang D (2012) Small sizes of TiO₂-NPs exhibit adverse effects at predicted environmental relevant concentrations on nematodes in a modified chronic toxicity assay system. *J Hazard Mater* 243:161-168.
- Wu HS, Lin YS, Lin SW (2013) Mechanisms of visible light photocatalysis in N-doped anatase TiO₂ with oxygen vacancies from GGA+U calculations. *Int J Photoenergy* 2013:1-7.
- Xiong D, Fang T, Yu L, Sima X, Zhu W (2011) Effects of nano-scale TiO₂, ZnO and their bulk counterparts on zebrafish: acute toxicity, oxidative stress and oxidative damage. *Sci Total Environ* 409:1444-1452.
- Xiong P, Hu J (2013) Inactivation/reactivation of antibiotic-resistant bacteria by a novel UVA/LED/TiO₂ system. *Water Res* 47:4547-4555.
- Yan X, He J, Evans DG, Duan X, Zhu Y (2005) Preparation, characterization and photocatalytic activity of Si-doped and rare earth-doped TiO₂ from mesoporous precursors. *Appl Catal B* 55:243-252.
- Ye L, Belloni P, Moller K (2012) Optical design of an UV-LED edge-lighting glass model. In: Jobbagy A (ed) IFMBE proceedings, Vol. 37, Springer Berlin Heidelberg, pp 327-330
- Zaleska A (2008) Doped-TiO₂: a review. *Recent Pat Eng* 2:157-164.

Zhang B, Powers R (2012) Analysis of bacterial biofilms using NMR-based metabolomics. *Future Med Chem* 4:1273-1306.

Zheng X, Chen D, Wang Z, Lei Y, Cheng R (2013) Nano-TiO₂ membrane adsorption reactor (MAR) for virus removal in drinking water. *Chem Eng J* 230:180-187.